Contents

List of figures

List of Tables

Estratto

Al giorno d'oggi le nuove tecnologie stanno permettendo un progressivo miglioramento nei trattamenti delle lesioni tumorali e conseguentemente nella vita del paziente. Una delle metodologie più innovative per il trattamento di tumori solidi è basata sull'elettroporazione (EP). L'applicazione di impulsi elettrici ad alta tensione sulla massa tumorale permette l'apertura di pori nella membrana cellulare e la conseguente morte cellulare direttamente causata dagli impulsi elettrici o in combinazione con chemioterapici. L'erogazione degli impulsi avviene tramite dispositivi medici "elettrodi" costituiti da aghi con diverse configurazioni geometriche, ma basati tutti sull'accoppiamento elettrico di una coppia di aghi ed in generale su due poli conduttivi.

In questo lavoro è presentato un nuovo dispositivo per elettroporazione, costituito da un singolo ago mininvasivo in cui sono presenti entrambi i poli di trattamento (elettrodo bipolare), in grado di trattare lesioni di ridotte dimensioni non facilmente raggiungibili. Il lavoro di tesi ha analizzato preliminarmente gli aspetti teorici dell'elettroporazione tramite modellizzazione Finite Element Methods (FEM) del campo elettrico, con software Comsol Multiphysics®. Questa analisi ha permesso l'identificazione di specifiche per la progettazione e realizzazione di primi prototipi di elettrodo bipolare utilizzati per le opportune verifiche funzionali mediante modelli pre-clinici (vegetale e animale). L'attività di tesi ha portato all'identificazione di alcuni modelli di elettrodo bipolare ritenuti d'interesse per un possibile sviluppo futuro ad uso clinico.

Abstract

Nowadays, new technologies are allowing a progressive improvement in the treatment of cancer lesions and consequently in the life of the patient. One of the most innovative methods for the treatment of solid tumours is based on electroporation (EP). The application of high voltage electrical impulses on the tumour mass allows the opening of pores in the cell membrane and the consequent cellular death directly caused by electrical impulses or in combination with chemotherapy. Pulse delivery is achieved by medical devices "electrodes" consisting of needles with different geometrical configurations, but all based on the electric coupling of a pair of needles and generally on two conductive poles.

In this work a new electroporation device is studied, consisting of a minimally invasive single needle in which are present both the treatment poles (bipolar electrode), able to treat small lesions not easily attainable. In this thesis project has preliminary analysed the theoretical aspects of electroporation through Finite Element Methods (FEM) modelling of the electric field, with Comsol Multiphysics software. This analysis has allowed the identification of design specifications for the realization of the first prototypes of bipolar electrode used for the appropriate functional verifications using pre-clinical models (vegetable and animal). Thesis work has led to the identification of some bipolar electrode models considered of interest for a possible future development for clinical use.

Chapter 1

Introduction

The following chapter introduces the purpose of the device that will be treated in the following master thesis work, specifying the steps and tests carried out for the creation of the prototype and the mode of subsequent use.

Electroporation (EP) is a technique that developed around 1970 which allows the electropermeabilization of cells. EP is an innovative technique which it has developed in the fields of biotechnology and medicine. The aim of this technique is to increase the efficacy of chemotherapy, creating pores (several nm in diameter) on the cell membrane to send molecules inside. EP is based on the application of an electric field on a cell. This external electric field leads to an induced transmembrane voltage which is proportional to the field itself. Several companies have worked in this field, an example is the company IGEA S.p.A., it has been working in biophysics field for more than 20 years and it is improving the technology, based on electroporation.

Over the years, guidelines have been drawn up to allow the correct use of electroporation, its parameters and devices. One of the first medical device developed to use this technique is the electroporator Cliniporator^{TM} and its accessories (produced by IGEA). The technology has improved, and several medical devices have been developed to use electroporation in the treatment of solid tumours.

This master thesis work aims to analyse the main steps for the development of a prototype of a new electrode to be used with the Cliniporator^{TM}. This device is an electrode, a special needle that will allow the use and application of electroporation. It will be different from the commercially available electrodes for geometric design and the conditions of use. It will improve the invasiveness of the device.

A device will be designed that can hold on the single electrode (needle) both conductive poles (positive and negative) so as to simplify use, instead of having two different needles acting as opposite poles. The device under examination, thanks to its small diameter, should allow to treat organs in a minimally invasive way, such as liver and pancreas using a single

electrode instead of minimum two needles. The following master thesis work is divided into chapters summarized below.

Chapter 1 is the present introductory part.

Chapter 2 introduces the state of the art of electroporation. Explains how the tumour volume is treated with this technique, the guidelines adopted and reported in European Standard Operating Procedures for Electrochemotherapy (ESOPE). The devices on the market with which it is possible to use electrochemotherapy. The steps to follow in order to carry out this technique.

Chapter 3 provides an overview of the materials and methods used to design this device. It is also reported the software that allowed the theoretical simulations (FEM) and the variation of the electrical and geometrical parameters.

Chapter 4 this chapter reporting all the analysed geometric configurations and the results obtained during the Finite Element Methods *(*FEM) simulations. Furthermore, it describes the study and activities to create all necessary prototypes and the results of using them on vegetable models and animal models.

Chapter 2

State of art

The following chapter will introduce the state of the art of electroporation, the technique, the devices on the market and the guidelines introduced for the correct use of parameters and electrodes on the patient.

2.1 Electroporation

Electroporation (EP) also known as Electropermeabilization (Figure 2.1 [1]) is an innovative technique which it has developed in the fields of biotechnology and medicine. The aim of EP is to increase the efficacy of chemotherapy, creating pores (several nm in diameter) on the cell membrane to send molecules inside. The permeability of the cell by electroporation allows the use of Electrochemotherapy (ECT). The latter is the technique that, in combination with electrical impulses that penetrate the cell membrane, allows the sending of a dose of non-permeant drugs, in particular chemotherapy drugs such as cisplatin or bleomycin.

In the last years, the number of researchers has increased, and the first theoretical experiments using electroporation and the results of these studies were published in 1970. [2] In general, electroporation and electropermeation are both used to indicate structural changes in the cell membrane due to the creation of an electrical field.[3]

As mentioned above, electroporation is based on the application of an electric field on a cell. This external electric field leads to an induced transmembrane voltage which is proportional to the field itself. In the case of elevated electric fields, it is possible to arrive at non-physiological effects such as structural rearrangements of the lipids in the membrane, resulting in the formation of pores through the membrane. This formation of the pores allows the entry and the transport through the membrane of molecules which would not otherwise be penetrate in the cytosol.

As will be seen in the project dealt with in this thesis, electroporation depends on different parameters such as:

- applied voltage;
- the number of pulses;
- the duration of pulses;[4]

Which are just the electrical parameters. Electroporation also depends on characteristic cell parameters such as:

- cell size;
- membrane composition;
- cytoskeletal structure.[3]

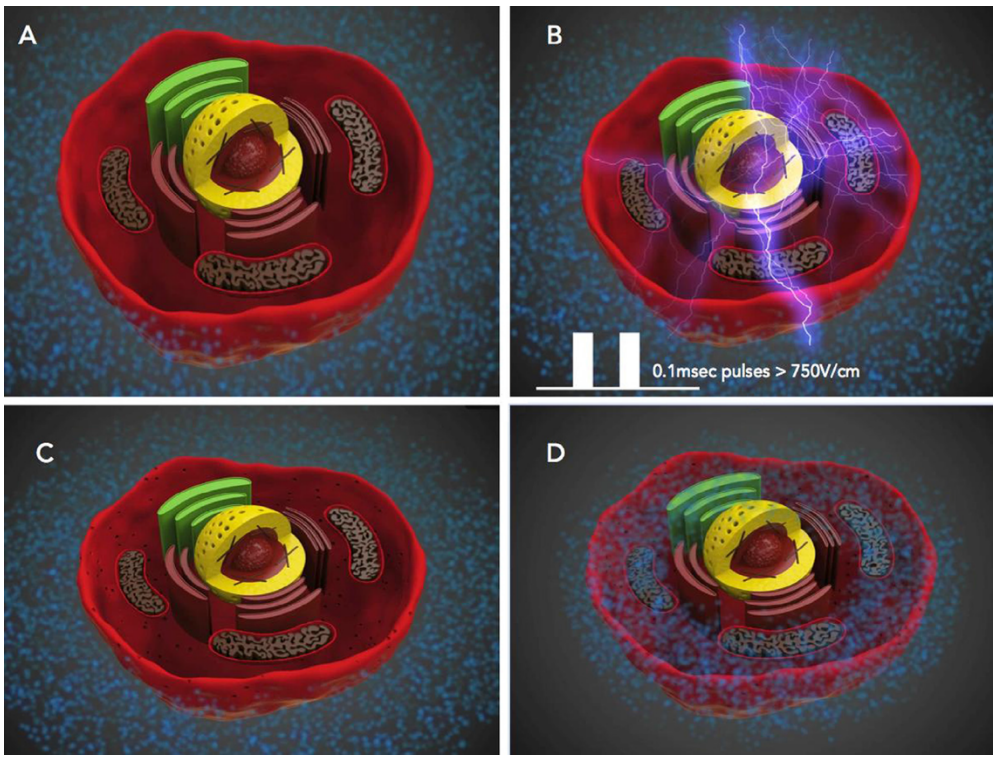

Figure 2.1 **Electroporation.** A) Delivery of drugs. B) Application of electrical field. C) Creation of nanopores. D) Input of the drug.

As visible in figure 2.2, the electric field induces the change in the resting transmembrane potential of the cell which is negative. The first part of the membrane that will be permeabilized is those facing the anode (positive pole). If the induced electric field is below the permeability threshold no effect is observed on the cell and therefore there is no permeability. If the applied electric field is greater than a minimum value, either the reversible electroporation or the irreversible electroporation occurs. The application of

electric field on cell, causes a rearrangement of the structure of the cell membrane for which the process of permeation is formed as a function of the applied voltage and therefore of the energy fed into the system, this process may be reversible or irreversible. [5]
The transmembrane voltage, as mentioned above depends on several factors that can be highlighted in the following equation:

$$\Delta\Phi_m = \frac{3}{2} ER \cos\theta$$

- $\Delta\phi_m$ = induced transmembrane voltage;
- E = electric field;
- R = radius;
- θ =angle between E and R.

This equation relates the induced transmembrane voltage to the direction of the electric field and the radius.[6]

In particular, in function not only of the tension but also of the number of pulses, re-sealed pores of the cellular membrane can be obtained; if this happens, there is reversible electroporation otherwise irreversible electroporation (leading to cellular death). Cell death is also related to the loss of control of Ca^{2+} transport that spreads into the cytoplasm and disrupts the cytoplasmic reticule.[7]

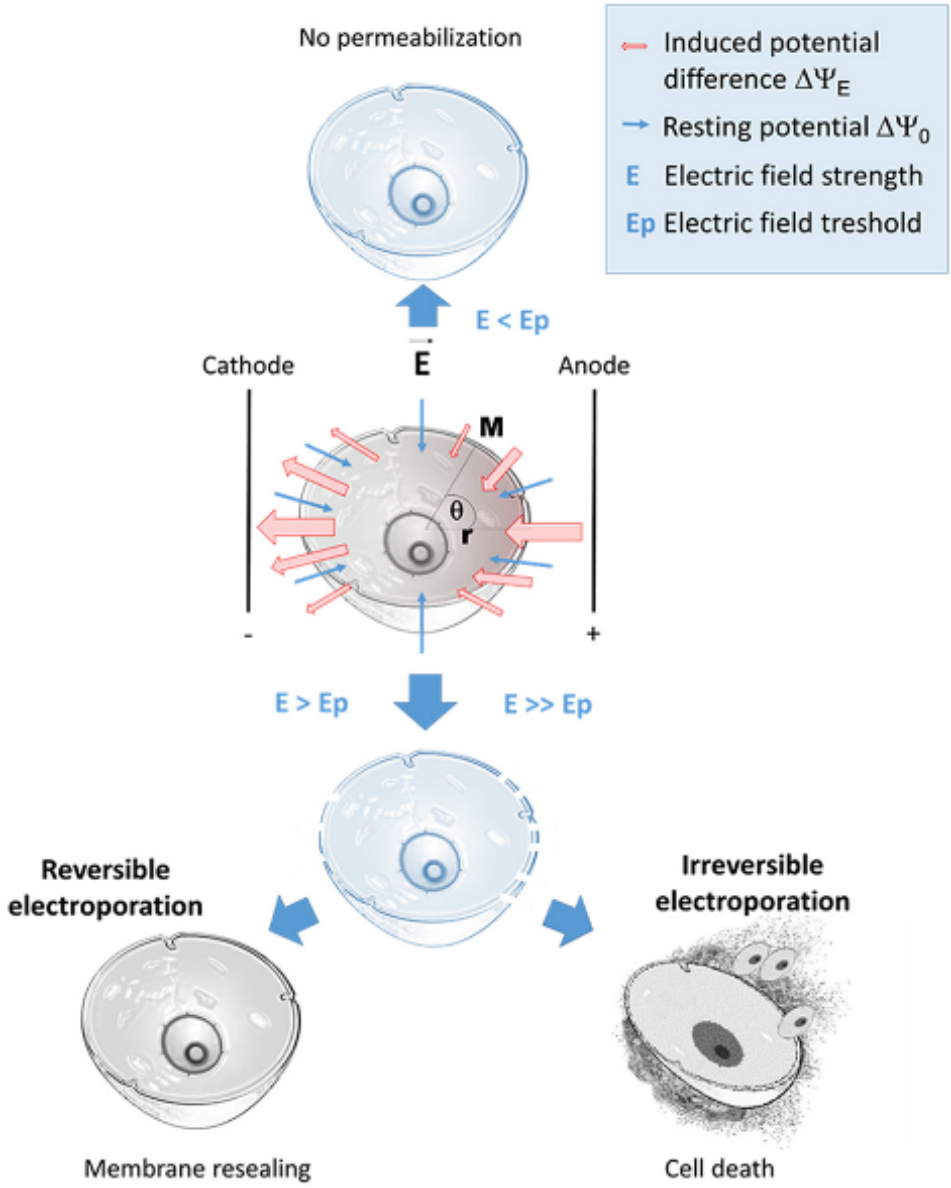

Figure 2.2 **Reversible and Irreversible electroporation.** Electric field induces the change in the resting transmembrane potential of the cell which is negative. If the induced electric field is below the permeability threshold no effect is observed on the cell and therefore there is no permeability. If the applied electric field is greater than a minimum value, either the reversible electroporation or the irreversible electroporation occurs.

Another important aspect regarding the EP is also related to the electrode because the cells near the electrode could be irreversibly damaged while moving away the characteristics of the cell membrane are maintained and reversible. In addition, the amplitude of the electric field, moving away from the electrode, decreases without causing pore formation on the cell membrane. So, it can be said that the electroporation efficiency is linked to the electrical parameter applied. Studies have shown that the electropermeability of the cell membrane can be achieved by increasing the number of pulses or the duration of the pulses in the case of the amplitude of the electrical field which is not optimal. At this point it was possible to introduce the concept of the optimal absorbed dose which is proper function of the electric field, the number of pulses and its duration. This relationship has been demonstrated in the studies conducted by Ongaro et al., the depth of the electropermeation increases when the number of impulses sent is greater, even if the voltage is kept constant. Electropermeation applications can be electrotransfer of low permeability drugs such as bleomycin and cisplatin so that tumour cells can be spread into the cytoplasm. The graph in figure 2.3 shows how the electric field threshold necessary to obtain electropermeation can be lowered if you increase the impulses sent. [4]

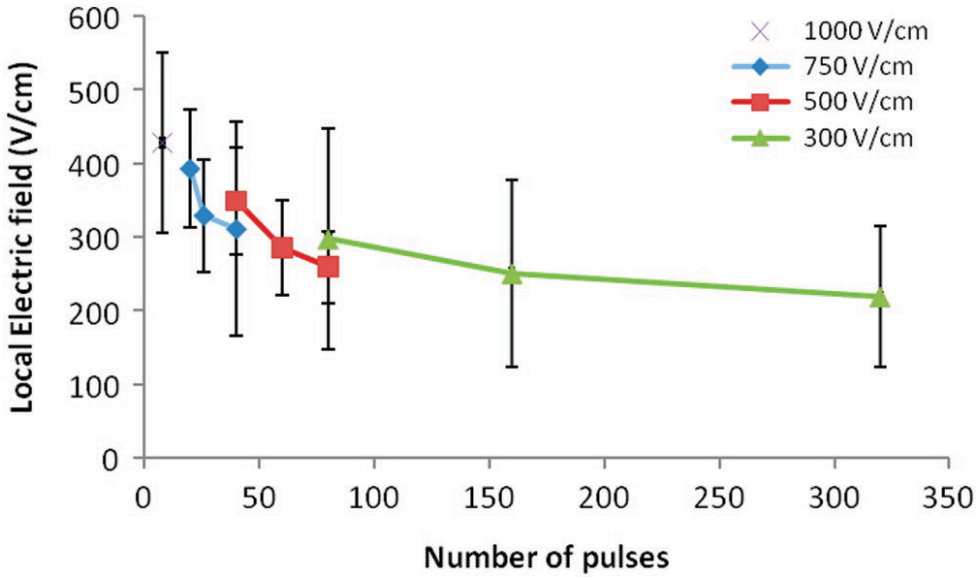

Figure 2.3 **Electrical field development as a function of the number of pulses.** The threshold of the electric field decreases as the number of pulses applied increases.

Several studies have been conducted to arrive at the optimal parameters usable but also to be able to analyse which chemotherapy drugs to be used in combination with electroporation, they have arrived at the conclusion of cisplatin and bleomycin.[3] With the use of the drug, it is necessary to combine either a high electric field and low pulse duration or a low voltage and a long duration. [8]

Electroporation can be divided into gene or drug electrotransfer, in particular it is characterized by different clinical applications. For the genes it is divided into DNA or RNA while for the drugs it differs according to the metastasis to hit: cutaneous metastasis such as melanomas or head and neck, non-cutaneous metastasis such as bones, liver or brain and primary tumours such as the ovaries, breasts or pancreas.[3]

2.2 Cell Membrane

The basis of a human being's life is the cell. It is the fundamental unity of living organisms, and each cell has a specific function to ensure life. One of the characteristics of the cell is that it has a plasma membrane that protects it from the external environment. This is an important regulatory barrier for transport into and out of the molecules and ions; it maintains the balance of chemical and electrical gradients.[9]

Transmembrane transport can be achieved by ionic channels (allow the flow of ions and can be opened or closed by some electrical or chemical signals), aqueous pores (formed from proteins) and ionic pumps (allow the transport of ions). The lipid bilayer into the membrane is permeable only to water, O_2 and CO_2 and polar compounds like DNA, RNA, carbohydrates, proteins and ions. The carriage is possible thanks to the macromolecules and the presence of ion channels allow the control of Na^+, Cl^-, Ca^{2+}, K^-. [9]

The permeabilization of the cell membrane (Figure 2.4 [9]**)** is composed by 4 important step:

- Balance of gradient (a) among $Ca^{2+,}$ K^+ and Na^+ and high content of ATP.[9]
- Permeabilization of cell (b), K^+ and ATP leave the cell and Ca^{2+} and N^+ get in.[9]
- Resealed cell (c) allows the cell to retrieve ion gradient.[9]
- Damaged cell (d), if the membrane do not reseal or reseal too slowly, there will be an excessive cellular $Ca^{2+.}$ Cell death by necrosis and apoptosis.[9]

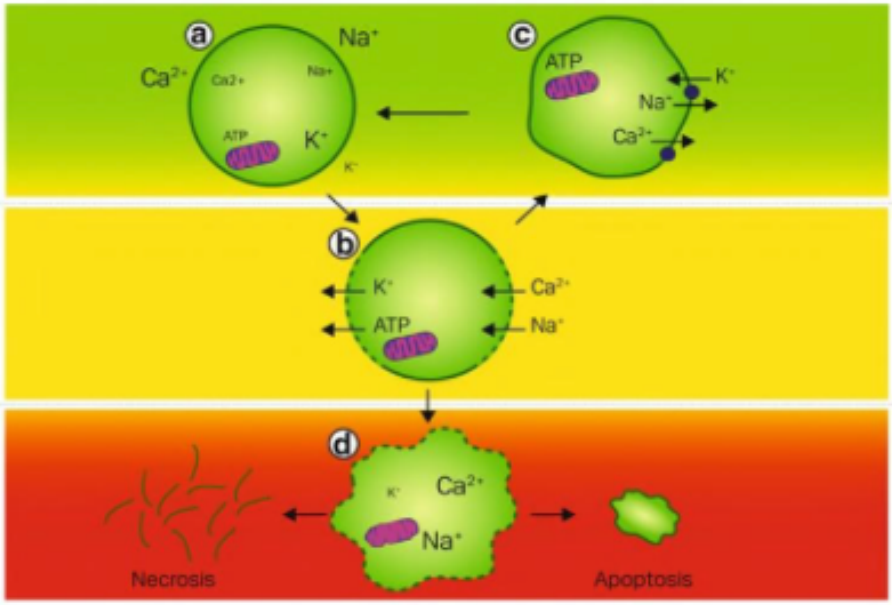

Figure 2.4 **Effects of permeabilization on the cell.** A) Balance of gradient. B) Permeabilization of cell. C)Resealed cell. D) Damaged cell.

The cell membrane acts as a barrier to prevent the influx of hydrophilic drugs, macromolecules and peptides and the permeability of cellular membrane increases with electroporation thanks to the application of an electric field.[1] [9]

As said before, the electroporation allows to increase the permeability of the cell membrane, however, leading to a loss of homeostasis and disturbance of normal functions. One of the most important aspects is that electroporation will also cause a large influx of calcium, due to the high gradient through the membrane. Calcium is one of the main agents involved in cell damage.[9]

The cell membrane is flexible and self-sealing, and this allows the membrane to repair itself when a hole is caused, as happens in electroporation. Nonpermeating tracers allow to investigate the permeabilization and the resealing (Figure 2.5 [9]) to figure out the cell's survival. In normal condition tracers' drug do not enter into the cell. The permeabilization allows the gained access into the cell thanks to pores and when the membrane is resealed the tracers drug cannot leave the cell. [9]

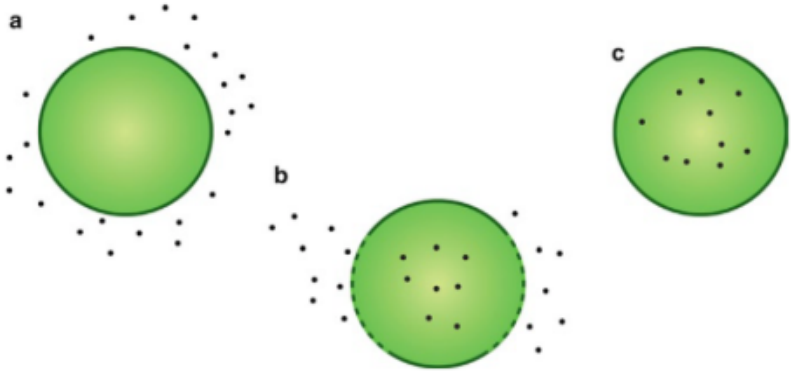

Figure 2.5 **Tracer drug.** A) Non-permeable tracer drug is added. B) The permeability is allowed and therefore the tracer drug can enter. C) When the membrane is closed, no tracer drug can be washed out.

2.3 Equipment for patient treatment with electroporation

The electroporation system mainly consists of a pulse generator and a pulse applicator with specific roles.

Figure 2.6 **Flowchart of equipment for patient treatment.**

2.3.1 Pulse generator

The pulse generator, which is controlled by a computer, allows to generate electrical impulses so as to create the effect of electroporation and thanks to the pulse applicator that transmits these pulses to the tissue to be treated. The pulse generator is the electronic part of the electroporator, it must create an electrical signal. [8]

The electroporator in order to create this signal must have as inputs[8]:

- pulse amplitude;

- time of this pulse;
- number of times the signal must be applied;
- number, distance, type and polarity of the electrodes.

All these characteristics allow to determine the volume to be treated.[8]

2.3.1.1 *Electroporators*

There are several electroporators on the market in the area of electroporation.

- Angiodynamics is the manufacturer of the Nanoknife™ system: device for irreversible electroporation, therefore with high electric field. It allows the sending of high voltages between two electrodes. It is not intended to be used in combination with chemotherapy or other therapeutic substances. This device is designed to use six applicators at the same time. It has been set up so that the operator can use a default configuration or allow the operator can choose the features to use. The applicators are designed to be used exclusively with Nanoknife™ and can be used to treat smaller or larger cancers. [8]

Figure 2.7 **Nanoknife™.** Device for irreversible electroporation.

- Ichor is the manufactured of the TriGrid™ (Figure 2.11). It is used to send intramuscular or intradermal DNA. It was built specifically for sending DNA plasmid to muscle or skin. Ichor medical device uses electrical fields to improve this sending. It has three main purposes: therapeutic cancer vaccines, infectious diseases and therapeutic proteins. It is made up of three parts: the pulse generator, the integrated applicator on which there are electrodes and which allows easy use by the operator and finally the application cartridge which is sterile and consists of both electrodes and the substance to be sent.

Figure 2.8 **Trigrid™.** It is used to send intramuscular or intradermal DNA.

Among the most important and most used are the IGEA electroporators. These devices will also be used for conducted thesis work. The Cliniporator™ allowed to write the European Standard Operating Procedures for Electrochemotherapy that allows the use of electrochemotherapy on the basis of predefined rules so that there were fewer human errors possible by the operator. Below, the two IGEA electroporators and their differences have been reported:

- IGEA is the manufacturer of Cliniporator™ and Cliniporator Vitae™ (Figure 2.9-2.10). They are both made up of a command and control section on which is installed the application that manages the software and a power unit that generates

impulses. Like other devices, they must be used in conjunction with the company's electrodes. Both are equipped with external control connected to the Cliniporator™ which allows to control the delivery and generation of electrical impulses. They allow you to check in real time that the procedure has been performed. These devices allow the procedures to be completed within minutes. They can also be used for clinical investigations or in pre-clinical or experimental studies according to the specifications described in the user manual. Moreover, unlike other devices, it is possible to treat also organs in the vicinity of the heart, thanks to a system of cardiac synchronization that allows the release of impulses during the period of absolute refractory nature of the heart.[10]

Figure 2.10 **Cliniporator**™. IGEA's electroporator.

Figure 2.9 **Cliniporator Vitae**™. IGEA 's electroporator.

2.3.1.2 *Input for electric field*

At the base of the pulses to be applied and the parameters to be put in input to the electroporator there is the choice between the current and the voltage to be imposed. [8]
The main waveform used by electroporators to create an electric field is (Figure 2.11) [8]:

- square wave pulse;

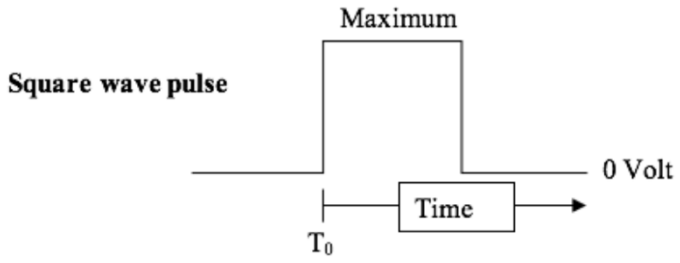

Figure 2.11 **Waveform.** The operators choose the pulse waveform to create the electric field.

2.3.2 Pulse applicators

The pulse applicators (applicator electrode and applicator cord) allows to transmit pulses from the generator to the tumour that has to be treated. There are many types of electrodes (needles, plates or pins) that can be used according to the area to be treated. The most important differences for pulse applicators are that they are divided in: penetrating or non-penetrating electrodes and in pre-set fixed geometry and custom variable geometry (Figure 2.12-2.13-2.14 [11]). The non-penetrating electrode usually consist of multiple rectangular thin plates and the tumour is placed near the space between plate electrodes. The electric field will move between the plates in the sequence present by the electroporator or chosen by the operator, depending on how many plates there are. Initially this device consisted of only two plates, in order to treat bulk tumour after the first application it was removed from the tissue, rotated and repositioned on the tumour tissue to give uniformity to the treated area. Over the years a new type of plate electrode has been built that could eliminate the rotation step, but that would be done by the electroporator itself, by switching between the pairs of plates. [8]

The configuration of the penetrating electrodes consists instead of needles with a tip to penetrate the tissue. Over the years, electrodes have developed with a pair of needles or an array of needles depending on the size and type of tumour tissue to be treated.[8]
There is a further difference between needle electrodes. Electrode linear arrays are used for small tumours, because the application is low voltage and are also ideal for local anaesthesia. Hexagonal needle electrode configuration is used for larger tumours, with general anaesthesia. Finger electrode configuration is used for tumours in the body cavity, such as the oral one. Finally the adjustable electrode configuration is used to give a support to the electrodes when it comes to tumours of different sizes, this electrode allows to vary the penetration depth of the device.[11]

When treating a tumour, the electrodes must be moved and positioned to cover the entire tumour area. They must be inserted up to the lower margin of the tumour in order to have a complete distribution of the electrical field. The selection of electrode depends on the size and position of the tumour to be treated. [12]

Examples of IGEA electrodes connected to the Cliniporator™ are in figure 2.12-2.13-2.14.[10]

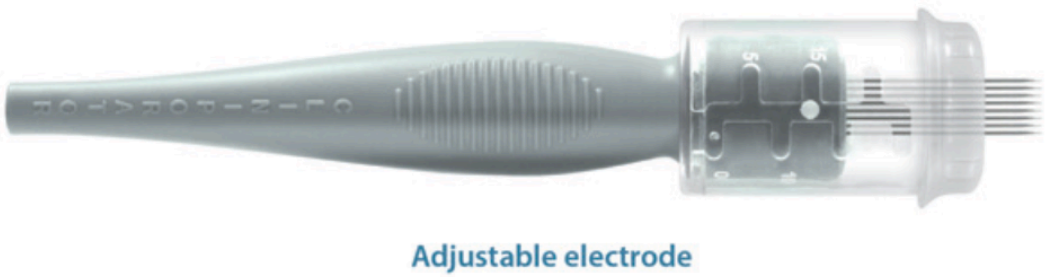

Figure 2.12 **Pulse applicators.** Adjustable electrode.

Figure 2.13 **Pulse applicators.** Linear array electrode.

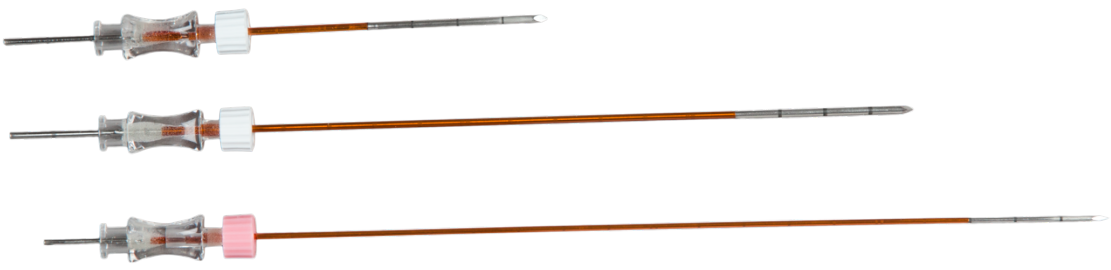

Figure 2.14 **Pulse applicators.** Needle electrode VGD, once positioned around or inside the tumor lesion allows the application of electroporation.

According to these devices on the market, the following thesis project will analyse and study a new electrode. This medical device will consist of a single electrode, like the VGD in the figure 2.12, but if normally each needle would have a conductive pole, in this case it was thought to get a single minimally invasive needle in which are present both treatment poles (bipolar electrode), to treat lesions that are not easily attainable.

2.4 Electrochemotherapy & European Standard Operating Procedures for Electrochemotherapy

Electrochemotherapy is a type of chemotherapy that is intended to introduce into cell membrane chemotherapeutic drugs. Its main purpose is to treat cancerous cells by sending a dose of non-permeant drug into the cell which is temporarily permeable thanks to the electroporation. It has greater success with the use of two non-permeant cytotoxic anti-cancer drugs such as bleomycin and cisplatin. The bleomycin is a small hydrophilic non-permeant anticancer cytotoxic drug. It is product by *Streptomyces verticillis* and it is used alone or with other drugs to treat cancer. [13]

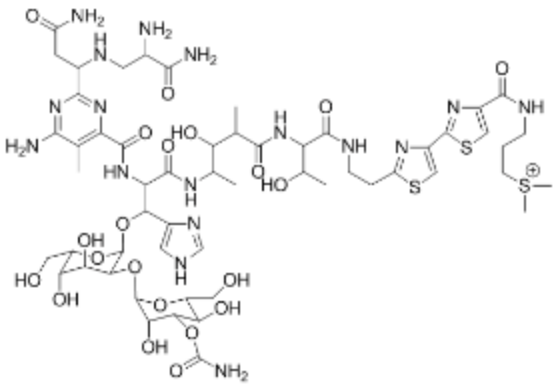

Figure 2.15 **Bleomycin**. Chemical structure of the drug used in electrochemotherapy.

In addition to bleomycin, there is cisplatin, a low-permeant cytotoxic drug. The first one is the molecules that in conjunction with electroporation has allowed an improvement in ECT. Only these two chemotherapeutic drugs have satisfied preclinical test and subsequently clinical trials. Overall, the application of electric pulse to the tumour cell causes decrease of perfusion and oxygenation of tumours. Electrochemotherapy it can be used in addition with chemotherapy or radiotherapy. [13]

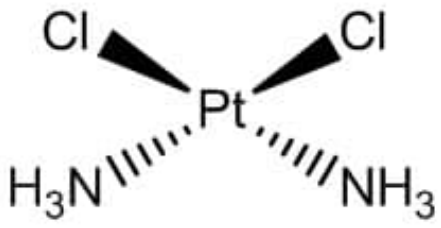

Figure 2.16 **Cisplatin**. Chemical structure of the drug used in electrochemotherapy.

Several animal tumour studies have been conducted to demonstrate the efficacy of ECT. It has been shown to be effective on fibrosarcoma, melanomas and carcinomas of mice, rats and rabbits. It is ideal for treating tumours that cannot be surgically removed due to the location. It can also be used before surgery as a cytoreductive. [12]

The advantages of electrochemotherapy can be summarized as follows. It is a technique also used to treat nodules with diameters smaller than 3 cm in diameter up to 7-8 cm. It can also be applied to different types of tumours, both cutaneous and subcutaneous. Another important advantage of this technique is the possibility of treating the nodules also on outpatient basis. It also provides an effective way to reduce blood loss. The main and most important advantage already highlighted in the previous chapters is that healthy tissue is less sensitive to electrochemotherapy than tumour tissue, compared to other methods such as ablation. Which is why you can use this technique over without being afraid to damage the healthy tissue easily. Low incidence of complications, which also entails a better quality of life. The advantage is the possibility of treatment repetition, if necessary. A study conducted by Campana et al. has allowed an investigation to be carried out on the quality of life after the application of electrochemotherapy. Going to analyse the healing and bleeding of the treated area, the aesthetic and everyday compromise.
The majority of patients reported a benefit in the disorders related to daily life activity (ADL). This is why the use of electrochemotherapy leads to an improvement in the quality of life of the patient. [12]

The European Standard Operating Procedures for Electrochemotherapy (ESOPE) allow to follow guidelines for the use of electrochemotherapy and treatment planning, also allowing too inexperienced doctors. The main point of the Standard Operating Procedures (SOP) is that a sufficient dose of the drug with an electric field distribution that can cover the entire tumour are the basis of good treatment.[12]
ESOPE treatment of the patient can be divided as follows[12]:

- Electroporator;
- Drug delivery;
- Anaesthesia;
- Electrodes;
- Patient response.

The publication of ESOPE (2006), has been the transition between previous techniques, with different chemotherapy drug and pulse parameters and wider standard procedures. The purpose of this study was to improve the regular technique of ECT of Standard Operating Procedures (SOP) based on the experience of European cancer centres on

Electrochemotherapy like Institute of Oncology in Llubljana, Cork Cancer Research Center and Herlev Hospital Copenhagen and this was also possible thanks to the realization of the first electroporator Cliniporator™ (IGEA, Carpi, Italy). Previous of this study, different procedures were applied to treat tumour or equal treatments were performed despite different clinical conditions. [12]
Before ESOPE, clinical trials were conducted in 247 patients (skin metastases of melanoma) treated with electrochemotherapy with bleomycin or cisplatin. After that, approximately 100 patients were studied for 2 years. They were analysed for different purposes, 41 evaluated for treatment response and 61 for toxicity.
Several parameters were analysed: the drug used (bleomycin or cisplatin), the route of administration (intratumoral or intravenous) and the type of electrode (plate or needle). 84.4% was obtained as a positive response, only a small part of a negative response was observed. These studies concluded that lower doses of bleomycin than those previously used are effective and there is greater tolerance by the tissues.[12]

Thanks to the clinical studies of ESOPE, this new approach has been adopted by several cancer centres, in particular for the treatment of cutaneous and subcutaneous tumour nodules. The quality of life of the patient should not be compromised, after the treatment. Electrochemotherapy treatments are safe and effective in palliative care. [12]
The ESOPE study resulted in positive responses regardless of tumour histology, type of drug administered, type of administration or type of electrode used. [1] The electroporator used in ESOPE studies is the Cliniporator™. [12]

2.4.1 Patient response

After a few hours of electrochemotherapy, since no treatment is required for the area, the patient is discharged. As visible in figure 2.17 ([12]) after an initial crust formation, it falls off after 4-12 weeks. The healing time of the area depending on the size and depth of the area. [12]

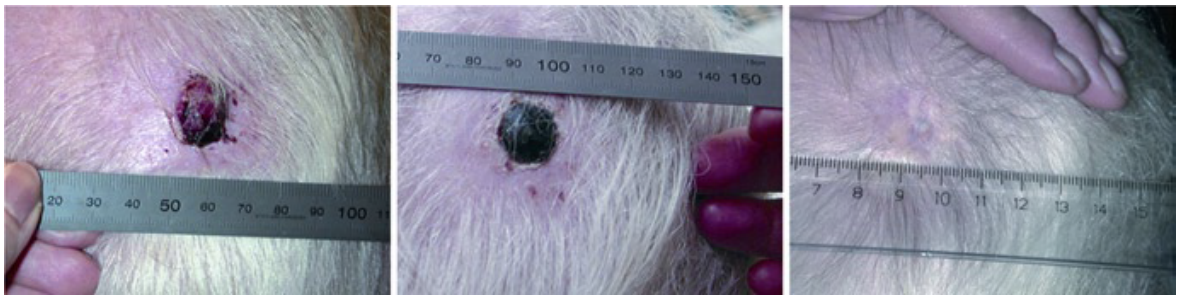

Figure 2.17 **Treatment of malignant melanoma metastases.** Example of electro-chemotherapy treatment of a malignant melanoma metastases of the head. It was treated with bleomycin and hexagonal electrode. On the left: the metastasis was ulcerated there was haemorrhage. At the centre: the response of the metastasis after one month with crust formation. On the right: the fall of the crust after six months.

The figure 2.17 shows the treatment of a malignant melanoma metastases of a bleomycin-treated patient. Marks of needle perforation in normal tissues are visible around the crust. It is evident that the tumour zone has become necrotic, the normal tissue has remained unchanged. The last image shows the fall of the crust and the healed area under the treated nodule. [12]

In the next chapter will be reported the study carried out for the simulation and the realization of a medical device, in particular an electrode to be used in electrochemotherapy with the Cliniporator™ (produced by IGEA®).

Chapter 3

Materials and method

This chapter describes the software used for electric field simulations and the theoretical model to simulate the device and relates characteristics, such as, geometry, materials and electrical parameters.

3.1 New electrode

Based on the electroporation and electroporators introduced in the previous chapter, the following study is conducted for the design of an electrode to be used with the electroporator Cliniporator™. This new electrode should facilitate operating procedures for treating deep lesions by reducing the invasiveness of treatment.
The initial hypothesis was to create a new electrode that could be used in electroporation and in particular usable with the Cliniporator™. It was thought to create a single electrode that could hold on the same needle both the positive and the negative pole. To obtain, a bipolar coaxial electrode, the two poles should have had the same axis of reference. In order to create this device, analyses on software and subsequently pre-clinical analyses have been done:

1. Modelling on software;
2. Test on vegetable model (potatoes);
3. Test on animal model (pig).

The project started from the simulation of different geometries to identify some optimal solutions. The analysis is performed using finite elements method. In order to model this medical device, a search was conducted and, among the several software available *Comsol Multiphysics®* has been identified.

3.1.1 Introduction to *Comsol Multiphysics* ®

Comsol Multiphysics® is a Finite Element Analysis (FEM) solver and multiphysics simulation software. [14]

Moreover, it is a software that allows to simulate, thanks to the coupling of one or more physical flows like AC/DC, of a fluid or mechanical structure, the structure of the desired model and its effects on the surrounding medium. It enables to model the device. In this thesis, *Comsol Multiphysics*® has been used because it lets to reproduce, at best, the geometry of the device and the considered physics, in this case the development of an electrical field created by an electrode in a medium, such as a tissue.

In the figure 3.1 is shown a flowchart in order to better understand the use of *Comsol Multiphysics* ® and the sequence of steps used in this project study.

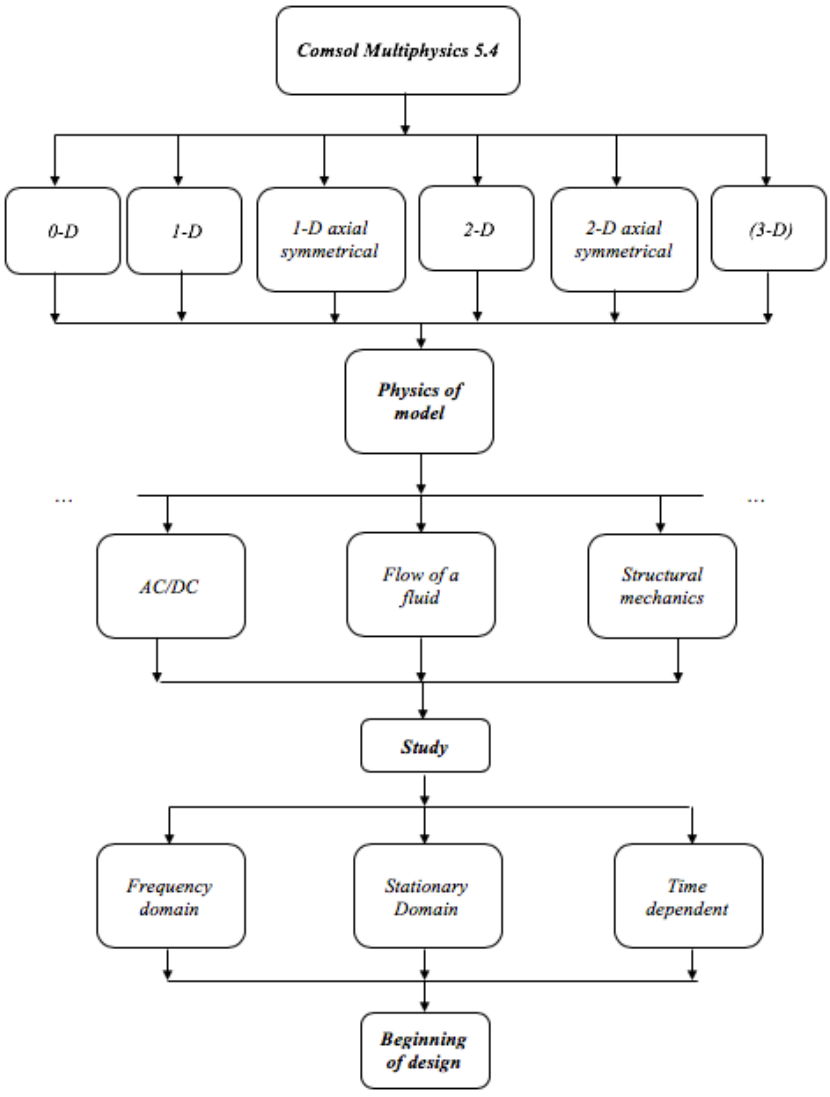

Figure 3.1 **Flowchart of *Comsol Multiphysics* ®**

3.2 *Comsol Multiphysics* ®

The software allows the user to choose modelling according to the following commands: 0 Dimension (*0-D*), 1 Dimension (*1-D*), 1 Dimension axial symmetrical (*1-D axial symmetrical*), 2 Dimension (*2-D*), 2 Dimension axial symmetrical (*2-D axial symmetrical*) and 3 Dimension (*3-D*). After the choice of the model, physics is chosen with the command "*physics of the model"*: alternating or continuous current (*AC/DC*), acoustic *study*, *transport of chemical species*, *flow of a fluid*, *heat transmission, radiofrequency, structural mechanics* and *mathematical models.* Another step is to select the type of "*study*" that can be in the *frequency domain*, *stationary* or *time dependent.*
Following these steps is possible to create the geometry of the device, to impose the conditions to the contour, to choose the constituent material of the electrode and of the means in which it is immersed.

In this case, 3D spatial dimension has been used and the study of the *electric currents* has been chosen, with dependent variables dependent on the electrical potential (Volt [V]). At the end, a *stationary study* was chosen for the electrode of this thesis.
The original idea, as mentioned in section 1, was to create a bipolar coaxial electrode, a simplification of the bipolar electrodes (two monopolar electrodes that together form a bipolar electrode), with two conductive poles on the same electrode. An attempt was made to create a concentric geometry of layers with *Comsol Multiphysics* ®, consisting of an alternation of conductive material and insulating material.

3.2.1 Electrode's geometry

The "*geometry"* of the medical device shall be created before the electrical field is studied. It may be made importing external images or creating a combination of existing geometries in *Comsol Multiphysics* ®.
In this case cylinders and cones were used to create the desired layer of the concentric geometry of the electrode. A parallelepiped of material, represents the tissue or organ into which the electrode would be introduced. In this thesis, various geometries of the electrode of interest have been analysed and realized.

The cone represents the tip while the hollow and solid cylinders represent the stainless-steel mandrel, the second pole and the insulating sheaths.
The tables 3.1 – 3.2 show the values for the first geometry created. Changes will be dealt in Section 4.

Electrode	**Comsol's geometry**	**Radius [R]**	**Height [H]**	**Thickness [T]**	**Unit of measure**
Tip	Cone	0.3-0.9	3		mm
Stainless-steel mandrel (Distal conductive pole)	Solid cylinder	0.5	47		mm
First insulating sheath	Empty cylinder	0.55	40	0.2	mm
Proximal conductive pole	Empty cylinder	0.7	35	0.2	mm
Second insulating sheath	Empty cylinder	0.85	25	0.2	mm

Table 3.1 **Values of the first geometry (electrode).**

	Comsol's geometry	**Width [W]**	**Height [H]**	**Depth [D]**	**Unit of measure**
Tissue/organ	Parallelepiped	80	80	80	mm

Table 3.2 **Values of the first geometry (tissue/organ).**

A qualitative image of the electrode structured with a concentric geometry is depicted in Figures 3.2-3.3-3.4.

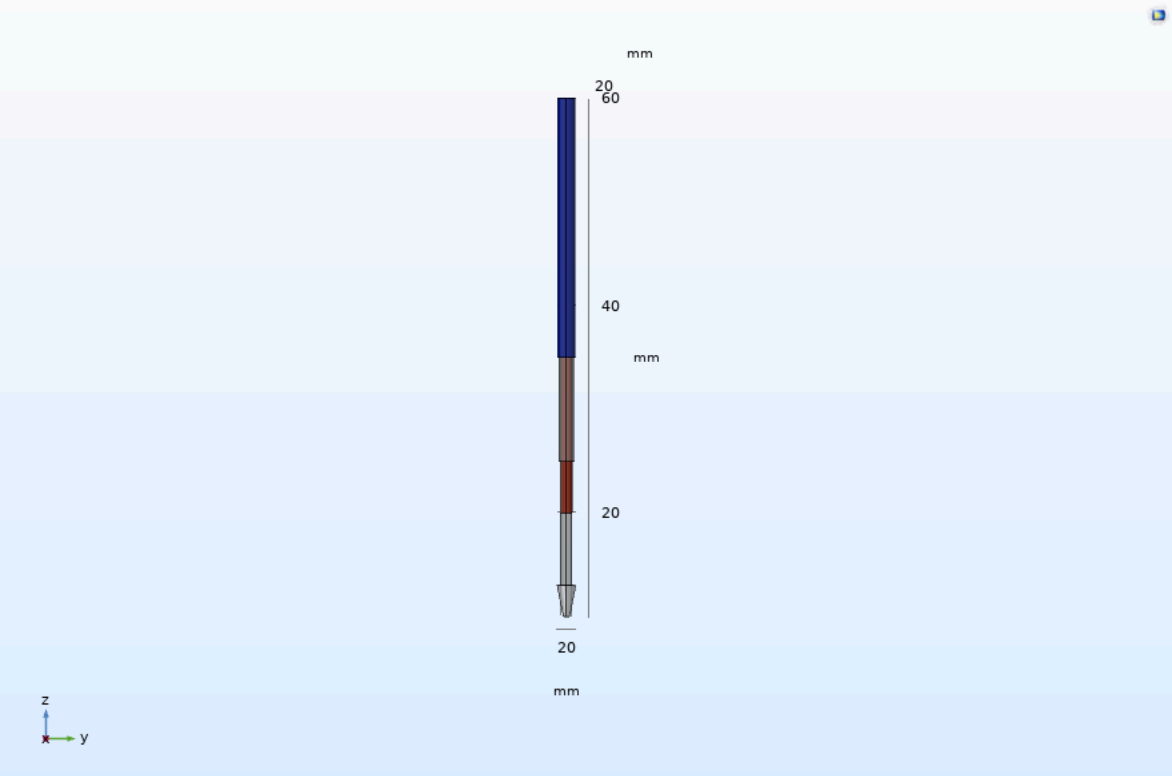

Figure 3.3 **Bipolar coaxial electrode.** First geometry recreated in *Comsol Multiphysics* ® of the device under examination.

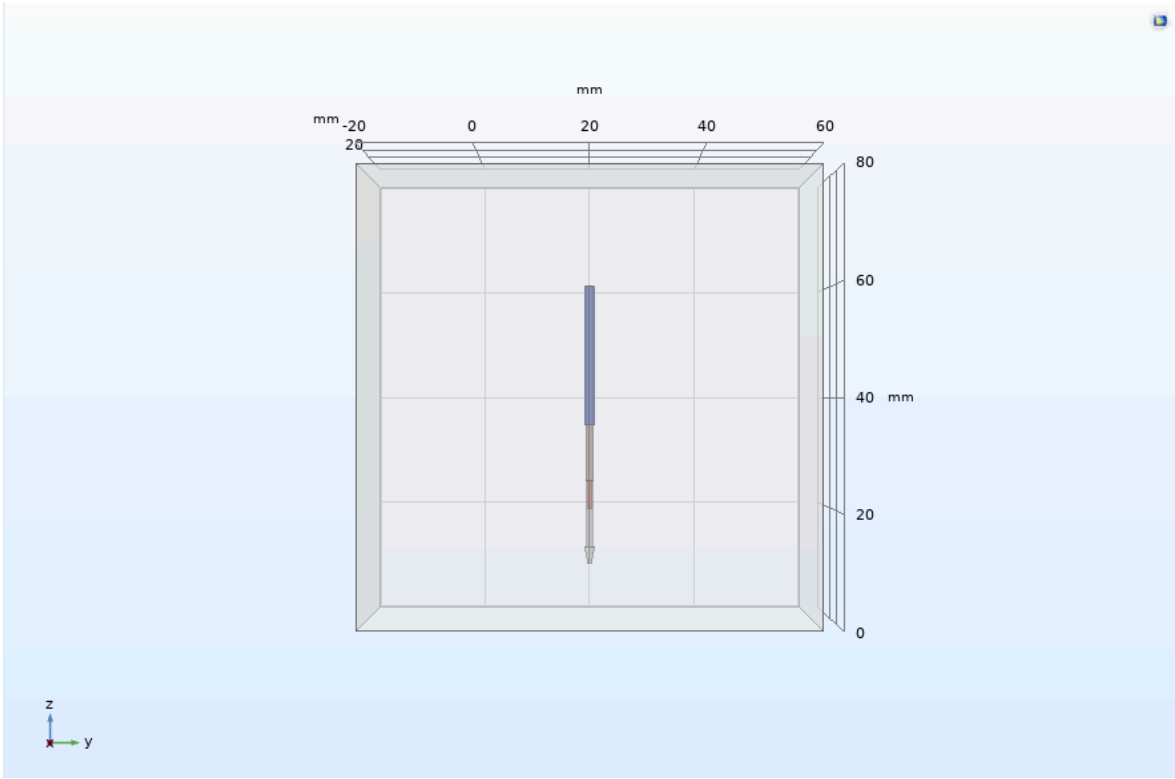

Figure 3.2 **Bipolar coaxial electrode with organ/tissue.** First geometry recreated in *Comsol Multiphysics* ® of the device under examination with tissue / organ.

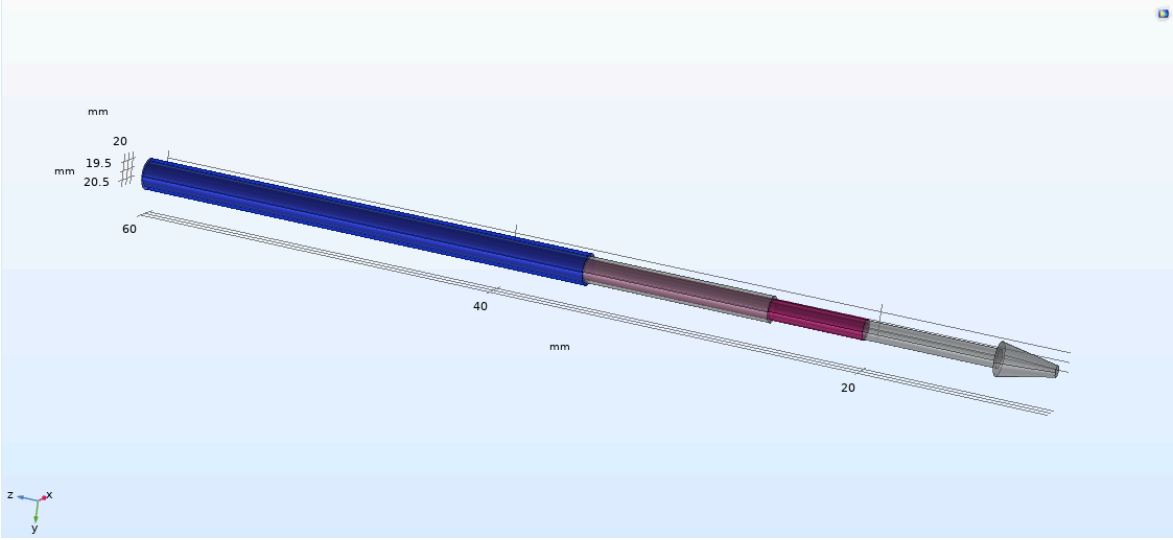

Figure 3.4 **Bipolar coaxial electrode.** Another view of the device in *Comsol Multiphysics* ®.

3.3 Materials

In order to make the electrode, the type of material for both the insulated and conductive part of the electrode was studied.

3.3.1 Conductive poles

Steel is a metal alloy that can appear in different types depending on the percentage of iron, carbon or other alloying elements. It is constituted by a certain percentage of iron and carbon. It can be extra soft, semi-hard, hard and extra hard depending on the amount of carbon. The steel considered for this device is stainless steel. The latter can be: ferritic, austenitic, martensitic, duplex. The most suitable phase for biomedical use is austenite, which however is difficult to have at room temperature. In order to allow austenite to be present at room temperature it is necessary to insert some stabilizers of gamma phase.
Austenitic stainless steel is chosen in the biomedical field because they have good mechanical properties and are resistant to corrosion, and besides being monophasic they are less difficult to reproduce.

There are different types of austenitic steels, one example being AISI 316 steel, which has a higher carbon content than AISI 316L steel, another one could be AISI 304.
The following table (Table 3.3) shows the percentage composition of the two steels studied.

AISI grade	C %	Si %	Mn %	Cr %	Ni %	Mo %
304	0.08	1.00	2.00	17.5-20	8-10.5	
316	0.08	1.00	2.00	16-18	10-14	2-3

Table 3.3 **Percentage composition of the steels.**

Steel AISI 316 and AISI 304 can be cold hardened and have a higher corrosion resistance. They are obtained by simple casting or casting into inert or vacuum gas.
AISI 304 has a chemical stability that guarantees a long life. Chemical stability and corrosion resistance are important aspects for the decision of the material of the device.

These two steels are chosen for their mechanical and electrical characteristics. The values are given in Table 3.4 [15].

PROPERTIES	304	316	UNIT OF MEASURE
Yield strength	290/300	280/290	MPa
Tensile strength	500/700	500/700	N/mm^2
Elongation	45	40	%
Hardness	215	215	HB
Density	7900	8000	kg/m^3
Young's modulus	$200*10^9$	$200*10^9$	Pa
Thermal conductivity	15	15	W/mK
Specific heat	500	500	J/kgK
Electric conductivity	0.73	0.75	$\Omega*mm^2/m$
Thermal expansion coefficient	16.5	16.5	$10^{-6}*K^{-1}$

Table 3.4 **Properties of steels.**

As shown, the properties of the two steels are very similar since they both are austenitic stainless steels. It has been chosen to use the AISI 304 steel as it is the already used for other IGEA's medical devices and it is more workable for the creation of electrode prototypes. Nevertheless, AISI 4340 has been used in the in *Comsol Multiphysics* ® simulation, because AISI 304 is not present in the bookcase of the software. Considering the many similarities in the properties between the two materials, this choice has been assessed as appropriate. Table 3.5 shows the characteristic values in the *Comsol Multiphysics* ® library of this steel.

PROPERTIES	AISI 4340	UNIT OF MEASURE
Density	7850	kg/m^3
Young's modulus	$205*10^9$	Pa
Thermal conductivity	44.5	W/mK
Specific heat	475	J/kgK
Electric conductivity	$4.032*10^6$	S/m
Thermal expansion coefficient	$12.3*10^{-6}$	K^{-1}
Relative permittivity	1	
Poisson's ratio	0.28	

Table 3.5 **Properties of AISI 4340.**

3.3.2 Insulating sheath

For the study of insulating sheaths, the study was carried out on different types of polymer. In particular, given their electrical insulating properties, the attention has been focused on: polyethylene terephthalate (PET) and polyimide (PI). These are two of the main polymers used in the biomedical field.

The first is a crystalline polymer, mostly used to make fibbers, films, and vines, especially in the prosthetic field. Mechanical characteristics of the PET are: resistant and light.

Both PET and polyimide are thermoplastic polymers, they can be softened and remodelled countless times. Thanks to their composition, it is possible to create and obtain the desired shape by processing the polymer in the state of polymeric fluid obtained by heating or by dissolving the polymers in a solvent.

They also have excellent mechanical characteristics that are kept constant even at high temperatures; in addition to these characteristics, they can withstand many chemical agents. They have a low coefficient of friction, good vibration-damping properties, and a good resistance to abrasion.
In this thesis, polyimide was chosen as material for the insulating sheaths. The choice is due to: its known biocompatibility (having already been used by IGEA); its immediate availability by the chosen company; its high dielectric strength, depending by the thickness of the wall, at the electroporation voltages.
Below (table 3.6) there are the properties of the material on *Comsol Multiphysics* ®.

PROPERTIES	POLYIMIDE	UNIT OF MEASURE
Density	1300	Kg/m^3
Young's modulus	$3.1*10^9$	Pa
Thermal conductivity	0.15	W/mK
Specific heat	1100	J/kgK
Electric conductivity	10^{-10}	S/m
Relative permittivity	4	
Poisson's ratio	0.28	

Table 3.6 **Properties of polyimide.**

3.3.3 Biological tissue

The last material to be simulated is the one in which the electrode will be inserted and will be in contact: the biological model as tissue or organ.
The tissues have different conductivity, this is due to different aspects such as the uneven tissue, anisotropy (cell orientation), physiological factors and of course the polarization of the electrode. In order to consider different biological models, in *Comsol Multiphysics* ® the simulation has been done with properties of:

- Water;

- Animal liver;
- Human liver;

varying different conductivity values.
As mentioned in section 3.2, the biological model will be simulated as a parallelepiped. The properties of these two materials are already present in *Comsol Multiphysics*® bookcase.
The tables 3.7-3.8-3.9 show the values in *Comsol Multiphysics*® of the properties of the material used as a medium.

PROPERTIES	WATER	UNIT OF MEASURE
Electric conductivity	0.4	S/m
Relative permittivity	80	

Table 3.7 **Properties of water.**

PROPERTIES	HUMAN LIVER	UNIT OF MEASURE
Density	1079	kg/m^3
Thermal conductivity	0.52	W/mK
Specific heat	3540	J/kgK
Electric conductivity	0.4	S/m
Frequency factor	$7.39*10^{39}$	1/s
Activation energy	$2.577*10^{5}$	J/mol
Relative permittivity	80	

Table 3.8 **Properties of human liver.**

PROPERTIES	ANIMAL LIVER	UNIT OF MEASURE
Electric conductivity	0.07	S/m
Relative permittivity	80	

Table 3.9 **Properties of animal liver.**

3.4 Electric field

After the definition of the geometry and the materials characterizing the medical device, the study to be carried out is set. In this case the variation of the electric field has been analysed thanks to the command "*Electric currents*". The equations used by *Comsol Multiphysics* ® for the calculation of the electric field are as follows:

$$\mathbf{J} = \sigma\mathbf{E} + \mathbf{J}_e$$

Ohm's law

$$\mathbf{E} = -\nabla V$$

Electric field in vacuum

$$\mathbf{D} = \epsilon_0 \epsilon_r \mathbf{E}$$

Electric field in material

Table 3.10 shows the variables used for *Comsol Multiphysics*® equations.

PHYSICAL VARIABLE	VALUE
Electric conductivity of material	σ
Electrical potential	V
Relative permittivity of material	ε_r
Gradient	∇
Current density	J
Electrical field in vacuum	E
Electrical field in the material	D

Table 3.10 **Physical variable.**

The reference values used for these equations are given in the table 3.11.

REFERENCE VALUES	VALUE
Reference impedance	Z_{ref} = 50 Ω
Temperature	T = 293,15 K

Table 3.11 **Reference values.**

3.5 Mesh

After the application of the electric field values, the mesh (figure 3.5) is run to perform the study and obtain the results.

The mesh cells "tetrahedral unstructured" shape has been chosen to obtain a more precise solution considering the electrode having more complex geometry.

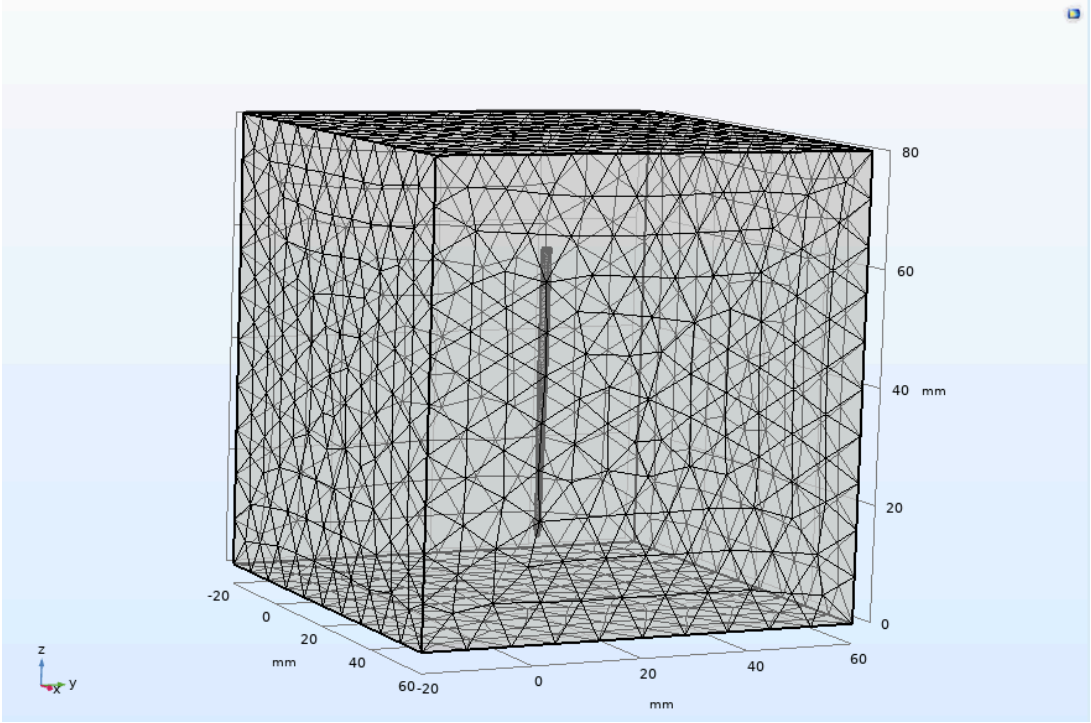

Figure 3.5 **Mesh.** Mesh cells "tetrahedral unstructured" shape to obtain a more precise solution.

Chapter 4

Bipolar coaxial electrode

The following chapter will deal with the simulations carried out in Comsol Multiphysics ®, the choice of electrodes to be used on a vegetable model based on the results of the initial simulations, and the choice of electrodes for the animal model.

4.1 Introduction

The chapter 4 will follow the creation of the first prototype of electrode. These electrodes have been used and tested on vegetable (potatoes) and animal (pig) model, thanks to the simulations in *Comsol Multiphysics* ® that have allowed to analyse different parameters.
After the study and the characterization with *Comsol Multiphysics* ®, the first prototypes have been produced in IGEA.

4.2 Electrode configurations with *Comsol Multiphysics* ®

The purpose of this study is to analyse the geometric and electrical parameters in order to obtain and realize a minimally invasive electrode. The purpose of the device was to treat a spherical tumour area of about 1 cm in diameter.
As described in the previous section, a change in *Comsol Multiphysics*® parameters was made. The results obtained are analysed below.
This analysis was conducted by investigating several geometric and electrical parameters listed below:

- Diameters of electrode: the selected parameters are from 2.00 mm (about 14G) to 1.4 mm (17G). The larger one, should be compatible with the use in bone tissue while the smaller with the use in soft tissues;

- Voltage applied to the poles: the values were different to highlight the variation of the electric field. These tests were conducted starting from generic values to obtain more specific one for electroporation;
- Separation between the poles: the length of the insulating part. As already mentioned, the insulating element will be made of polyimide;
- Length of the conductive poles: it was analysed how the length of the poles affected the shape of electric field. It was possible to differentiate electrodes with symmetrical geometry from asymmetric geometry. In the first case the length of the two poles is equal while in the second case it is different from each other.
- Polarity inversion between the poles: the polarity inversion has been analysed to see its effect on the electroporate volume. The choice of polarity was also due to the type of electroporator in use. The first Cliniporators™ had software that allowed the choice of polarity of the device during the pulses. The new Cliniporators™ (Cliniporator Vitae™) are designed with 8 pulses that automatically reverse the polarity of the device at each group of four pulses. The simulations in *Comsol Multiphysics* ® were conducted by choosing which pole was 0 V and which pole was with selected potential.

The figure 4.1 represents the geometry used to analyse these parameters and the resulting electric field.

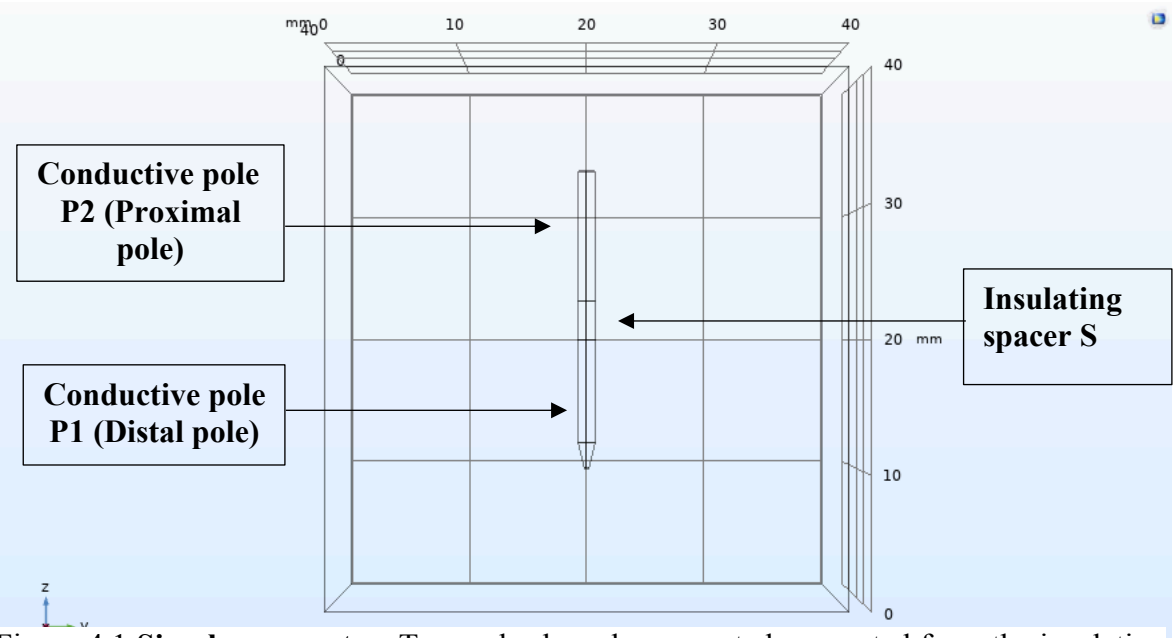

Figure 4.1 **Simpler geometry.** Two poles have been created, separated from the insulating sheath, having the same axis in common.

4.3 Results

The electric field of the simulations in *Comsol Multiphysics* ® will be conducted by analysing how it develops on the plane "yz", along the two axes: z (major axis) and y (minor axis). The table 4.1 summarizes the tests carried out in the symmetric case and in the asymmetric case in *Comsol Multiphysics* ®. The tests were all conducted with a threshold of 400 V/cm. Based on the purpose defined in the previous section, to obtain an electroporate volume of 1 cm, the electric field analysed will be that between 40000 V/m and 35000 V/m (red zone). An example of the areas analysed is shown in figure 4.2.

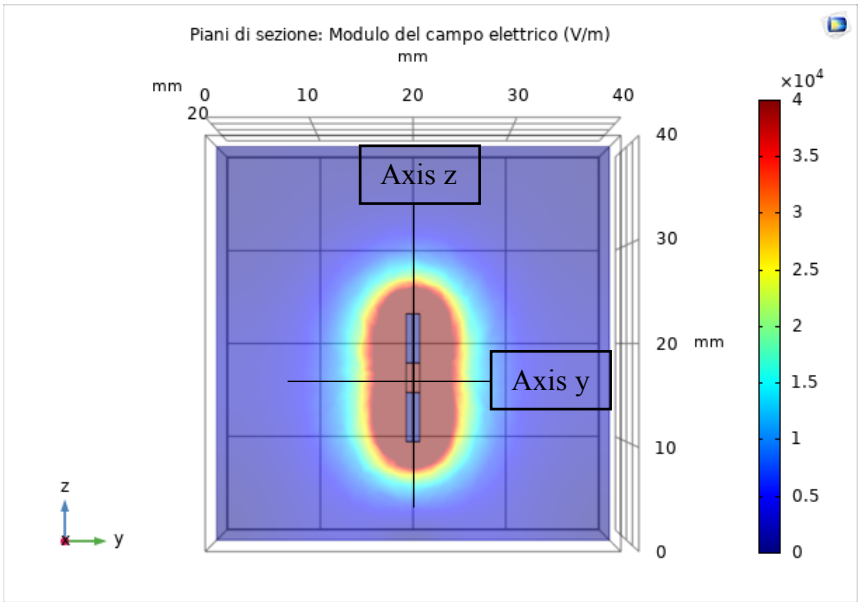

Figure 4.2 **An example of the results.**

Test session	Conductive Pole P1	Insulating Pole S	Conductive Pole P2	Voltage	Diameter D
1	5.00 mm	3.00 mm	5.00 mm	1000 V	**1.40 mm**
	5.00 mm	3.00 mm	5.00 mm	1000 V	**1.50 mm**
Diameters	5.00 mm	3.00 mm	5.00 mm	1000 V	**1.60 mm**
	5.00 mm	3.00 mm	5.00 mm	1000 V	**1.80 mm**
	5.00 mm	3.00 mm	5.00 mm	1000 V	**2.00 mm**
2	5.00 mm	3.00 mm	5.00 mm	**500 V**	1.40 mm
Voltage	5.00 mm	3.00 mm	5.00 mm	**1000 V**	1.40 mm
	5.00 mm	3.00 mm	5.00 mm	**1500 V**	1.40 mm
3	5.00 mm	**3.00 mm**	5.00 mm	1000 V	1.40 mm
Spacer	5.00 mm	**5.00 mm**	5.00 mm	1000 V	1.40 mm
	5.00 mm	**7.00 mm**	5.00 mm	1000 V	1.40 mm
4	**3.00 mm**	3.00 mm	**3.00 mm**	1000 V	1.40 mm
Conductive	**5.00 mm**	3.00 mm	**5.00 mm**	1000 V	1.40 mm
pole	**10.00 mm**	3.00 mm	**10.00 mm**	1000 V	1.40 mm
	15.00 mm	3.00 mm	**15.00 mm**	1000 V	1.40 mm
5	5.00 mm	3.00 mm	10.00 mm	**500 V**	1.40 mm
Voltage	5.00 mm	3.00 mm	10.00 mm	**800 V**	1.40 mm
6	5.00 mm	3.00 mm	10.00 mm	**500 V**	**1.40 mm**
Voltage	5.00 mm	3.00 mm	10.00 mm	**500 V**	**1.50 mm**
&	5.00 mm	3.00 mm	10.00 mm	**800 V**	**1.40 mm**
Diameters	5.00 mm	3.00 mm	10.00 mm	**800 V**	**1.50 mm**
7	5.00 mm	**3.00 mm**	10.00 mm	500 V	1.40 mm
Spacer	5.00 mm	**5.00 mm**	10.00 mm	500 V	1.40 mm
8	**20.00 mm**	3.00 mm	**5.00 mm**	500 V	1.40 mm
	15.00 mm	3.00 mm	**5.00 mm**	500 V	1.40 mm
Conductive	**10.00 mm**	3.00 mm	**5.00 mm**	500 V	1.40 mm
Pole	**10.00 mm**	3.00 mm	**3.00 mm**	500 V	1.40 mm
	5.00 mm	3.00 mm	**20.00 mm**	500 V	1.40 mm
	5.00 mm	3.00 mm	**15.00 mm**	500 V	1.40 mm
	5.00 mm	3.00 mm	**10.00 mm**	500 V	1.40 mm
	3.00 mm	3.00 mm	**10.00 mm**	500 V	1.40 mm

Table 4.1 **Tests carried out in *Comsol Multiphysics*®.** In bold the values changed.

4.3.1 Symmetric geometry

The first cycle of simulations conducted was the following, changing only the diameter of the electrode but keeping constant the length of the poles and the voltage at 1000 V. An example of the first type of study is given in figure 4.3-4.4.

Electrode	Conductive pole P1	Insulating Pole S	Conductive pole P2	Voltage	Diameter D
1	5.00 mm	3.00 mm	5.00 mm	1000 V	**1.40 mm**
2	5.00 mm	3.00 mm	5.00 mm	1000 V	**1.50 mm**
3	5.00 mm	3.00 mm	5.00 mm	1000 V	**1.60 mm**
4	5.00 mm	3.00 mm	5.00 mm	1000 V	**1.80 mm**
5	5.00 mm	3.00 mm	5.00 mm	1000 V	**2.00 mm**

Table 4.2 **Values for the first cycle of simulations (variable D).**

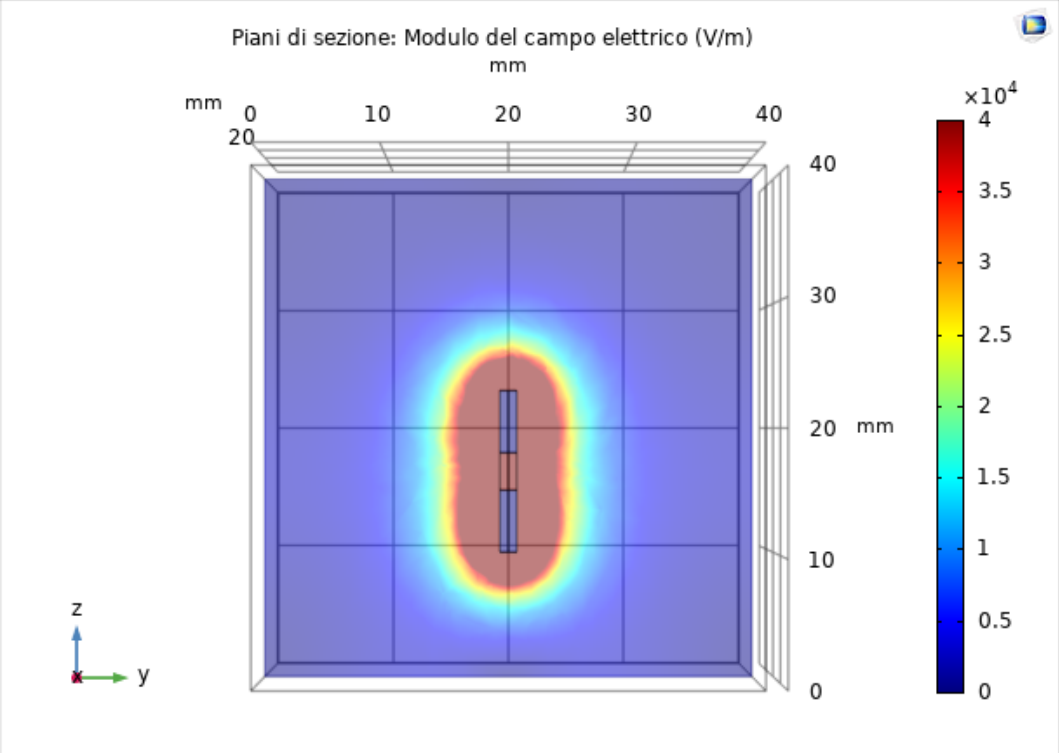

Figure 4.3 **First cycle of simulations - D=1.40 mm.** The sidebar expresses the amplitude of the electric field (V/m) around the electrode, from higher values (red) to lower values (blue).

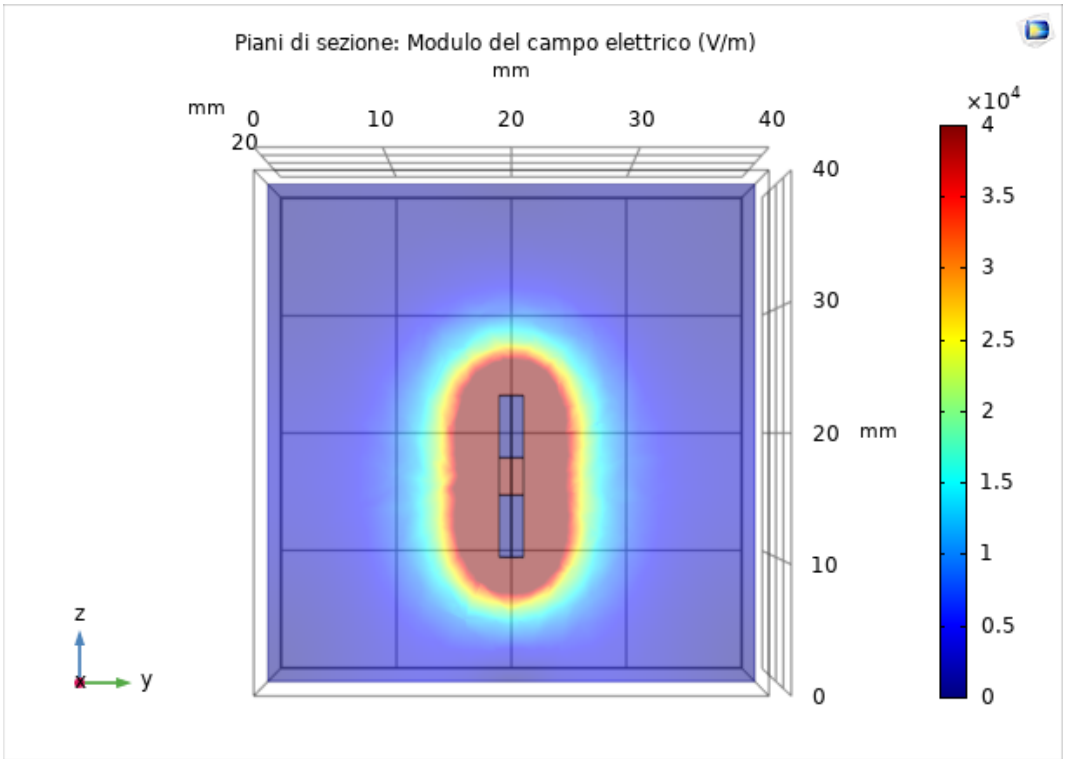

Figure 4.4 **First cycle of simulations - D=2.00 mm.** The sidebar expresses the amplitude of the electric field (V/m) around the electrode, from higher values (red) to lower values (blue).

The graph shows the values of the maximum diameters measured at the distal pole (P1), spacer (S) and proximal pole (P2) according to the section of the electrode. It is observed a minimal increase of the electric field measured at increasing the electrode diameter.

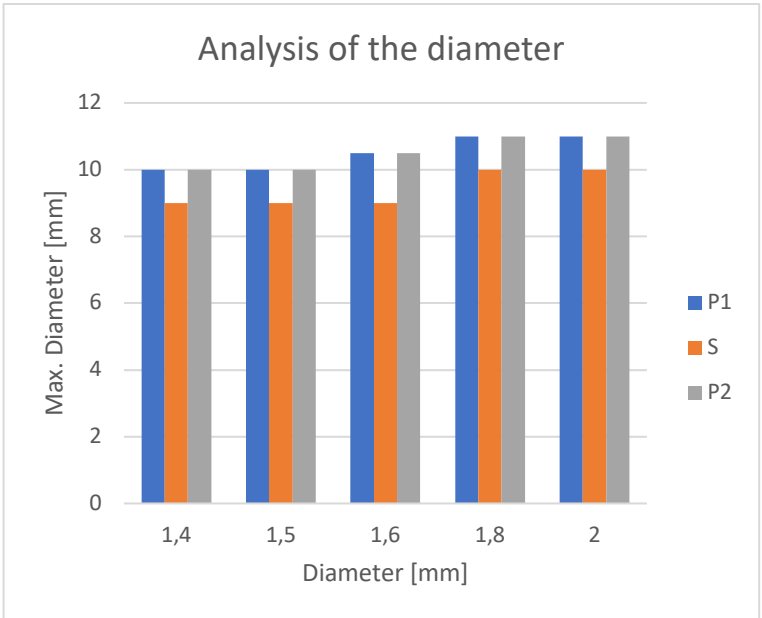

Figure 4.5 **Analysis of the diameter.** Values of the maximum diameters measured at the distal pole (P1), spacer (S) and proximal pole (P2) according to the section of the electrode.

One of the purposes of this electrode was to cover the tissue with a spherical volume electric field of about 1 cm in diameter. It has been shown, however, that the slight increase in the diameter of the device slightly varies the size of the electric field. Having seen the behaviour of the electric field around the electrode, it was decided to make new changes in values. It was decided to continue future simulations using the electrode of 1.40 mm ϕ, as we show that the diameter does not affect the electrical field size. The second cycle of simulations was conducted to study the influence of voltage applied on the electric field size. The table 4.3 shows the values used. An example of the second type of study is given in figure 4.6-4.7.

Electrode	Conductive pole P1	Insulating Pole S	Conductive pole P2	Voltage	Diameter D
1	5.00 mm	3.00 mm	5.00 mm	**500 V**	1.40 mm
2	5.00 mm	3.00 mm	5.00 mm	**1000 V**	1.40 mm
3	5.00 mm	3.00 mm	5.00 mm	**1500 V**	1.40 mm

Table 4.3 **Values for the second cycle of simulations (variable voltage applied).**

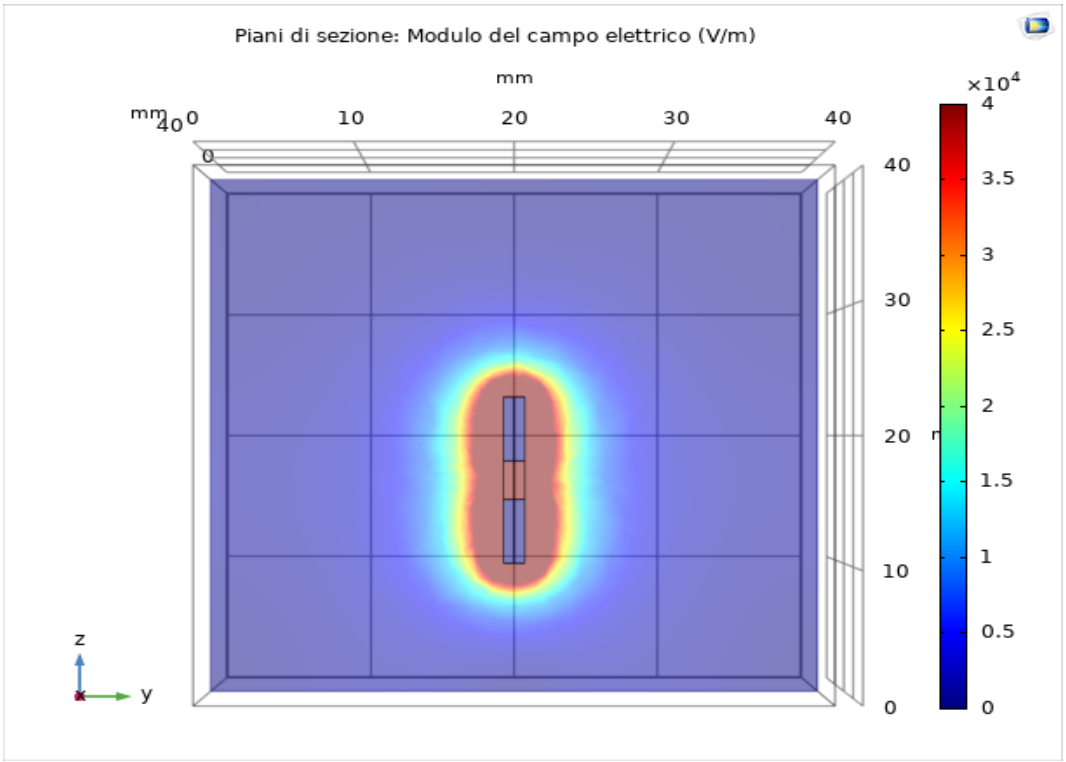

Figure 4.6 **Second cycle of simulations - 500 V.** The sidebar expresses the amplitude of the electric field (V/m) around the electrode, from higher values (red) to lower values (blue).

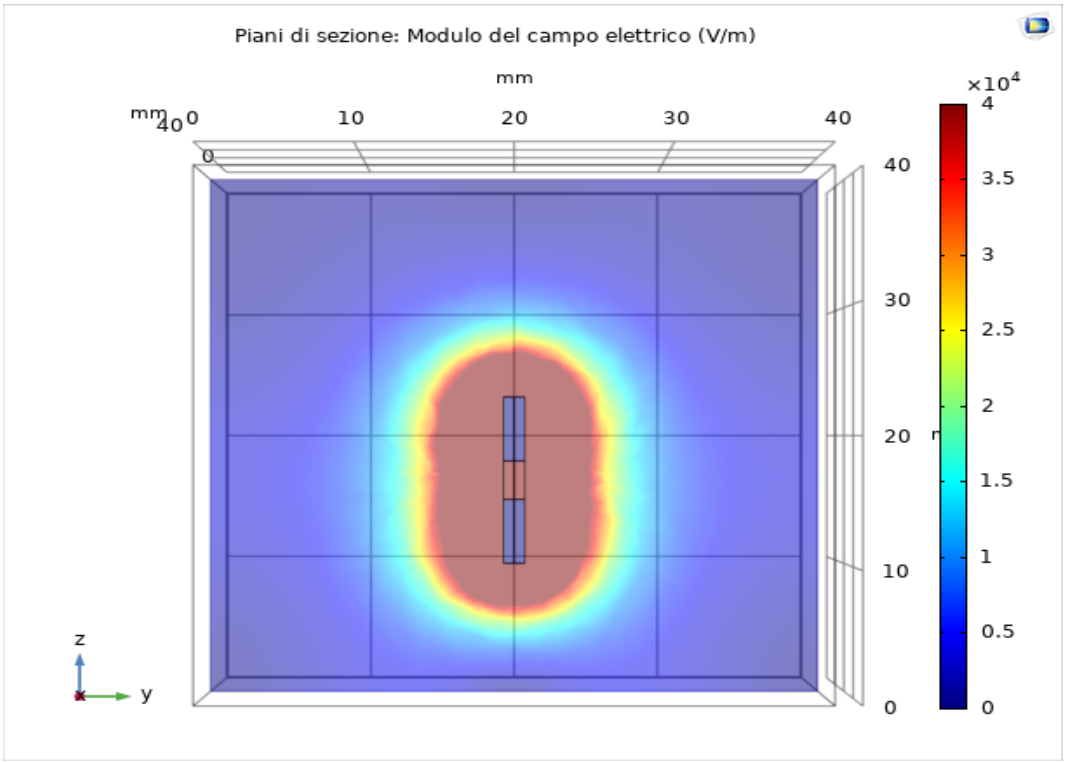

Figure 4.7 **Second cycle of simulations - 1500 V.** The sidebar expresses the amplitude of the electric field (V/m) around the electrode, from higher values (red) to lower values (blue).

The graph shows the values of the maximum diameters of the distal pole (P1), spacer (S) and proximal pole (P2) according to the voltage applied to the electrode.

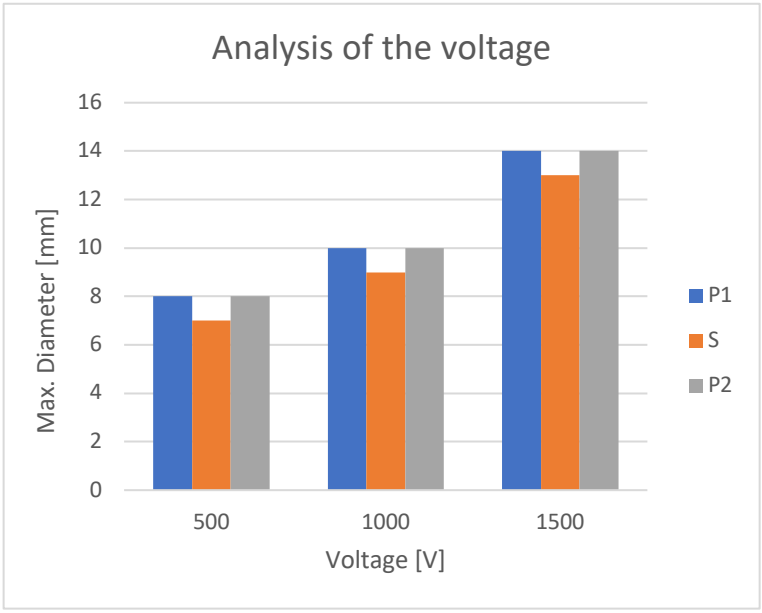

Figure 4.8 **Analysis of the voltage.** Values of the maximum diameters of the distal pole (P1), spacer (S) and proximal pole (P2) according to the voltage applied to the electrode.

The area covered by the electric field is greater than 1 cm in diameter.

We performed a new cycle of simulations, to see if increasing the length of the insulating pole, the width of electric field changes. From the simulations carried out above this area was covered only in case of voltage equal to 500 V. It was thought, however, to continue the simulations using higher voltages as 1000 V.

In this third simulation cycle we tested the effect of changing the length of the insulating pole, keeping constant the voltage applied. An example of the third type of study is given in figure 4.9-4.10.

Electrode	Conductive pole P1	Insulating Pole S	Conductive pole P2	Voltage	Diameter D
1	5.00 mm	**3.00 mm**	5.00 mm	1000 V	1.40 mm
2	5.00 mm	**5.00 mm**	5.00 mm	1000 V	1.40 mm
3	5.00 mm	**7.00 mm**	5.00 mm	1000 V	1.40 mm

Table 4.4 **Values for third cycle of simulations (variable S).**

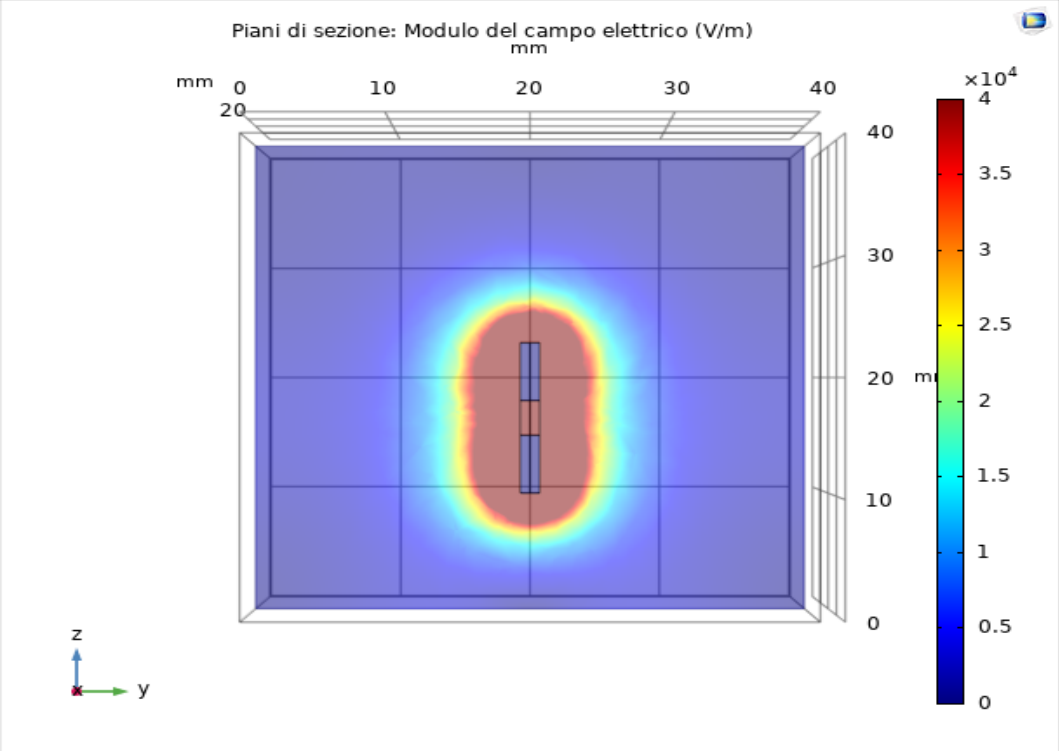

Figure 4.9 **Third cycle of simulations - S=3.00 mm.** The sidebar expresses the amplitude of the electric field (V/m) around the electrode, from higher values (red) to lower values (blue).

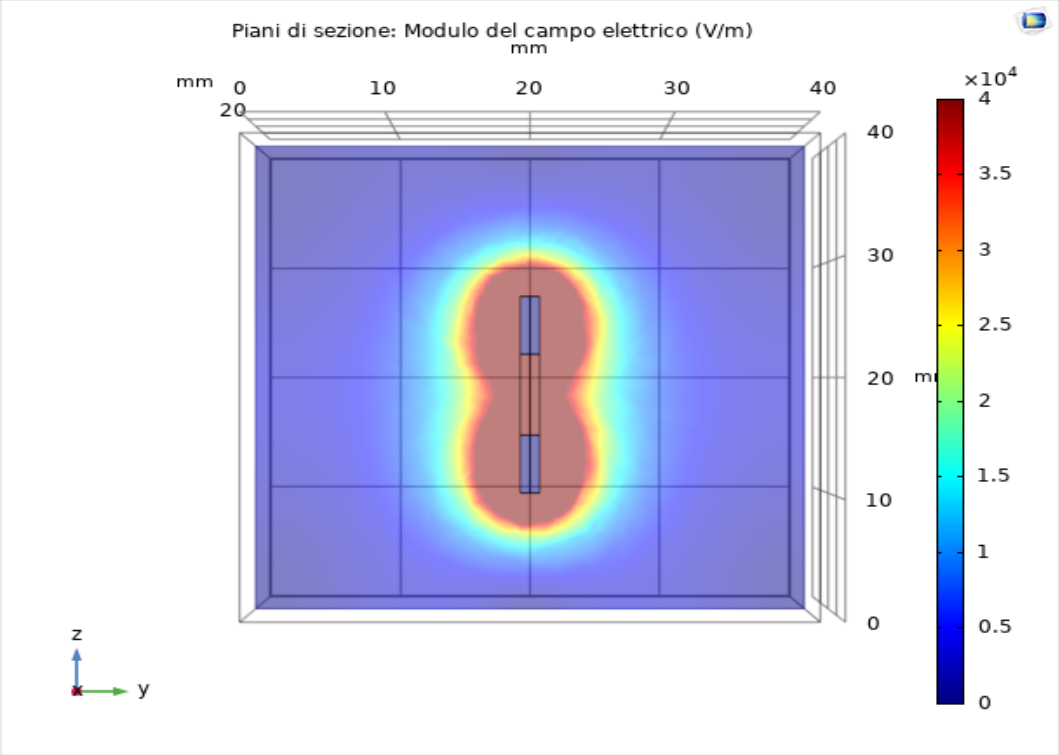

Figure 4.10 **Third cycle of simulations - S=7.00 mm.** The sidebar expresses the amplitude of the electric field (V/m) around the electrode, from higher values (red) to lower values (blue).

The graph shows the values of the maximum diameters of the distal pole (P1), spacer (S) and proximal pole (P2) according to the length of the insulating pole of the device.

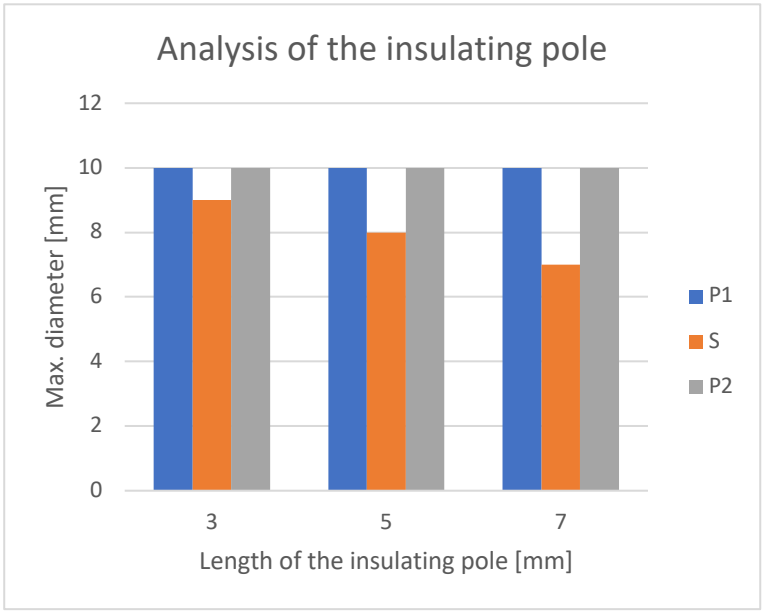

Figure 4.11 **Analysis of the insulating pole.** Values of the maximum diameters of the distal pole (P1), spacer (S) and proximal pole (P2) according to the length of the insulating pole of the device.

With this third cycle of simulations it has been evidenced that maintaining constant the diameter and the tension but varying only the length of insulating pole, the electric field does not vary along the y axis (for conductive poles) but along the major axis of the device, z axis. It was also pointed out that around the insulating pole, the greater its length the less will be the width of the electric field; in fact, it is possible to see a shape no longer regular around the pole.

In conclusion, another cycle of simulations was performed. In order to see how the electrical field varied according to some values, the length of the conductive poles has been varied. A voltage value of 1000 V, 1.40 mm diameter and 3.00 mm insulating pole length was always maintained. An example of the fourth type of study is given in figure 4.12-4.13.

Electrode	Conductive pole P1	Insulating Pole S	Conductive pole P2	Voltage	Diameter D
1	**3.00 mm**	3.00 mm	**3.00 mm**	1000 V	1.40 mm
2	**5.00 mm**	3.00 mm	**5.00 mm**	1000 V	1.40 mm
3	**10.00 mm**	3.00 mm	**10.00 mm**	1000 V	1.40 mm
4	**15.00 mm**	3.00 mm	**15.00 mm**	1000 V	1.40 mm

Table 4.5 **Values for fourth cycle of simulations (variable P1 and P2).**

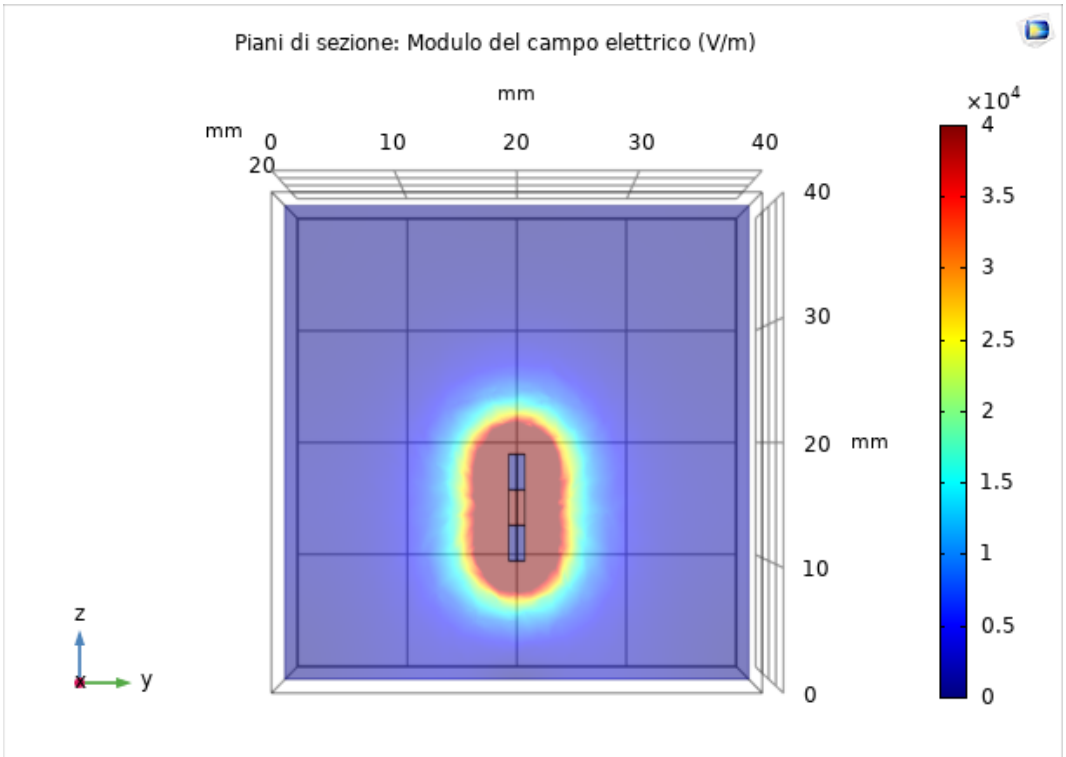

Figure 4.12 **Fourth cycle of simulations - P1 & P2=3.00 mm.** The sidebar expresses the amplitude of the electric field (V/m) around the electrode, from higher values (red) to lower values (blue).

In order to better visualize the electric field in the case of conductive poles with a length of 15.00 mm, the size of the parallelepiped had to be increased.

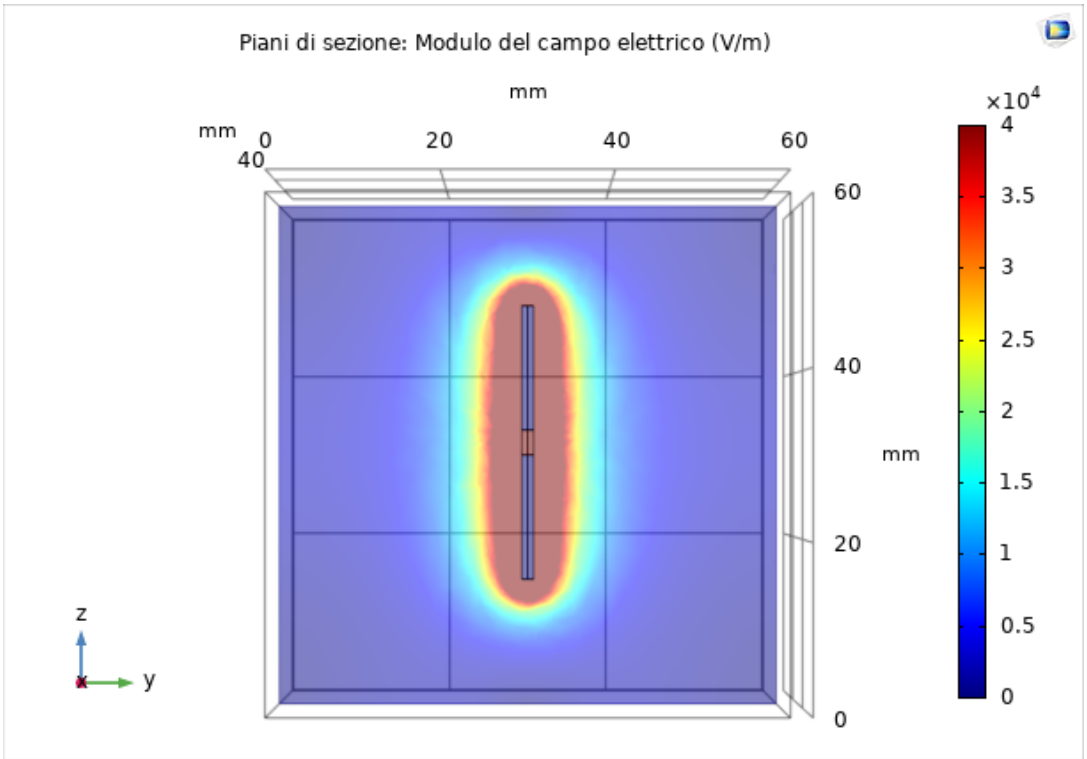

Figure 4.13 **Fourth cycle of simulations - P1 & P2=15.00 mm.** The sidebar expresses the amplitude of the electric field (V/m) around the electrode, from higher values (red) to lower values (blue).

The graph shows the values of the maximum diameters of the distal pole (P1), spacer (S) and proximal pole (P2) according to the length of the conductive pole of the device.

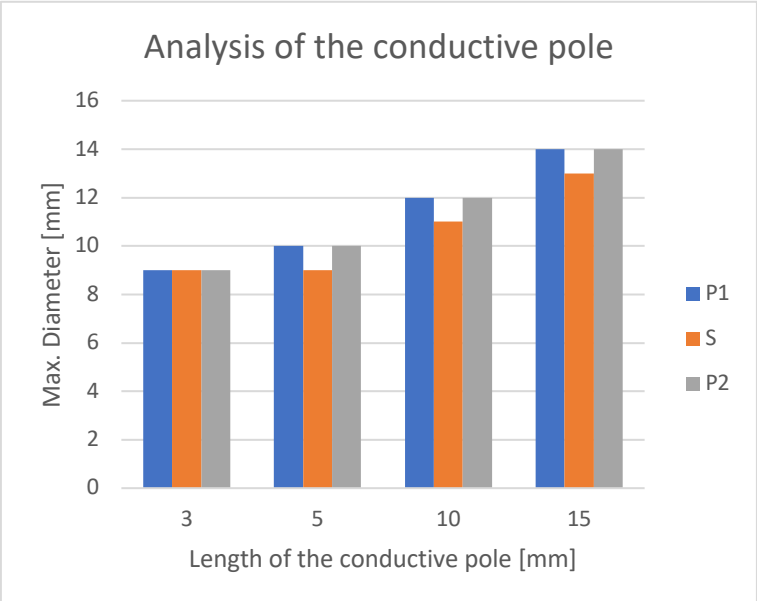

Figure 4.14 **Analysis of the conductive pole.** values of the maximum diameters of the distal pole (P1), spacer (S) and proximal pole (P2) according to the length of the conductive pole.

The conducted simulations show how the length of the conductive poles influences the electric field along the z axis, less evident is the expansion along the y axis, than even if slowly also along this axis is varied. This effect is also present at the insulating pole, which has been kept constant (3 mm). The total length of the electrode influences the electric field also around that insulating part although very slightly, being a length 3 mm very small compared to the total 30 mm of the conductive poles.

In conclusion, it can be noted that the electric field is mainly influenced by the length of the poles and the applied voltage. In particular, increasing the voltage applied shows high values of electric field along the y and z axis of the conductive pole area while increasing the length of the conductive poles leads to an electric field increasing along the axis z. The increase in length of the insulating spacer gives a less regular shape of the electric field.

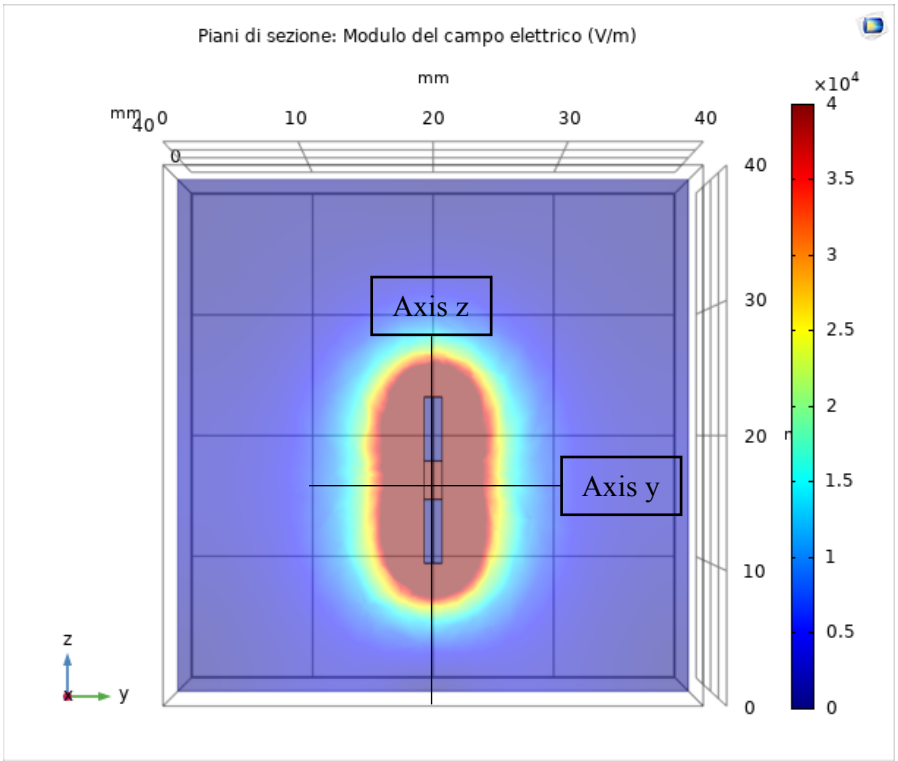

Figure 4.15 **An example of the results for symmetric geometry.**

Then, the same tests were conducted on asymmetric electrodes. In asymmetric geometry simulations, only the geometric values that were found to be of interest were used to conduct experiments.

4.3.2 Asymmetric geometry

The same study carried out for electrodes with symmetric geometry (conductive poles with same length) was also conducted for electrodes with asymmetric geometry (conductive poles with different length). In this case, the aim was to analyse more critical cases in order to limit the invasiveness of the electrode. Studies were carried out using 1.40 mm and 1.50 mm diameters, poles are of different lengths and different applied voltages. The tests were all conducted with a threshold of 400 V/cm. An example of the fifth type of study is given in figure 4.16-4.17.

Electrode	Conductive pole P1	Insulating Pole S	Conductive pole P2	Voltage	Diameter D
1	5.00 mm	3.00 mm	10.00 mm	**500 V**	1.40 mm
2	5.00 mm	3.00 mm	10.00 mm	**800 V**	1.40 mm

Table 4.6 **Values for fifth cycle of simulations (variable voltage applied).**

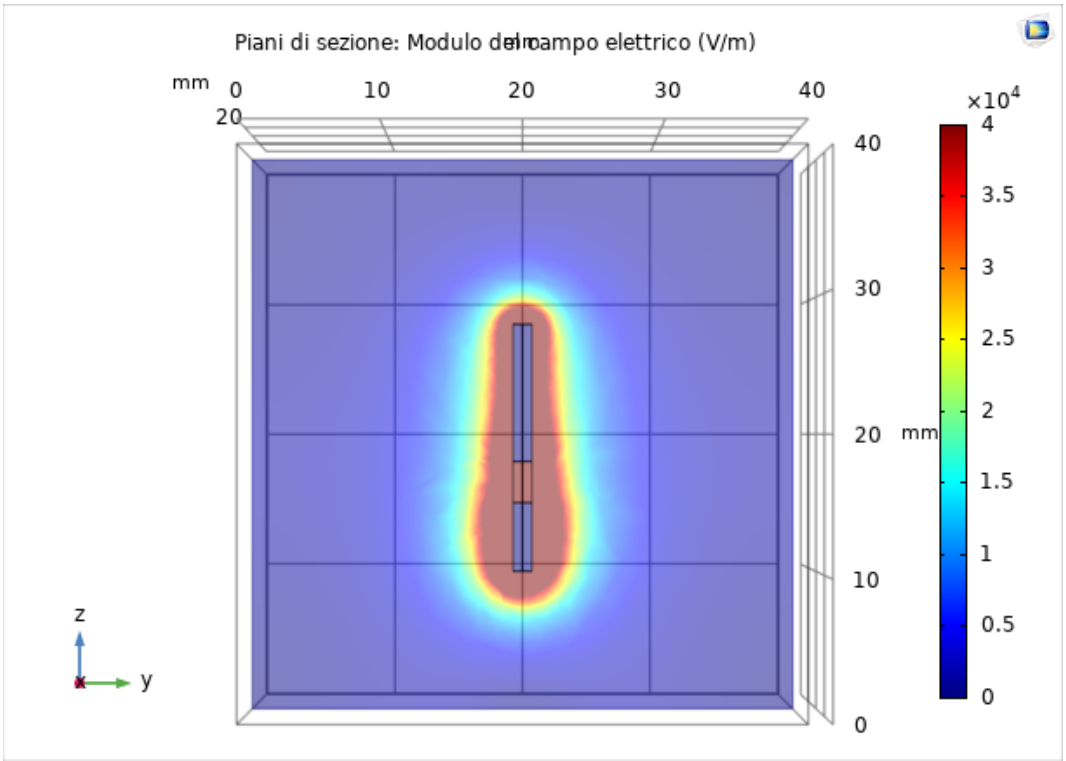

Figure 4.16 **Fifth cycle of simulations - V=500.** The sidebar expresses the amplitude of the electric field (V/m) around the electrode, from higher values (red) to lower values (blue).

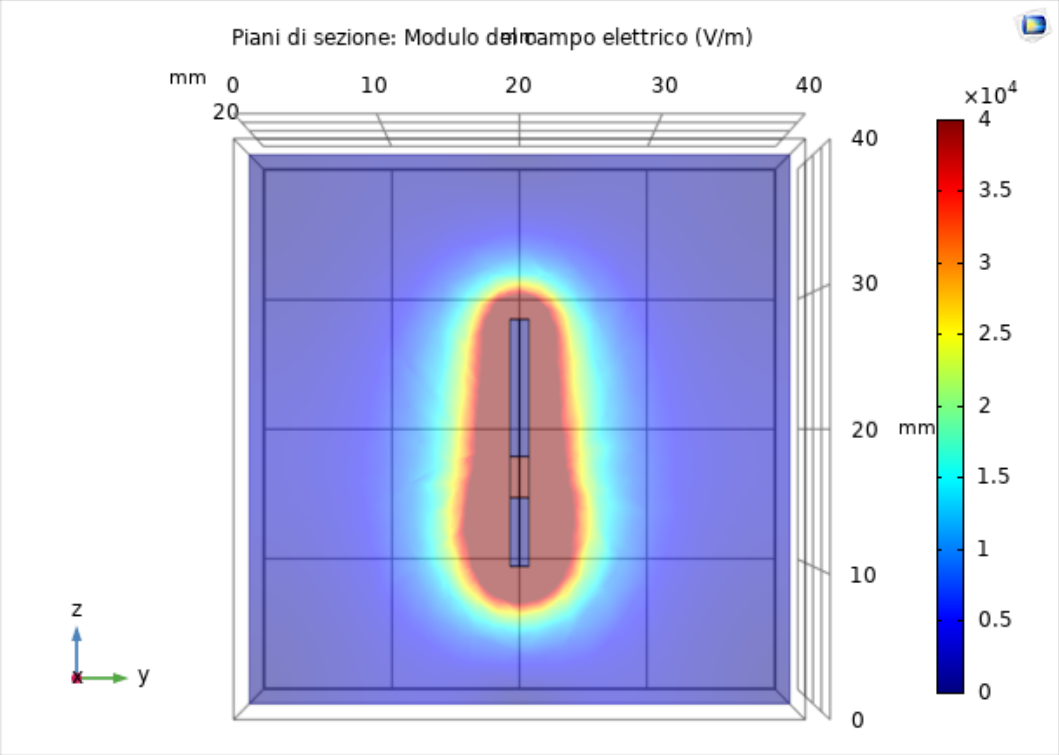

Figure 4.17 **Fifth cycle of simulations - V=800.** The sidebar expresses the amplitude of the electric field (V/m) around the electrode, from higher values (red) to lower values (blue).

The graph shows the values of the maximum diameters of the distal pole (P1), spacer (S) and proximal pole (P2) according to the voltage applied.

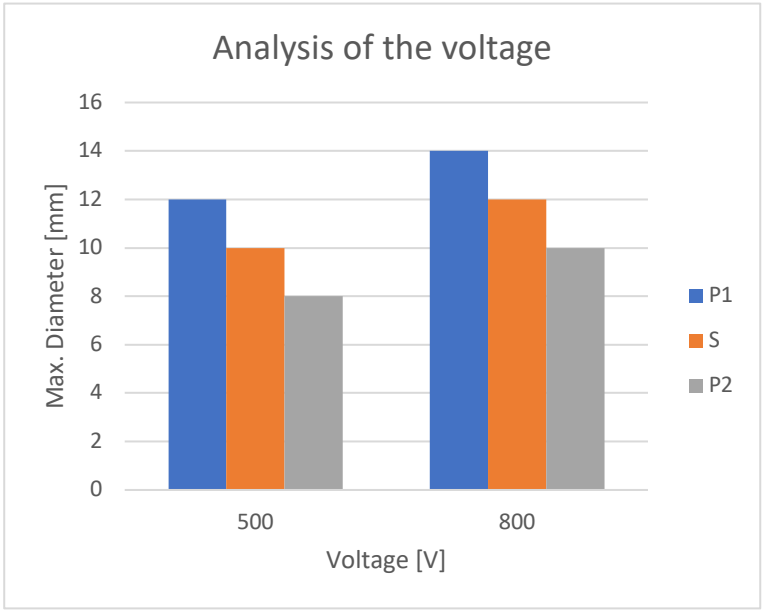

Figure 4.18 **Analysis of the voltage.** values of the maximum diameters of the distal pole (P1), spacer (S) and proximal pole (P2) according to the voltage applied.

The effect of the change of applied voltage is evident keeping constant poles length and electrode diameter, the electric field is higher at the long pole (P1) compared to the short one (P2).

The second cycle of simulations for asymmetric electrode, tested the effect of electrode diameter and of the amplitude of the applied electric field. Results of the simulations are given in figures 4.19-4.20-4.21-4.22.

Electrode	Conductive pole P1	Insulating Pole S	Conductive pole P2	Voltage	Diameter D
1	5.00 mm	3.00 mm	10.00 mm	**500 V**	**1.40 mm**
2	5.00 mm	3.00 mm	10.00 mm	**500 V**	**1.50 mm**
3	5.00 mm	3.00 mm	10.00 mm	**800 V**	**1.40 mm**
4	5.00 mm	3.00 mm	10.00 mm	**800 V**	**1.50 mm**

Table 4.7 **Values for sixth cycle of simulations (variable D).**

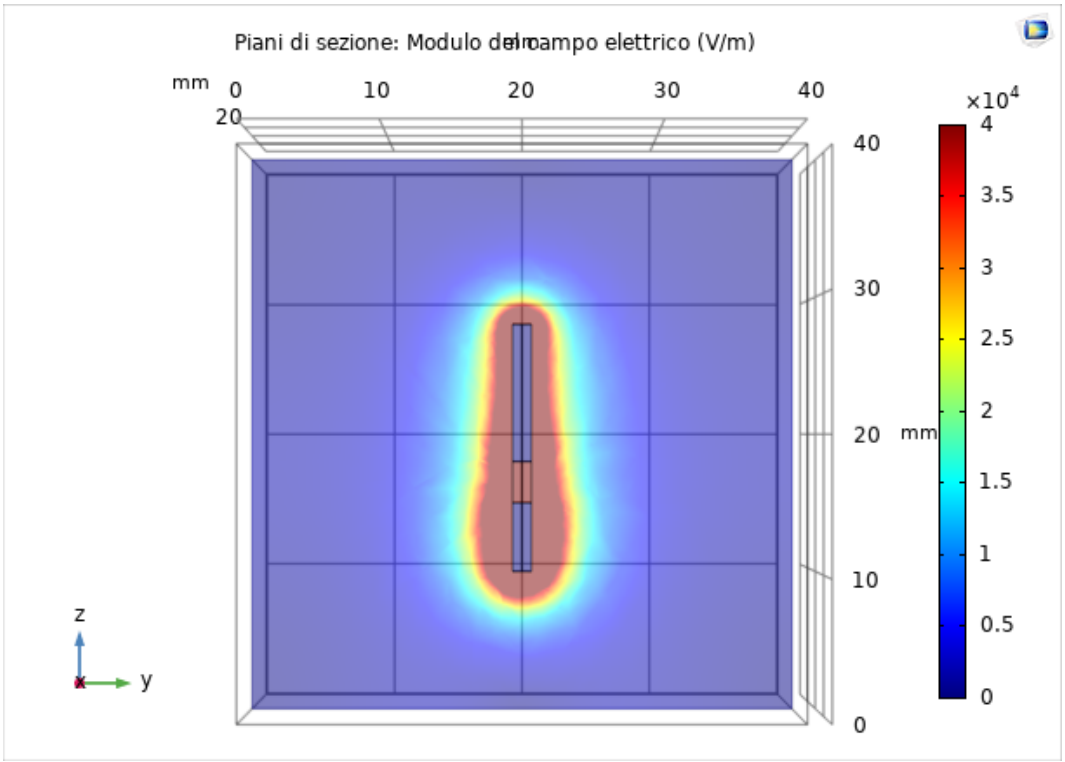

Figure 4.19 **Sixth cycle of simulations - D=1.40 mm & V=500V.** The sidebar expresses the intensity of the electric field (V/m) around the electrode, from higher values (red) to lower values (blue).

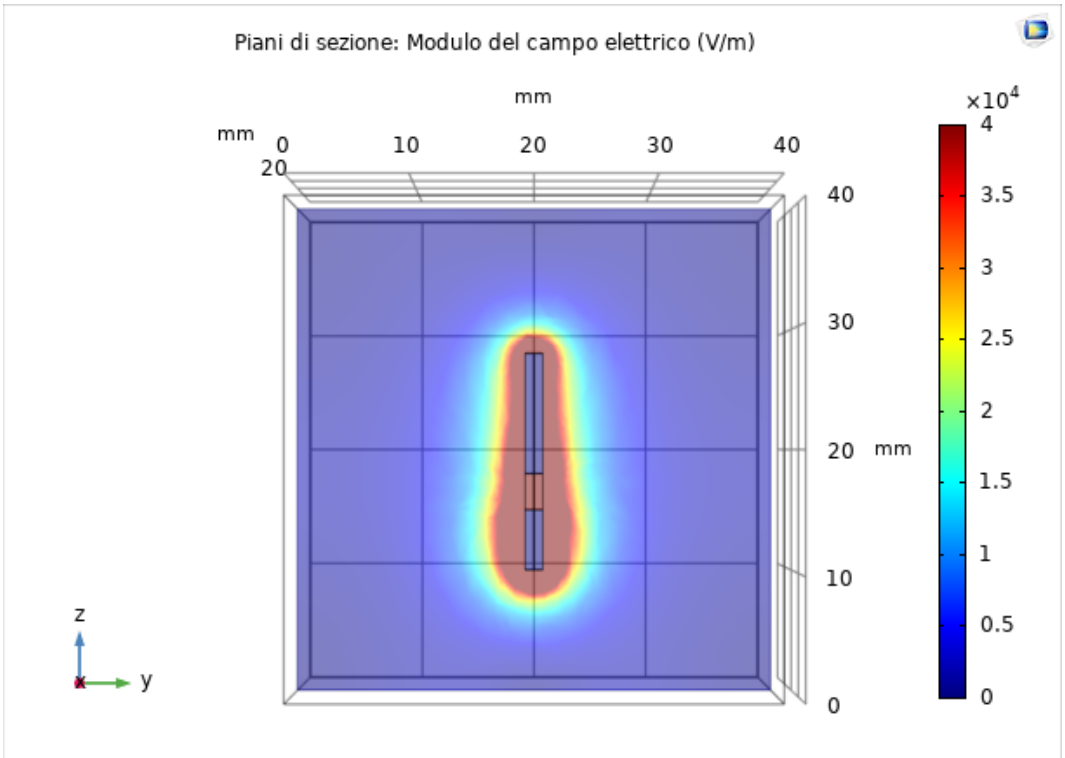

Figure 4.20 **Sixth cycle of simulations - D=1.50 mm & V=500 V.** The sidebar expresses the intensity of the electric field (V/m) around the electrode, from higher values (red) to lower values (blue).

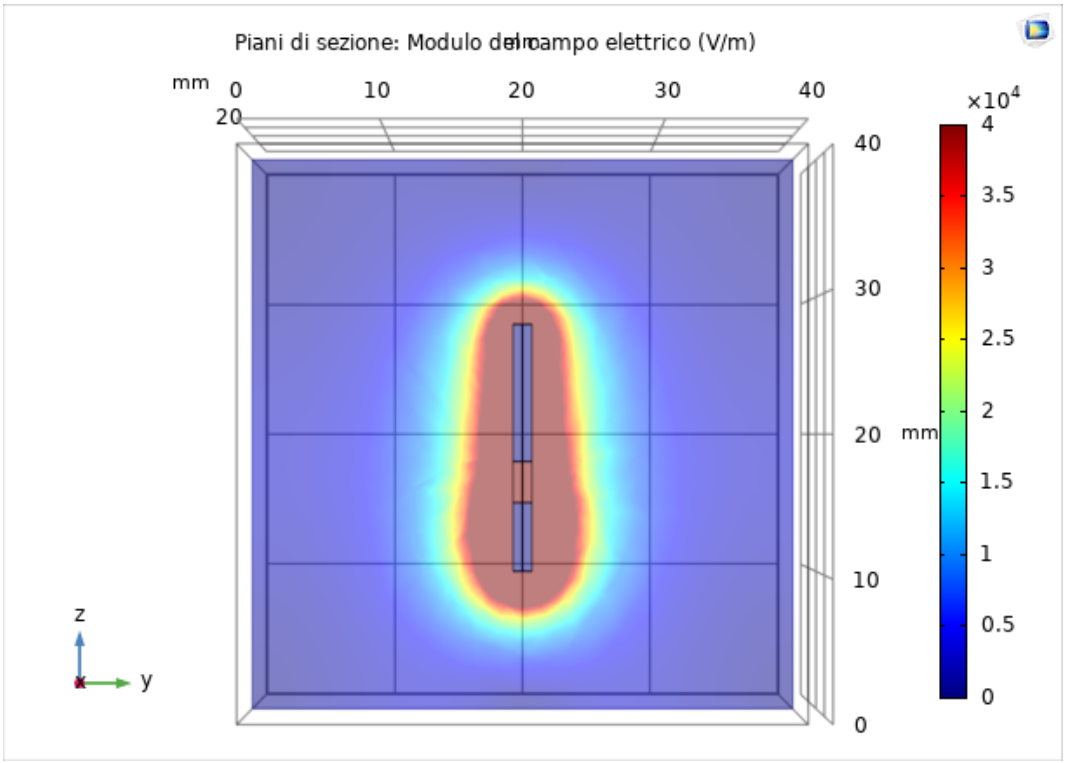

Figure 4.21 **Sixth cycle of simulations - D=1.40 mm & V=800 V.** The sidebar expresses the intensity of the electric field (V/m) around the electrode, from higher values (red) to lower values (blue).

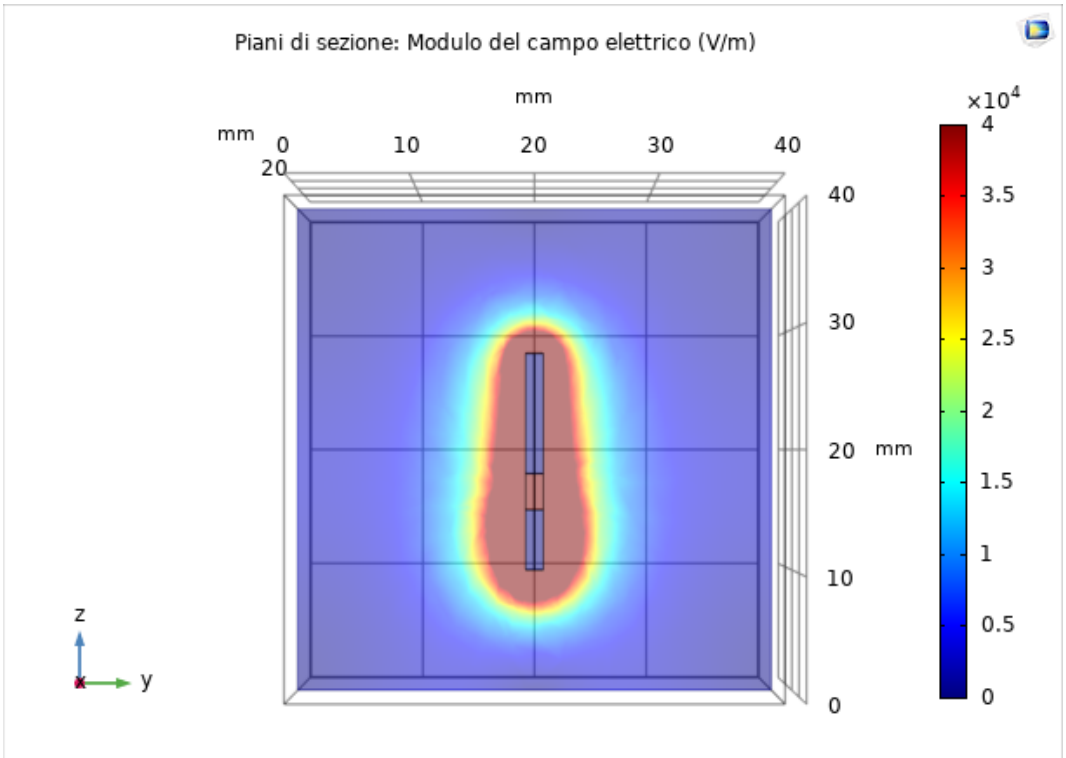

Figure 4.22 **Sixth cycle of simulations - D=1.50 mm & V=800 V.** The sidebar expresses the intensity of the electric field (V/m) around the electrode, from higher values (red) to lower values (blue).

The graph shows the values of the maximum diameters of the distal pole (P1), spacer (S) and proximal pole (P2) according to the voltage of the device, differentiating case diameter to 1.40 mm (the first one) and 1.50 mm (the second one).

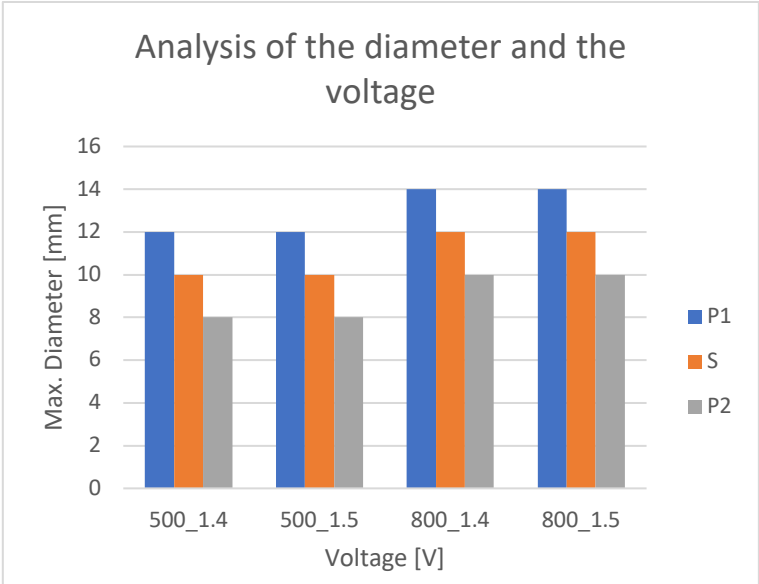

Figure 4.23 **Analysis of the diameter and the voltage.** Values of the maximum diameters of the distal pole (P1), spacer (S) and proximal pole (P2) according to the voltage of the device, differentiating case diameter to 1.40 mm (the first one) and 1.50 mm (the second one).

The same voltage applied to the different electrode diameter the extension of the electric field around the electrode is the same, as it was observed for symmetrical geometry simulations. Higher applied voltage leads to a larger are covered by the electric field. Then the effect of change in the length of the insulating pole was investigated, keeping the voltage constant and the electrode diameter of 1.40 mm. An example of the results is shown in figures 4.24-4.25.

Electrode	Conductive pole P1	Insulating Pole S	Conductive pole P2	Voltage	Diameter D
1	5.00 mm	**3.00 mm**	10.00 mm	500 V	1.40 mm
2	5.00 mm	**5.00 mm**	10.00 mm	500 V	1.40 mm

Table 4.8 **Values for seventh cycle of simulations (variable S).**

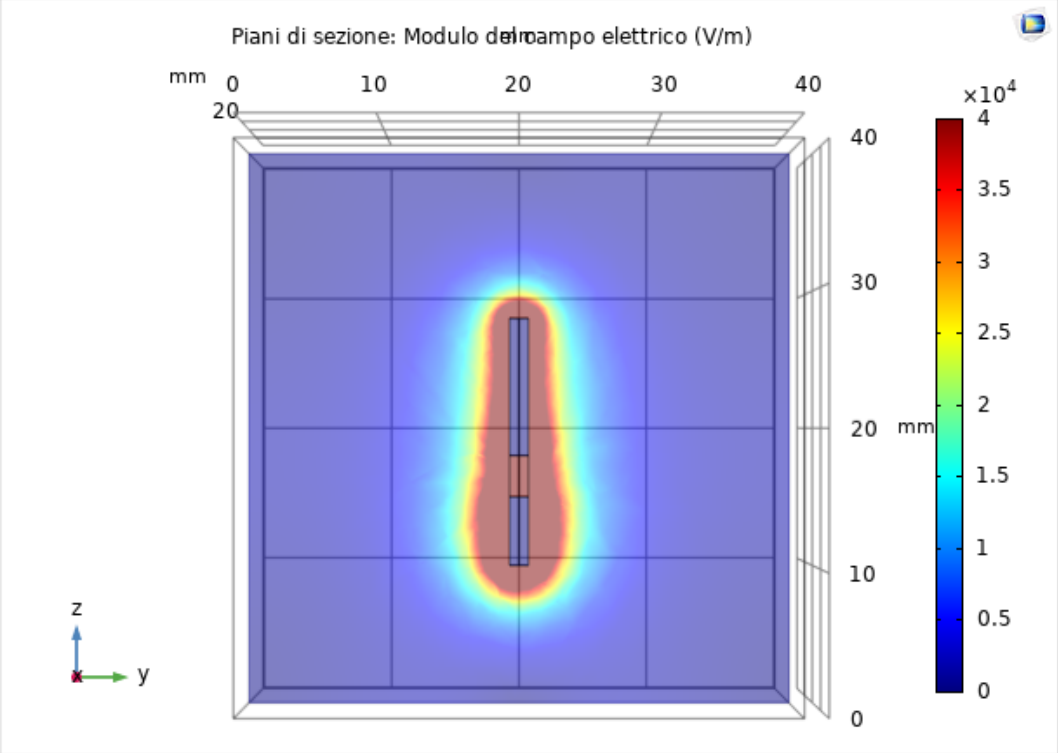

Figure 4.24 **Seventh cycle of simulations - S=3 mm.** The sidebar expresses the intensity of the electric field (V/m) around the electrode, from higher values (red) to lower values (blue).

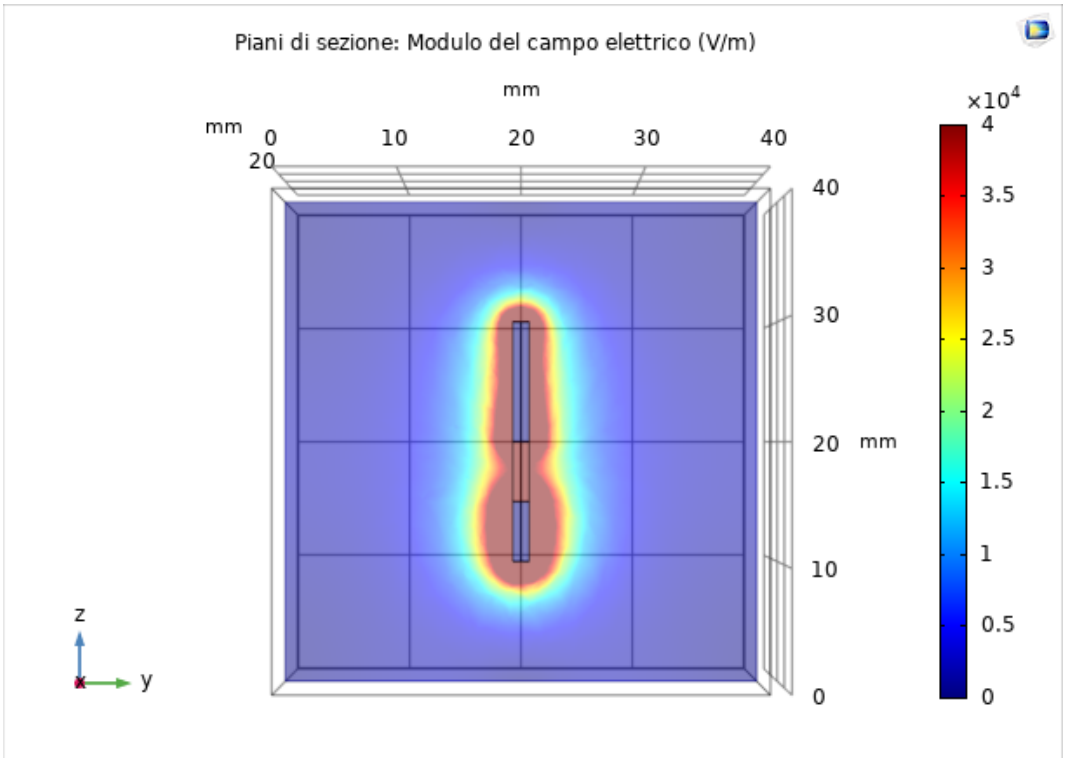

Figure 4.25 **Seventh cycle of simulations - S=5 mm.** The sidebar expresses the intensity of the electric field (V/m) around the electrode, from higher values (red) to lower values (blue).

The graph shows the values of the maximum diameters of the distal pole (P1), spacer (S) and proximal pole (P2) according to the length of the insulating pole.

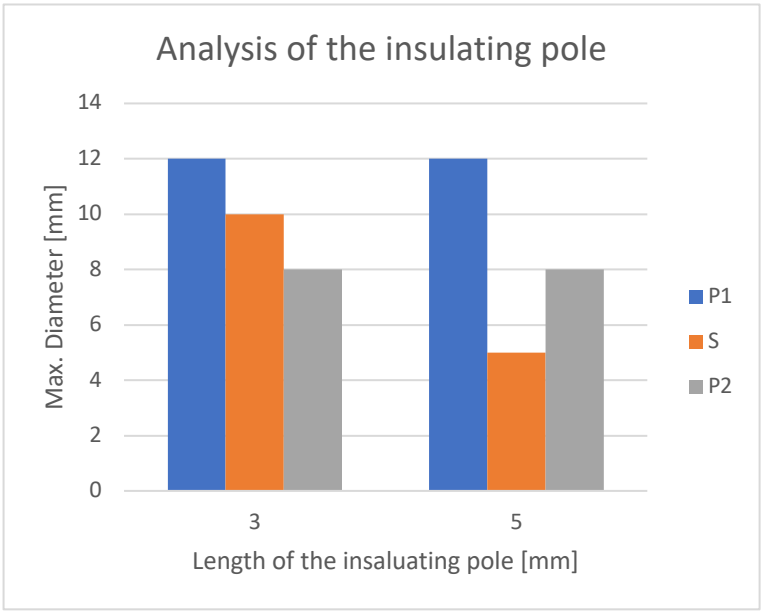

Figure 4.26 **Analysis of the insulating pole.** Values of the maximum diameters of the distal pole (P1), spacer (S) and proximal pole (P2) according to the length of the insulating pole.

This new simulation cycle shows that increasing the length of the insulating spacer decreases the electrical field around it. The red zone in the above figure (between 35000 V/m and 40000 V/m) is smaller for longer lengths. The last simulation cycle was carried out by varying the length of the conductive poles only, keeping the voltage and diameter constant. Results are shown in figure 4.27-4.28-4.29-4.30-4.31-4.32-4.33-4.34.

Electrode	Conductive pole P1	Insulating Pole S	Conductive pole P2	Voltage	Diameter D
1	**20.00 mm**	3.00 mm	**5.00 mm**	500 V	1.40 mm
2	**15.00 mm**	3.00 mm	**5.00 mm**	500 V	1.40 mm
3	**10.00 mm**	3.00 mm	**5.00 mm**	500 V	1.40 mm
4	**10.00 mm**	3.00 mm	**3.00 mm**	500 V	1.40 mm
5	**5.00 mm**	3.00 mm	**20.00 mm**	500 V	1.40 mm
6	**5.00 mm**	3.00 mm	**15.00 mm**	500 V	1.40 mm
7	**5.00 mm**	3.00 mm	**10.00 mm**	500 V	1.40 mm
8	**3.00 mm**	3.00 mm	**10.00 mm**	500 V	1.40 mm

Table 4.9 **Values for eighth cycle of simulations (variable P1 and P2).**

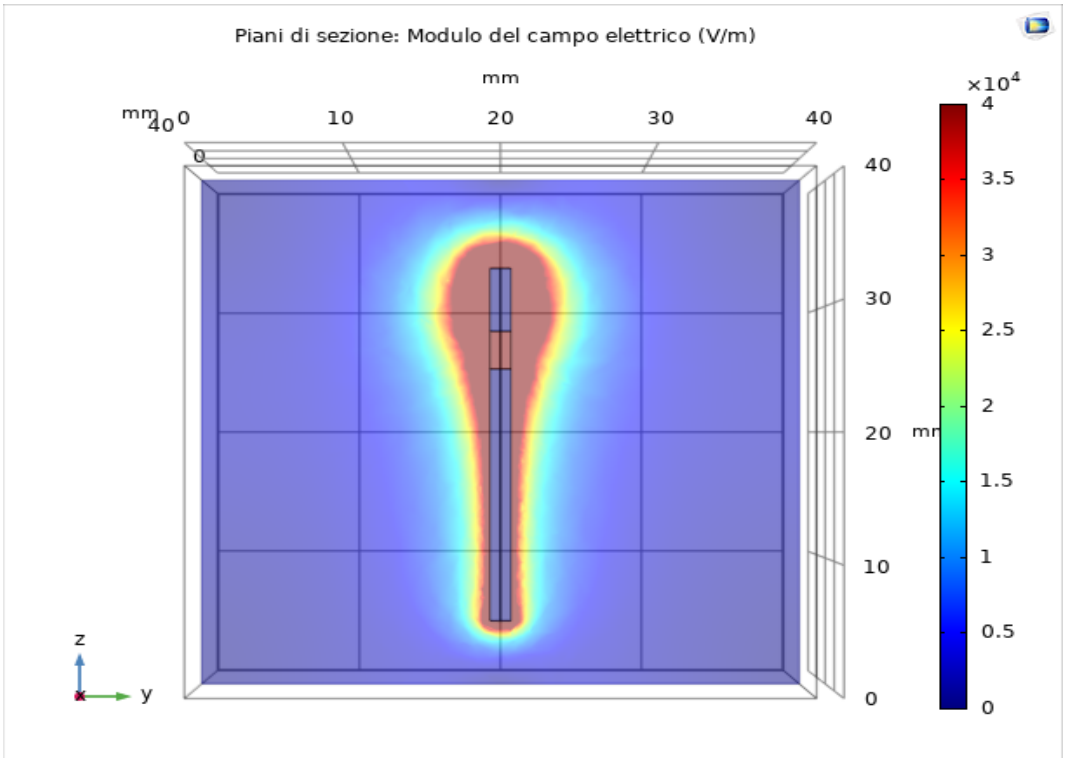

Figure 4.27 **Eighth cycle of simulations - P1=20.00 mm & P2=5.00 mm.** The sidebar expresses the intensity of the electric field (V/m) around the electrode, from higher values (red) to lower values (blue).

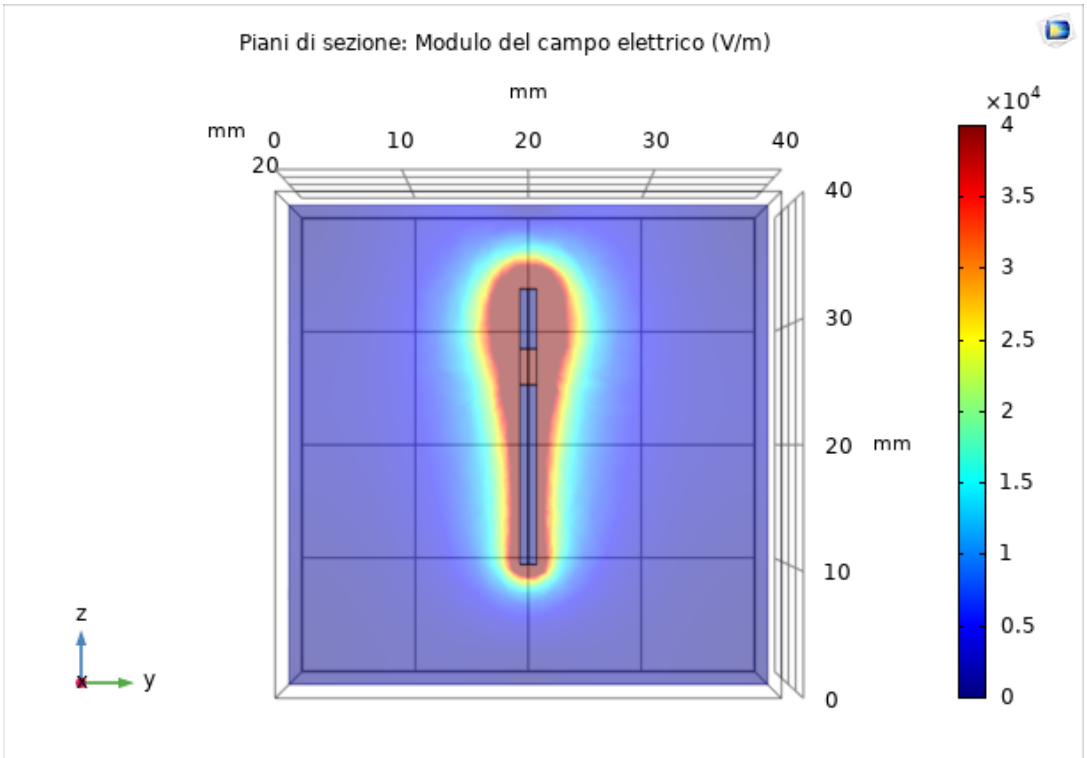

Figure 4.28 **Eighth cycle of simulations - P1=15.00 mm & P2=5.00 mm.** The sidebar expresses the intensity of the electric field (V/m) around the electrode, from higher values (red) to lower values (blue).

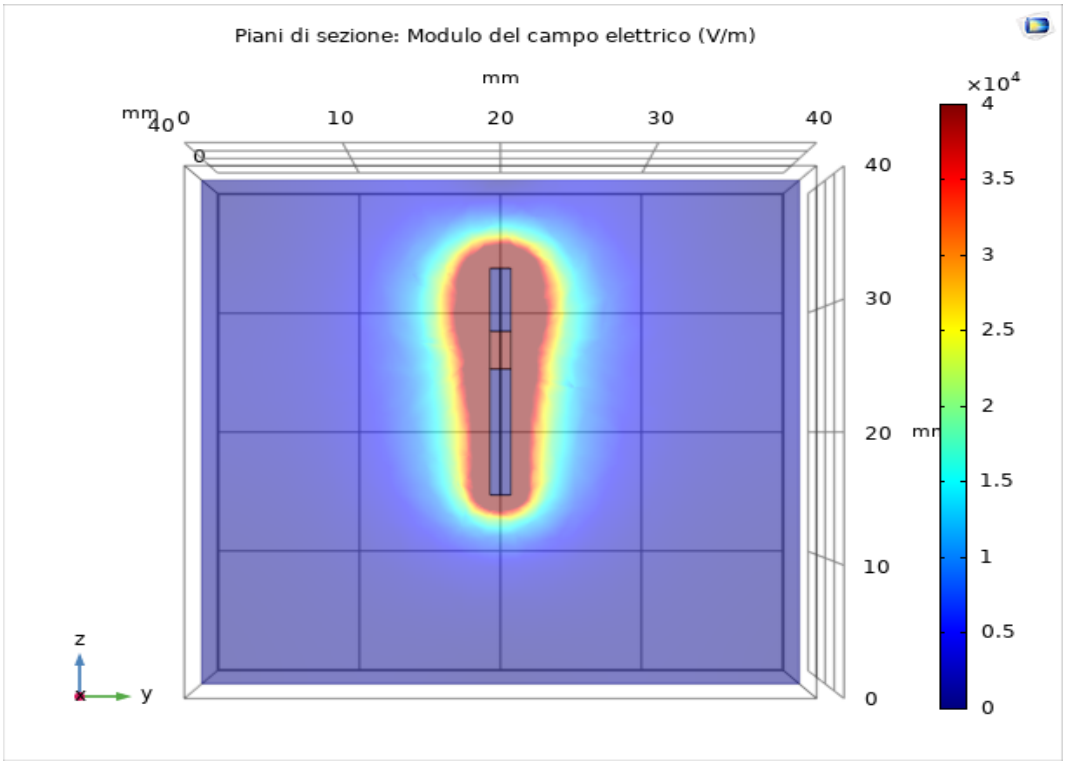

Figure 4.29 **Eighth cycle of simulations - P1=10.00 mm & P2=5.00 mm.** The sidebar expresses the intensity of the electric field (V/m) around the electrode, from higher values (red) to lower values (blue).

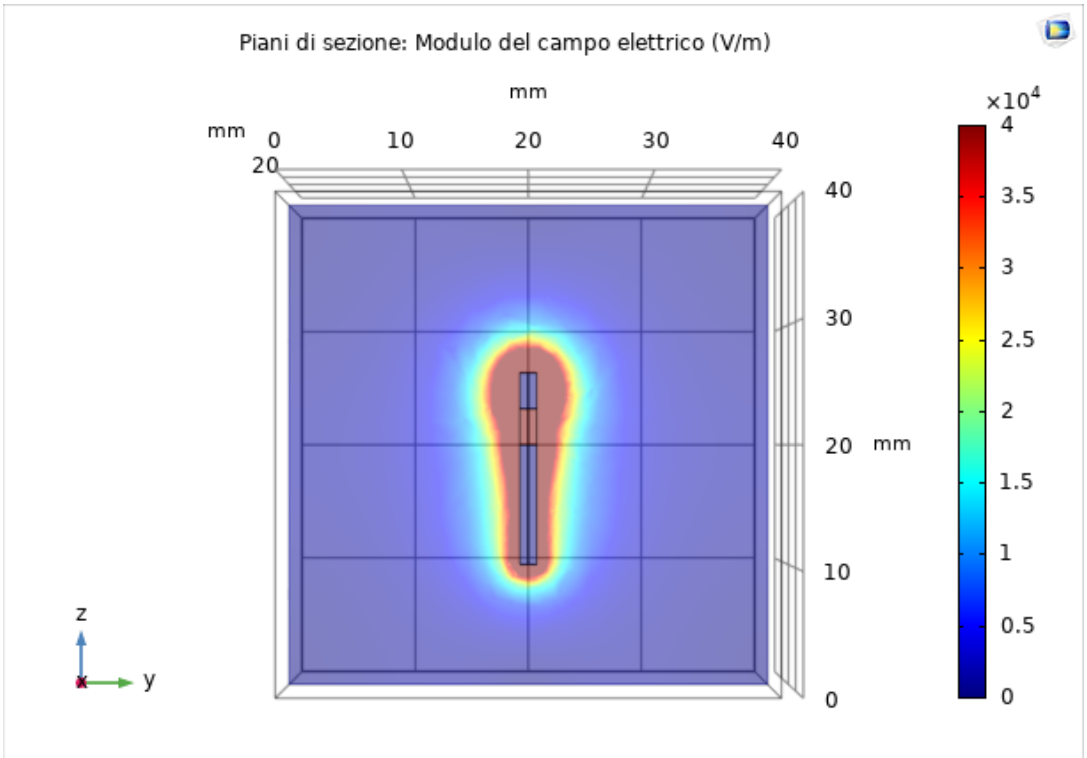

Figure 4.30 **Eighth cycle of simulations - P1=10.00 mm & P2=3.00 mm.** The sidebar expresses the intensity of the electric field (V/m) around the electrode, from higher values (red) to lower values (blue).

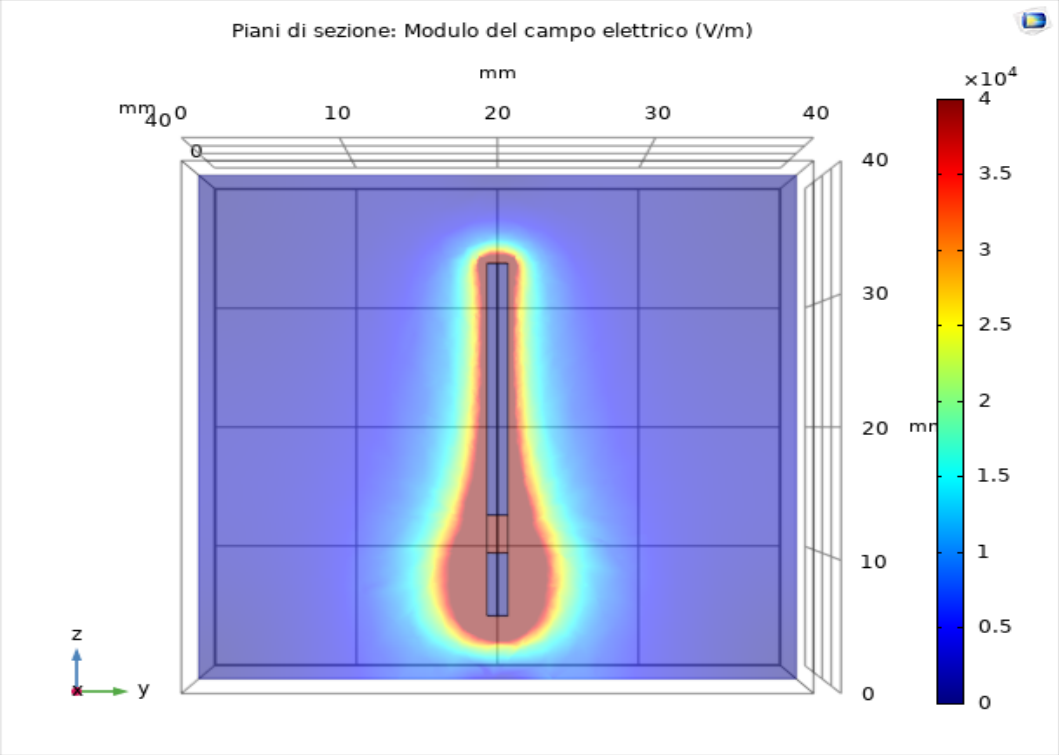

Figure 4.31 **Eighth cycle of simulations – P1=5.00 mm & P2=20.00 mm.** The sidebar expresses the intensity of the electric field (V/m) around the electrode, from higher values (red) to lower values (blue).

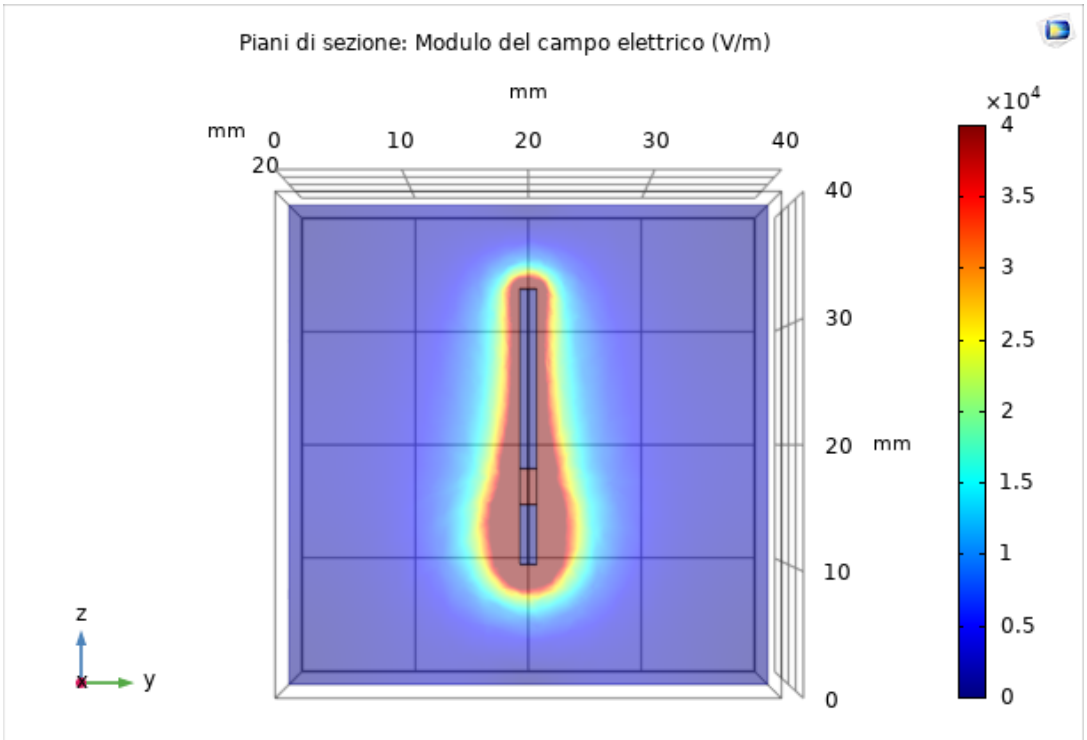

Figure 4.32 **Eighth cycle of simulations - P1=5.00 mm & P2=15.00 mm.** The sidebar expresses the intensity of the electric field (V/m) around the electrode, from higher values (red) to lower values (blue).

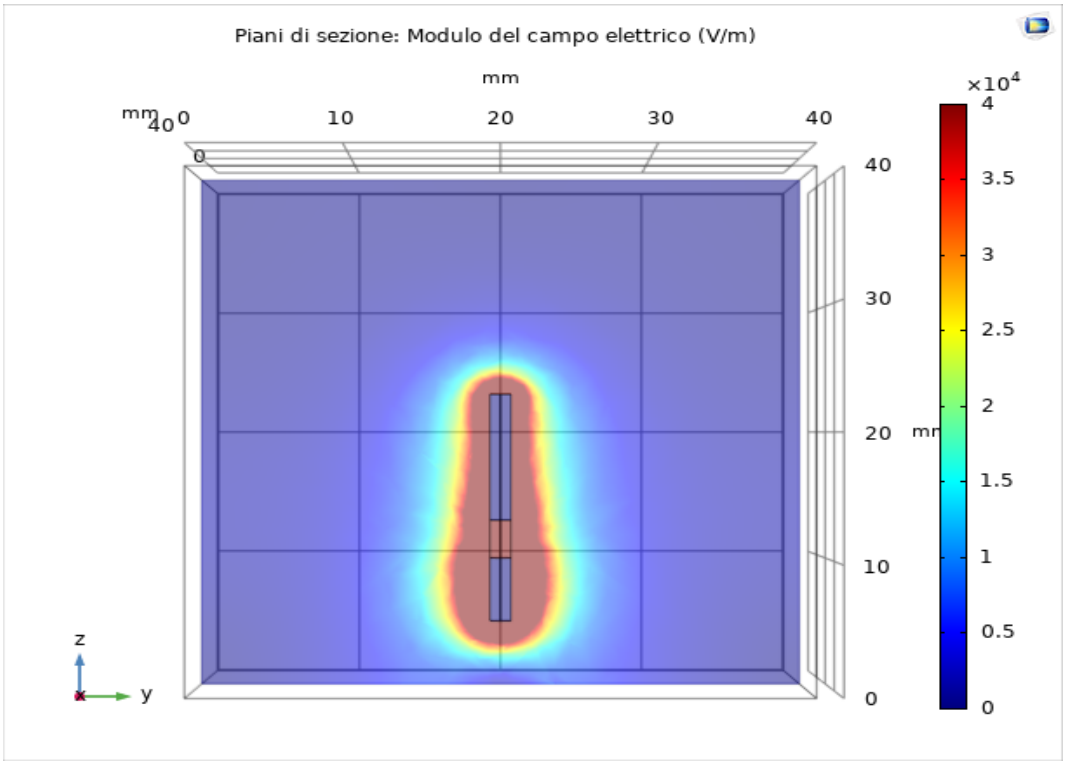

Figure 4.33 **Eighth cycle of simulations - P1=5.00 mm & P2=10.00 mm.** The sidebar expresses the intensity of the electric field (V/m) around the electrode, from higher values (red) to lower values (blue).

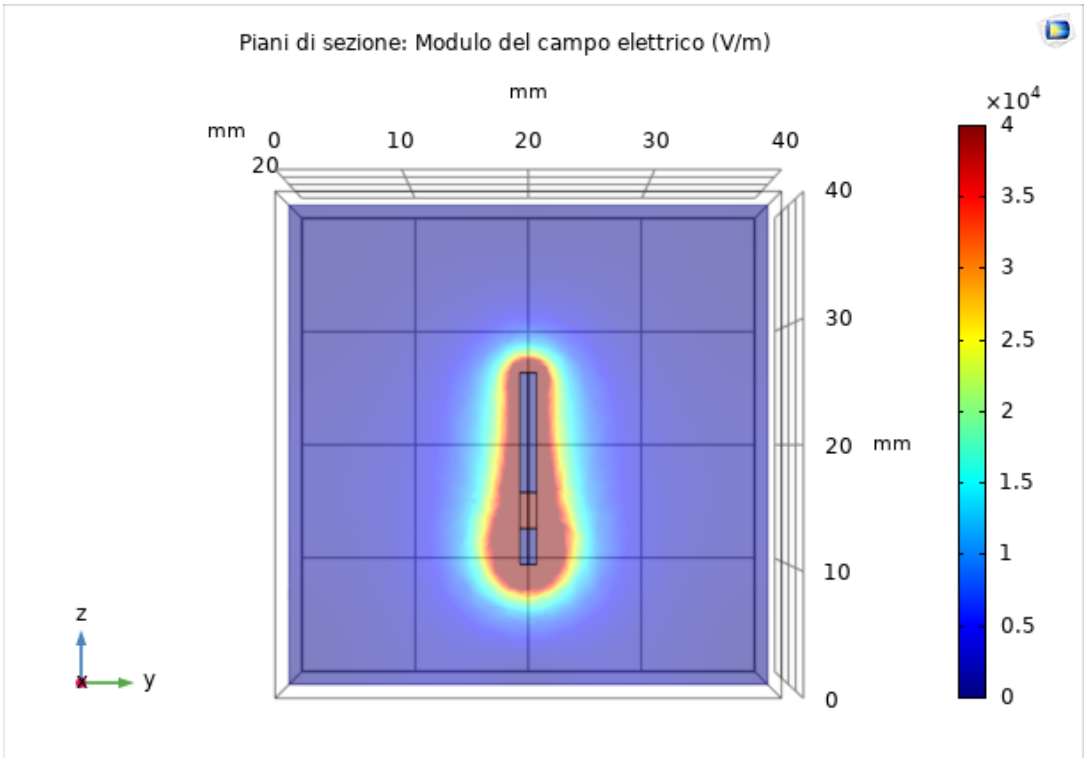

Figure 4.34 **Eighth cycle of simulations - P1=3.00 mm & P2=10.00 mm.** The sidebar expresses the intensity of the electric field (V/m) around the electrode, from higher values (red) to lower values (blue).

The graph shows the values of the maximum diameters of the electric field of the distal pole (P1), spacer (S) and proximal pole (P2) according to the total length of the poles.

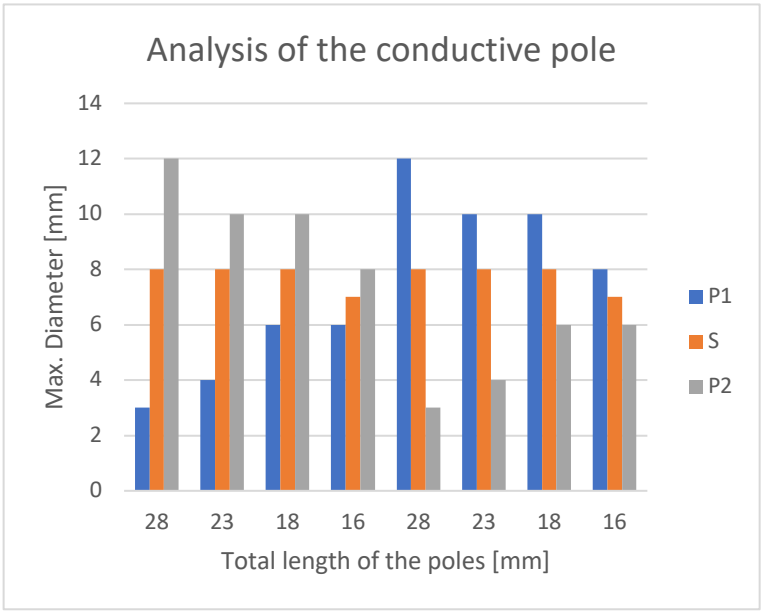

Figure 4.35 **Analysis of the conductive pole.** values of the maximum diameters of the electric field of the distal pole (P1), spacer (S) and proximal pole (P2) according to the total length of the poles.

The last cycle of simulations confirmed previous results, keeping constant diameter and voltages but changing the length of the poles, the electric field zones change with greater values, particularly along the major axis of the electrode (z-axis). With the last simulations carried out, it was also possible to analyse the reversal of the poles. Results show that the field will be always greater around the shorter pole compare to the long one, whether it is proximal or distal.

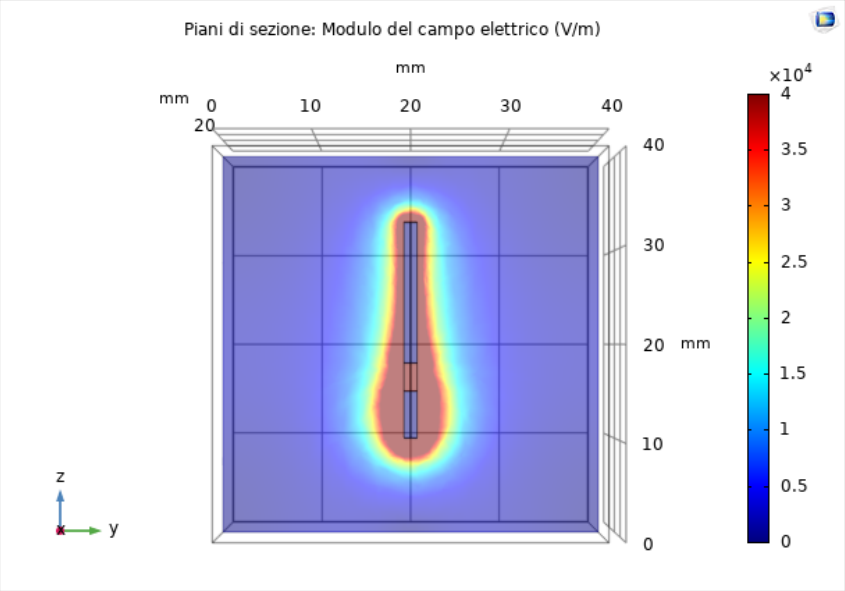

Figure 4.36 **An example of the results for asymmetric geometry.**

4.3.3 Conclusions

A number of conclusions could be drawn from these simulation cycles on *Comsol Multiphysics*® for both cases (symmetric and asymmetric geometry of the electrode).

The simulations carried out in the two previous sections allow to understand which parameters most influenced the electric field shape and therefore the dimensions of the tissue volume that can be treated around the electrode.

In conclusion the fundamental parameters are:

1. the applied voltage (*second and five cycle of simulations*) is the parameter that influences the maximum diameter of the electric field, and allows to electroporate the larger volume around the electrode;

2. the length of the conductive poles and insulating spacer (*third, four, seven and eight cycle of simulations*), generate a greater electric field along the main axis of the electrode;
3. the length of the insulating spacer (*third and seven cycle of simulations*) allows to obtain a form of the electric field less "regular" as the increase of its length results in a decrease in the diameter of the electric field diameter around it;
4. in the case of electrodes with asymmetric geometry (*eight cycle of simulation*), the electroporate volume will be greater around the conductive pole with shorter length.

4.4 Prototype design

Once the preliminary tests had been carried out in *Comsol Multiphysics* ® it was possible to decide to create the first prototypes in order to investigate and verify the device qualitatively. Thanks to the study carried out with *Comsol Multiphysics* ® it was possible to start a design phase to create the prototypes of the electrode with parameters aligned to those of the theoretical model for use on vegetable and animal model. As mentioned in the previous sections, one of the main objectives of this work was to minimize the invasiveness of the device. In this case, the geometry of the prototype will be different from the simulations but it will be like in the figure 4.37.

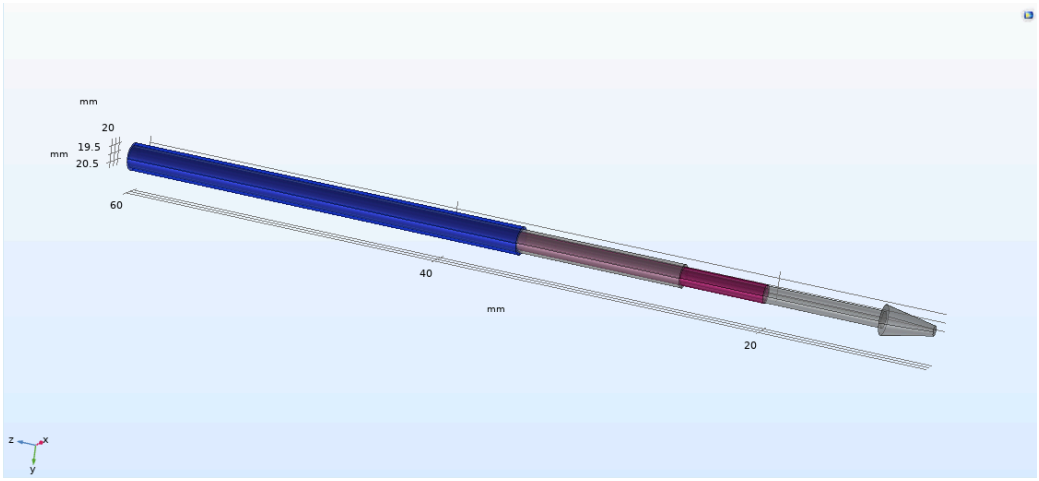

Figure 4.37 **Real electrode.** Real structure of the electrode in *Comsol Multiphysics* ®.

Among the studied diameters it was thought to continue the study and the creation of electrodes with diameter of 1.4 mm. As mentioned in the previous sections, it was possible to choose such a small diameter because it was decided to test in organs such as the liver. The company was then asked to investigate the creation of a stainless-steel mandrel, how much greater the reduction in diameter from 1.4 mm could be, a 0.8 mm reduction has been achieved. And so, the steel tube and the polyamide tubes to create the concentric structure were studied. The aim of achieving the greatest possible reduction was to create this structure of electrode that could contain alternating insulating and conductive tubes without creating any positive step. These concentric tubes had to be such as to reach a maximum diameter of 1.4 mm because having protrusions (positive step) of the tubes involved entry problems and a larger diameter of the hole in the treated tissue.

The first decision was to take a mandrel with an external diameter of 1.40 mm and a diameter reduction of 0.83 mm with a tolerance of +/- 0.02 mm. When the mandrel with its respective diameter reduction was achieved, it was possible to study the tube of insulating material to be inserted above.

One of the main characteristics of the insulated sheath between the two conductive poles was the greatest possible thickness to be able to isolate them during the application of a very high voltage (with the maximum functional objective of voltage of 3000 V) as that required for cell membrane electroporation. In the technical sheets of the insulating tube considered for the realization it was also considered that they could have a high dielectric strength due to the high values of the electroporation used. In fact, the chosen material was the polyimide that had a dielectric strength of 4000/0.001". The study of the external and internal diameters of the first insulating sheath had to be interlocked with the tube. Being a first prototype, it has been decided to use tubes already available, combining these electrical and commercial requirements (also thanks to the time availability of material in IGEA). In the table 4.12 are reported the characteristics of the geometry of the prototype.

	Outside Diameter (OD)	Inside Diameter (ID)	Wall Thickness
Stainless Steel mandrel	1.4 +/0.02 mm	0.83 +/- 0.02 mm	-
First insulating sheath	0.9144 mm	0.8636 +/- 0.010 mm	0.0254 +/- 0.0064 mm
Second conductive pole	1.15 +/- 0.02 mm	0.95 +/- 0.02 mm	-
Secondo insulating sheath	1.3843 mm	1.1938 +/- 0.013 mm	0.0953 + /- 0.0239 mm

Table 4.10 **Measurements of the prototype.**

The first prototype of a bipolar coaxial electrode to be used initially on a vegetable model, which will be treated in section 4.5, was produced in IGEA. In this thesis was initially treated only the realization of the prototype without electrical connector design to be connected to the Cliniporator™, standard connections have been used for the use of the prototype on vegetable and animal models.

Once the materials have been obtained in the company, it has been possible to decide the configuration of the electrode for the vegetable model based on the simulations carried out in *Comsol Multiphysics*®. The prototypes for testing in vegetable models and the chosen geometry were used to conduct a qualitative verification of the device.

4.5 Test on vegetable model

These electrodes have been used and tested in potatoes. Potatoes are a good model to initially study the electroporation area (irreversible electroporation) as already seen in literature. They are a simplified model and can produce results very similar to those on tissues.[16][7]. In IGEA a trial has done to investigate the parameters studied and simulated with *Comsol Multiphysics*® to understand the shape of the electric field with different electrode configurations.

In order to be able to carry out the vegetable model tests, a protocol has been drawn up. The protocol would have made it possible to determine which model to use for animal model testing by critical analysis of the results. The concentric structure of the electrode is shown again in the images 4.38-4.39 to better understand geometry.

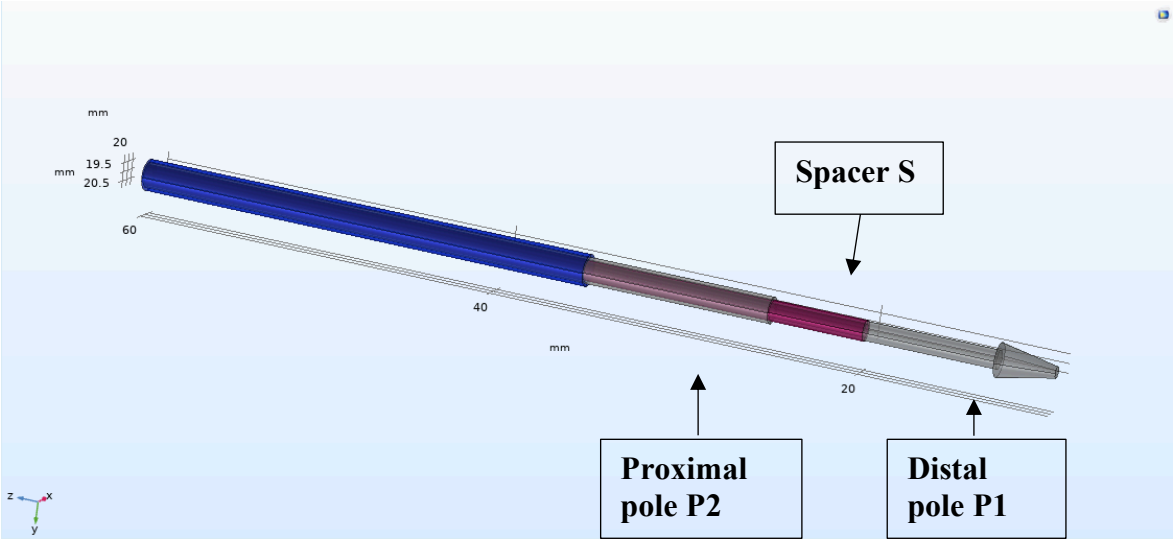

Figure 4.38 **View of electrode in *Comsol Multiphysics* ®.** Real structure of the electrode in *Comsol Multiphysics* ®.

Figure 4.39 **Example of real bipolar electrode.** Distal Pole: 10.00 mm, Spacer: 3.00 mm, Proximal pole: 5.00 mm.

It was decided to proceed with the tests described in the table 4.13. For values of insulating part of 3 mm a voltage of 500 V is applied and for a length of 5 mm a voltage of 800 V. For the short length of the insulating spacer it has been purposely decided to apply elevated voltage. All tests were conducted using 12 series of 8 pulses to perform treatments according to irreversible electroporation protocol. All tests shall use pulses of a length of 100 μs at frequencies of 1 kHz. Cliniporator Vitae™ has been used with automatic reversal of polarity in the 96 total pulses. The electrode will be inserted entirely in the potatoes maintaining a distance of 1 cm between the distal conductive pole and the outer edge of the potato. In this case the electrode will have a small tip made in IGEA that will facilitate the penetration and that will be included in the length of the first conductive pole P1. Once electroporation is carried out in the vegetable model, 24 hours will be expected for cutting in section to be able to visualize the area affected by the electric field. More than 50 tests were carried out on potatoes, the most significant ones are shown in the table 4.13 below.

Test number	P1 [mm]	S [mm]	P2 [mm]	V [V]	Pulse
1	10	3	10	500 V	96
2	10	5	10	800 V	96
3	10	5	10	500 V	96
4	10	3	5	500 V	96
5	5	5	10	800 V	96
6	5	3	5	500 V	96
7	5	5	5	800 V	96
8	5	3	15	500 V	96
9	5	5	15	800 V	96
10	3	3	3	500 V	96
11	3	5	3	800 V	96
12	3	3	10	500 V	96
13	3	5	10	800 V	96
14	3	5	10	500 V	96

Table 4.11 **Test on potatoes.**

The first test was carried out with a symmetric electrode with conductive poles of 10 mm and insulating part of 3 mm, the result of electroporation after 24 h is shown in the figure 4.40.

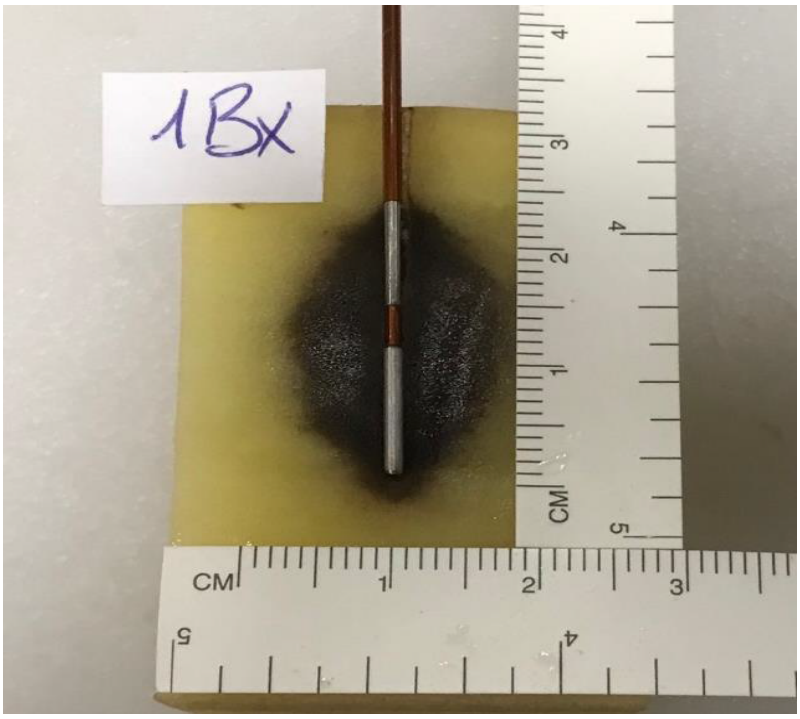

Figure 4.40 **Test 1 on vegetable model.** P1 & P2 = 10.00 mm, S=3.00 mm.

The second test was carried out with the same length of the conductive poles and different length of the insulating part (S = 5.00 mm) and the applied tension of 800 V (Figure 4.41).

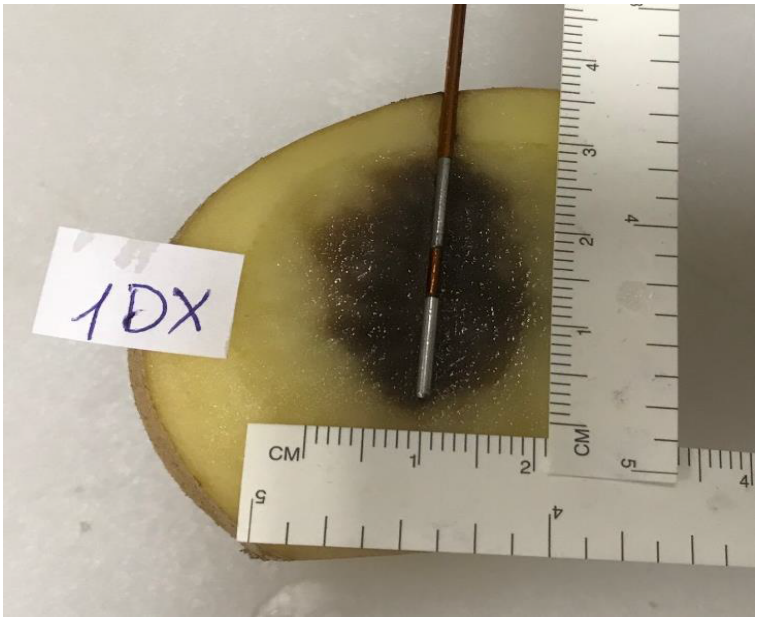

Figure 4.41 **Test 2 on vegetable model.** P1 & P2 = 10.00 mm, S=5.00 mm.

The third electrode (Figure 4.42) had the following geometry: P1 = 10.00 mm, P2 = 10.00 mm, S = 5.00 mm and then voltage of 500 V. The fourth test (Figure 4.43) was carried out with the device having P1 =10.00 mm, S = 3.00 mm, P2 = 5.00 mm and therefore voltage 500 V.

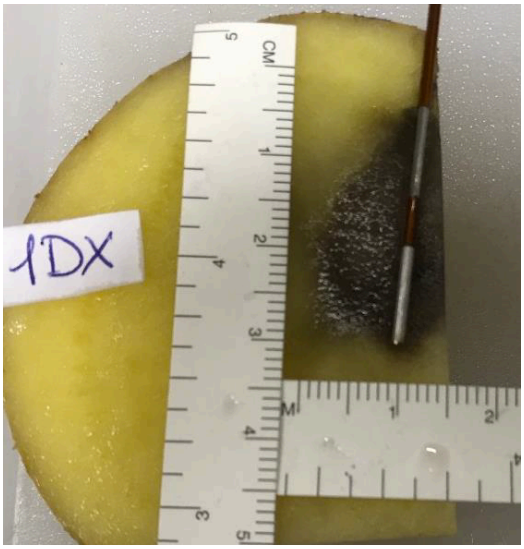

Figure 4.42 **Test 3 on vegetable model.** P1=10.00 mm, P2 = 10.00 mm, S=5.00 mm.

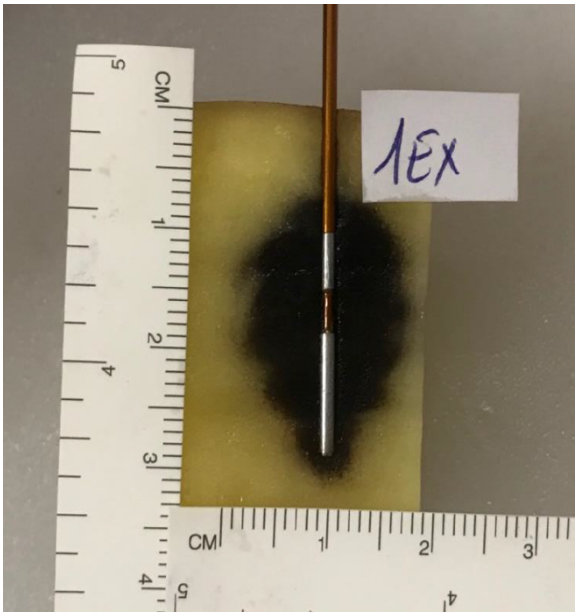

Figure 4.43 **Test 4 on vegetable model.** P1=10.00 mm, P2 = 5.00 mm, S=3.00 mm.

The electrodes used in these tests both had conductive poles P1 of 5.00 mm but differed by the length of the insulating part and P2. The electrode of the test (Figure 4.44) have P1= 5.00 mm, S = 5.00 mm and P2 = 10.00 mm while in the sixth test (Figure 4.45) P1 = 5.00 mm, S = 3.00 mm and P2 = 5.00 mm.

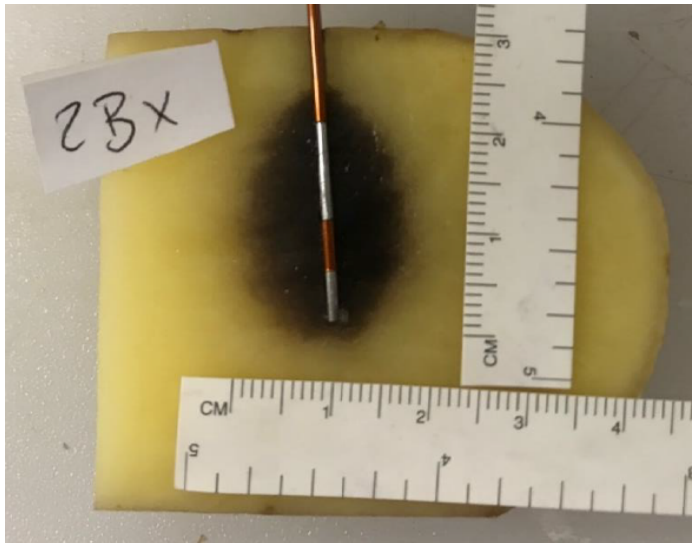

Figure 4.44 **Test 5 on vegetable model.** P1 = 5.00 mm, P2 = 10.00 mm, S=5.00 mm.

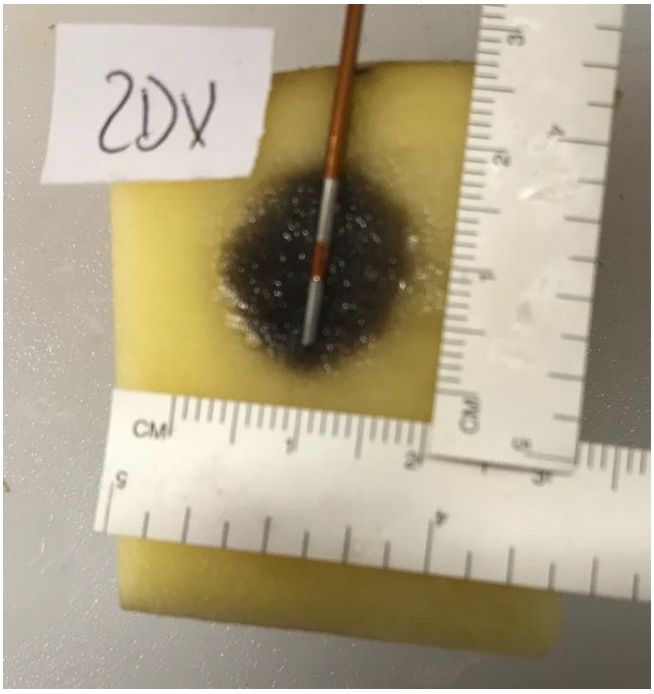

Figure 4.45 **Test 6 on vegetable model.** P1 & P2 = 5.00 mm, S=3.00 mm.

Both electrodes had P1 = 5.00 mm but in the case of the seventh electrode (Figure 4.46) the electrode is composed by P2 and S = 5.00 mm, while for the eighth (Figure 4.47) P2 = 15.00 mm and S = 3.00 mm.

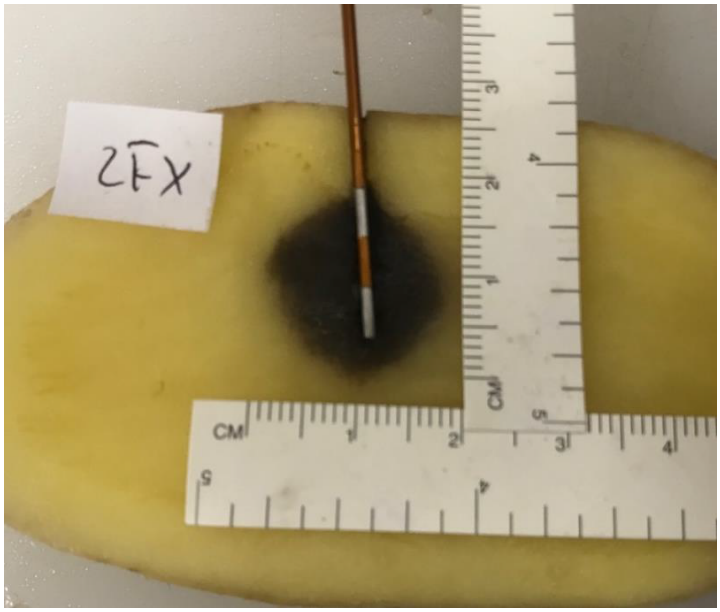

Figure 4.46 **Test 7 on vegetable model.** P1, P2 & S = 5.00 mm.

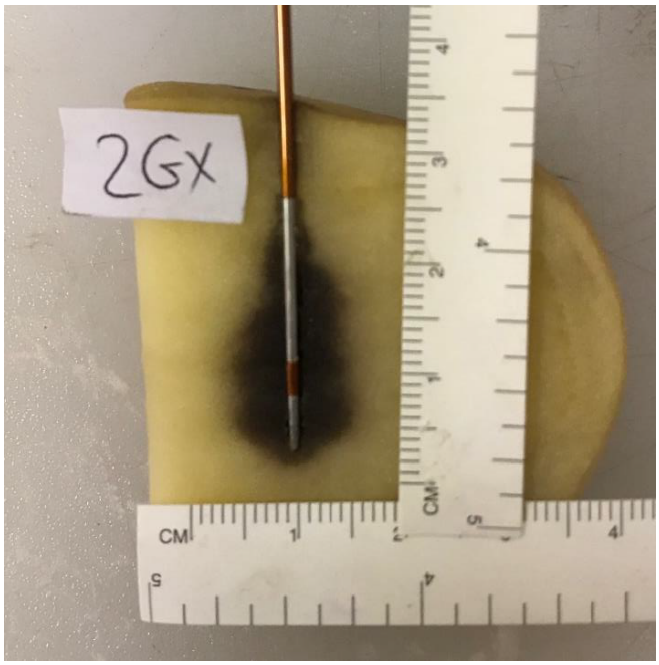

Figure 4.47 **Test 8 on vegetable model.** P1 = 5.00 mm, P2 = 15.00 mm, S=3.00 mm.

For the ninth test (Figure 4.48) the insulating spacer (S) will be 5.00 mm long, P1 = 5.00 mm and P2 = 15.00 mm and will have a voltage of 800 V while for the tenth test (Figures 4.49) the insulating spacer (S) will have a length of 3.00 mm, P1 = 3.00 mm & P2 = 3.00 mm and a voltage of 500 V.

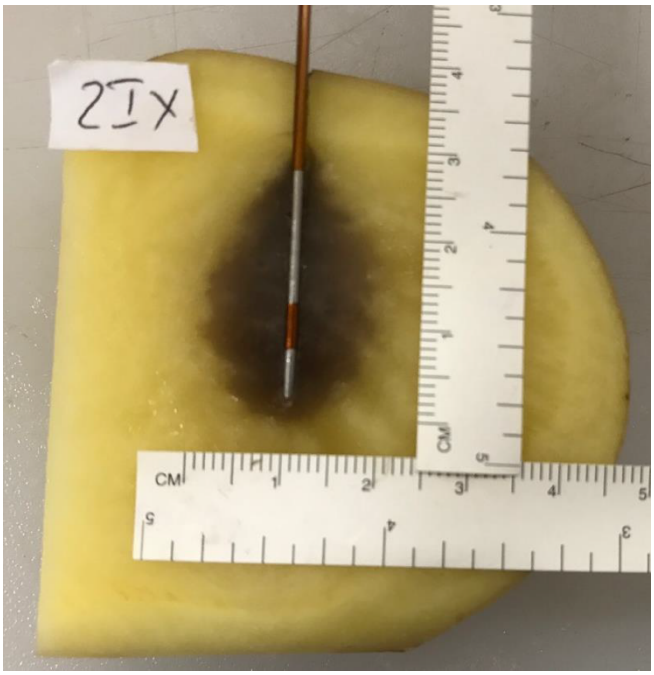

Figure 4.48 **Test 9 on vegetable model.** P1 & S = 5.00 mm, P2 = 15.00 mm.

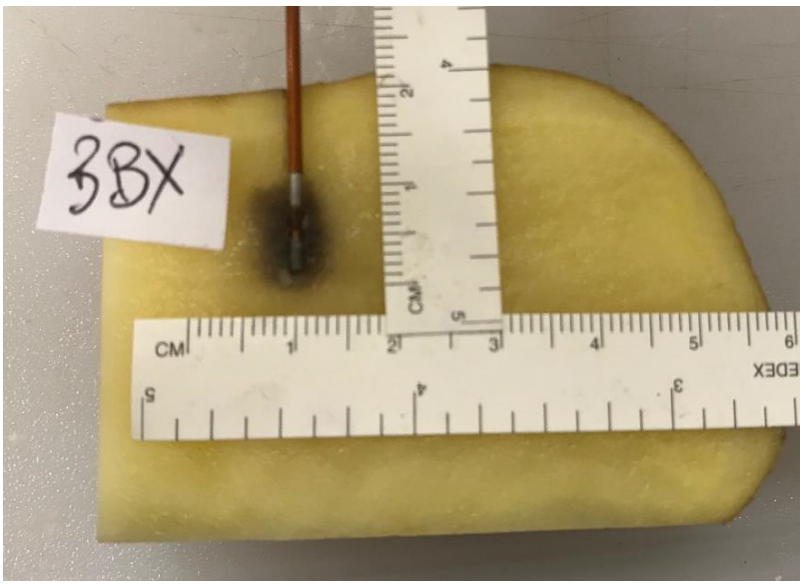

Figure 4.49 **Test 10 on vegetable model.** P1, P2 & S = 3.00 mm.

In the eleventh test the electrode (Figure 4.50) consisted of P1 and P2 equal to 3.00 mm but S = 5.00 mm and voltage equal to 800 V. For the electrode of the twelfth (Figure 4.51) P1 and S was 3.00 mm but P2 = 10.00 mm and therefore a voltage 500 V.

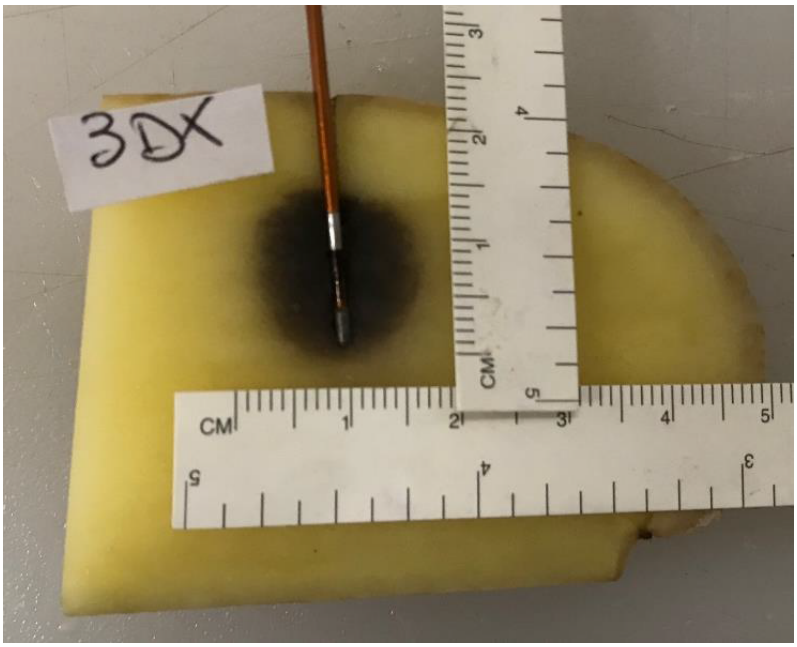

Figure 4.50 **Test 11 on vegetable model.** P1 & P2 = 3.00 mm, S = 5.00 mm.

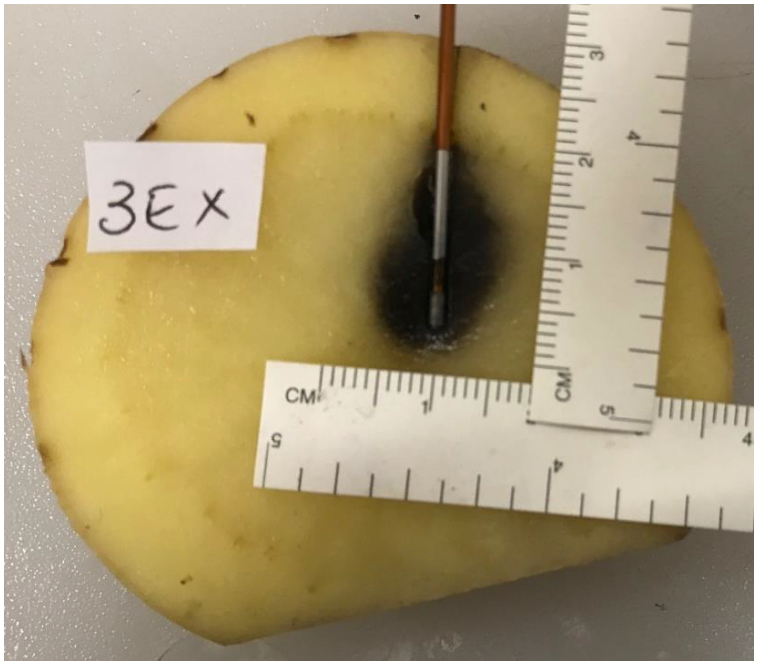

Figure 4.51 **Test 12 on vegetable model.** P1 & S = 3.00 mm, P2 = 10.00 mm.

In the last two tests carried out on a vegetable model, electrodes with asymmetric geometry were used. In the thirteenth (Figure 4.52) and fourteenth (Figure 4.53) test the electrode consisted of P1 = 3.00 mm, P2 = 10.00 mm and S = 5.00 mm but in the first case the voltage was 800 V while in the second was 500 V.

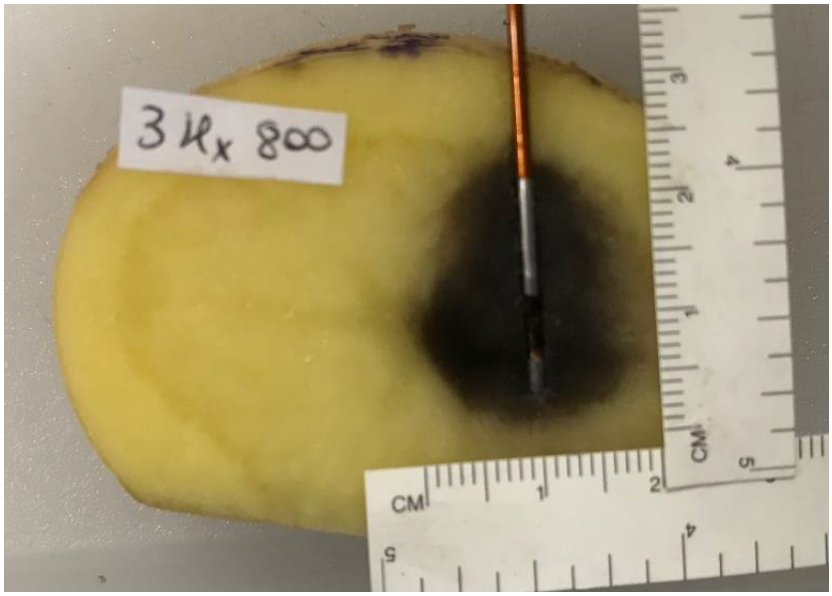

Figure 4.52 **Test 13 on vegetable model.** P1 = 3.00 mm, P2 = 10.00 mm, S = 5.00 mm.

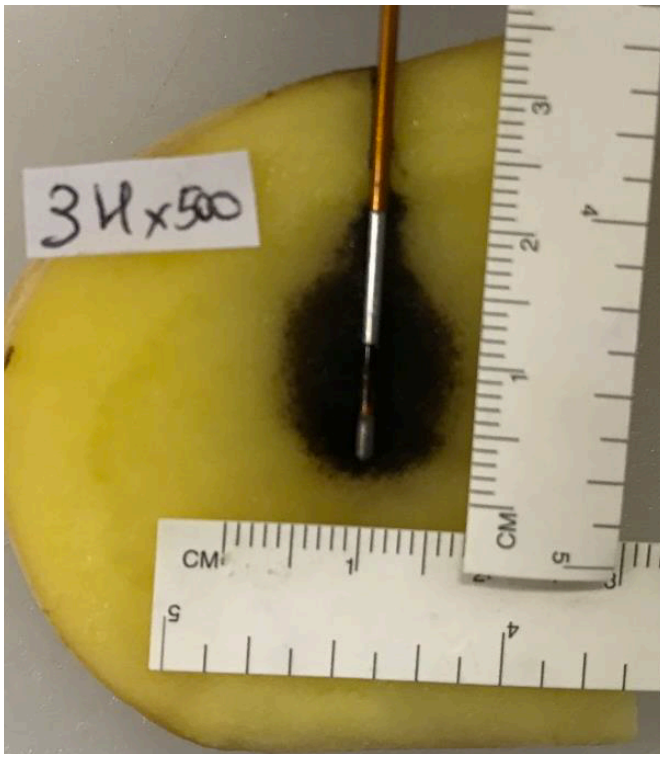

Figure 4.53 **Test 14 on vegetable model.** P1 = 3.00 mm, P2 = 10.00 mm, S = 5.00 mm.

4.5.1 Critical analysis of the results (vegetable test)

Similar conclusions to those found with the *Comsol Multiphysics* ® software were drawn from the vegetable model tests. The area in black is the part of potato hit by the electric field visible after 24 hours (IRE). The electric field develops along two directions that will be called "H" for the major axis, while "D" for the minor axis (figure 4.54).

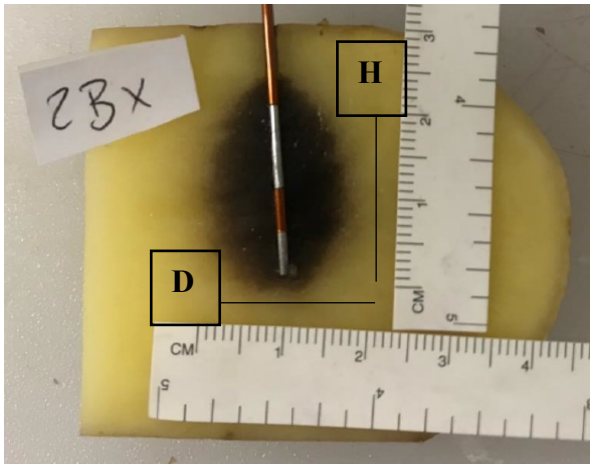

Figure 4.54 **Example of reading results on vegetable model.**

Test number	P1 [mm]	S [mm]	P2 [mm]	Total length [mm]	V [V]	Max. D [mm]
1	10	3	10	23	500 V	14.35
2	10	5	10	25	800 V	18.20
3	10	5	10	25	500 V	15.50
4	10	3	5	18	500 V	14.93
5	5	5	10	20	800 V	15.46
6	5	3	5	13	500 V	14.99
7	5	5	5	15	800 V	16.93
8	5	3	15	23	500 V	12.10
9	5	5	15	25	800 V	18.43
10	3	3	3	9	500 V	8.74
11	3	5	3	11	800 V	14.14
12	3	3	10	16	500 V	10.62
13	3	5	10	18	800 V	18.58
14	3	5	10	18	500 V	12.40

Table 12 **Test on vegetable model.** Maximum diameter of the electroporate zone.

In *Comsol Multiphysics* ® it was not possible to simulate the properties of the vegetable model; therefore, the diffusion effect of the electroporation involves a geometry slightly different from the theoretical model.

The values of the maximum diameters of the proximal, distal and spacer poles were used to analyze the results obtained in *Comsol Multiphysics* ® and on the vegetable model, also in order to make a better comparison. In the list below, it will be possible to see the similarity of the conclusions drawn in *Comsol Multiphysics* ® and on potatoes. The only difference obtained is that the diameters on potatoes are slightly higher than those of the theoretical model. This could be due to the number of pulses used on the vegetable model (96 impulses compared to single impulse on software), the type of cut carried out to obtain a clear image after 24 h or also to the type of material of which the potato is formed and therefore the way of diffusion of the electroporation.

It was, therefore, decided to analyze the maximum diameter of the electroporated zone for the vegetable model as the latter is not totally congruent due to the considerations made before compared to the theoretical ones. The maximum diameter is reported mainly for the symmetrical geometry of the electrode, and it was analyzed according to the maximum electrode length (P1+S+P2) in the histograms below.

The following conclusions could be drawn from the vegetable model tests:

- At the same total length of the poles (P1, S, P2), but different voltage applied it is evident that the greater diameter and therefore the electroporated volume is greater around the pole with shorter length. Test 13 (Max. D: 18.58 mm) & 14 (Max. D: 12.40 mm).

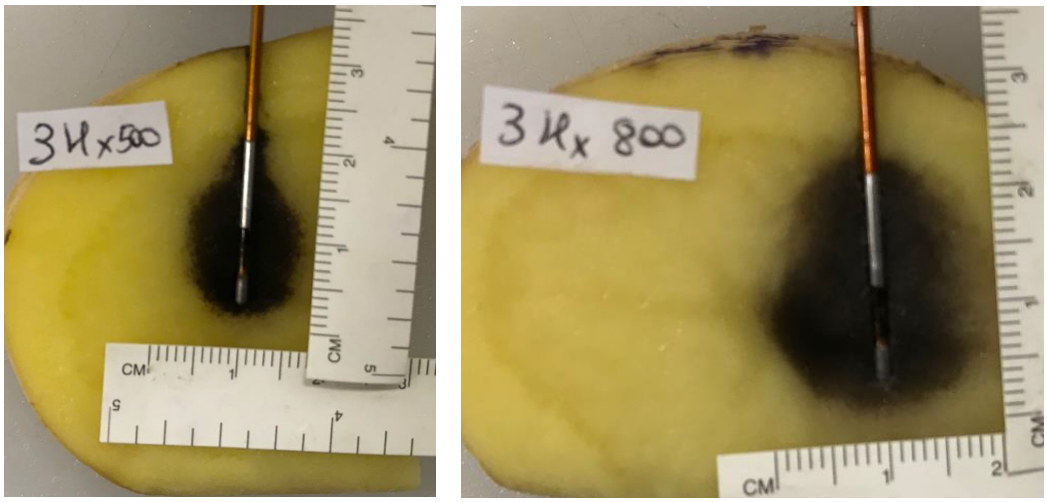

Figure 4.55 **Test 13 & 14.** At the same length of the poles (P1, P2 & S), but different voltage, greater diameter around the pole with shorter length.

- Using the same length of the insulating spacer and the same applied voltage but different length of the conductive poles it is possible to observe greater diameter of the electroporated zone around the electrode with greater length. Tests 6 (Max. D: 14.99 mm) & 10 (Max. D: 8.74 mm).

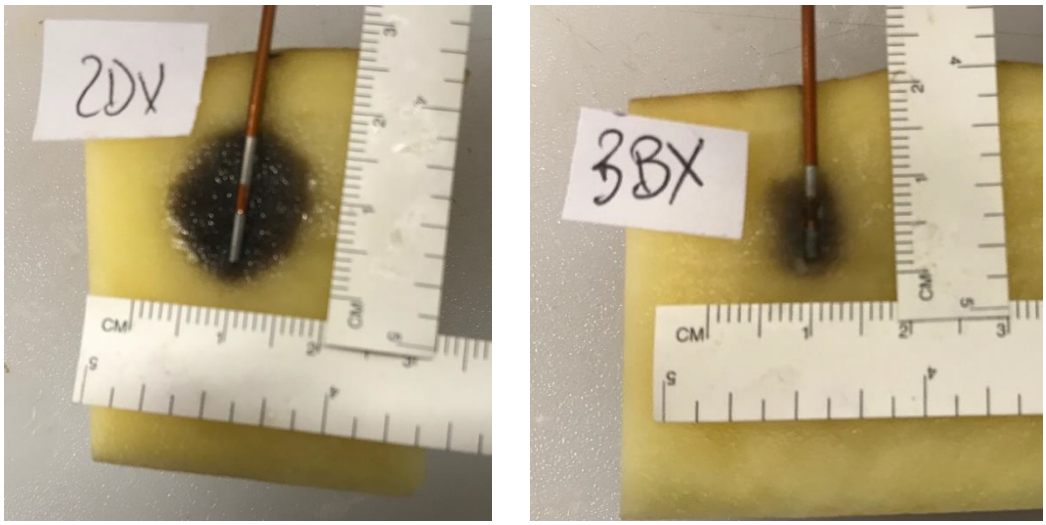

Figure 4.56 **Test 6 & 10.** Same length of the insulating spacer, same voltage but different conductive pole, greater diameter of electroporated zone around the electrode with greater length.

- Another aspect evidenced by the following tests is that with the same total length of the poles (P1+ P2+S) and the voltage applied in the figure on the left an electrode with symmetrical geometry is used, while in the right case it is asymmetric geometry. The shape of the electric field is different. A figure is formed more "regular" in the symmetrical case compared to the asymmetrical one that as in the first evaluation has greater diameter of the electroporate zone around the length of the smaller pole. Tests 1 (Max. D: 14.35 mm) & 8 (Max. D: 12.10 mm).

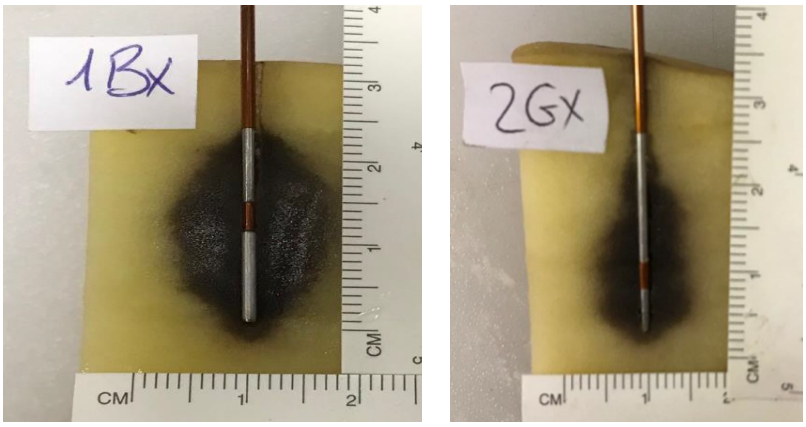

Figure 4.57 **Test 1 & 8.** Same total length of poles, same applied voltage but different geometry: asymmetrical and symmetrical one. Regular electroporated volume around symmetrical geometry compared to asymmetric geometry.

- The last variable analysed also in *Comsol Multiphysics* ® is the influenced of the length of the insulating spacer. In this case it is evident that as the length of the insulating pole increases, the maximum diameter of the electroporated zone around the spacer decreases. Tests 4 (Max. D: 14.93 mm) & 14 (Max. D: 12.40 mm).

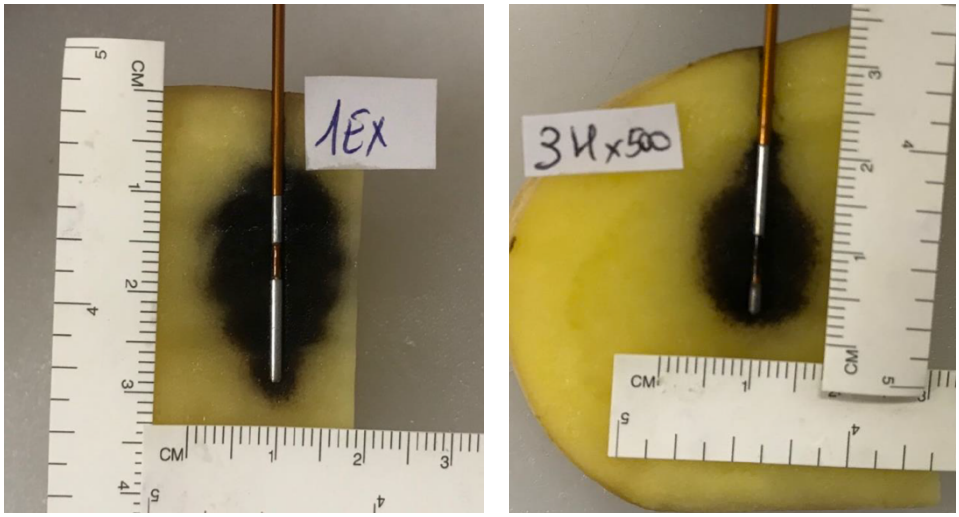

Figure 4.58 **Test 4 & 14.** Same applied voltage, same length of the conductive poles but different spacer, as the length of S increases, the electroporate volume decreases.

In conclusion the test performed with the vegetable are in line with results of the modelling performed with *Comsol Multiphysics*®. The variables that most influence the electroporated volume are the voltage and the total length of the poles. They will influence the distribution of the electric field in the tissue in both directions: H and D.

From the graphs below, the trend of the maximum diameter according to the total length of the electrode (P1+S+P2) can be summarized. The tests were divided into 500 V and 800V. In both, if the length increases the diameter of the electroporated volume increases. The few exceptions observe can attributed to the characteristics of the potatoes in use.

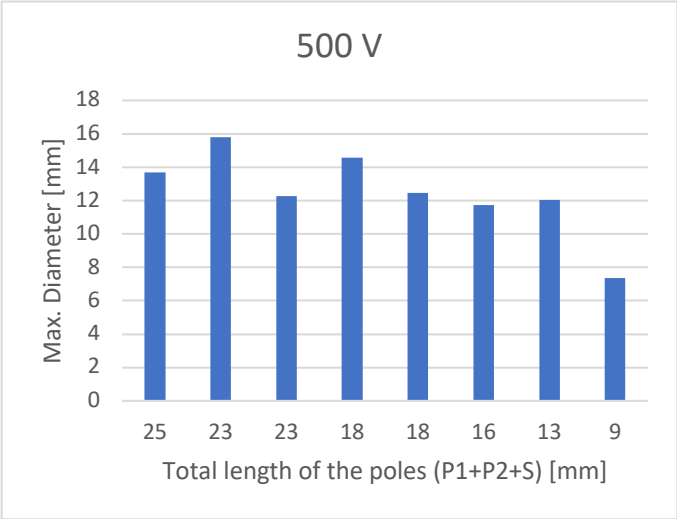

Figure 4.60 **Analysis of the vegetable model to the voltage 500 V.** Values of the maximum diameters of the electric field according to the total length of the poles

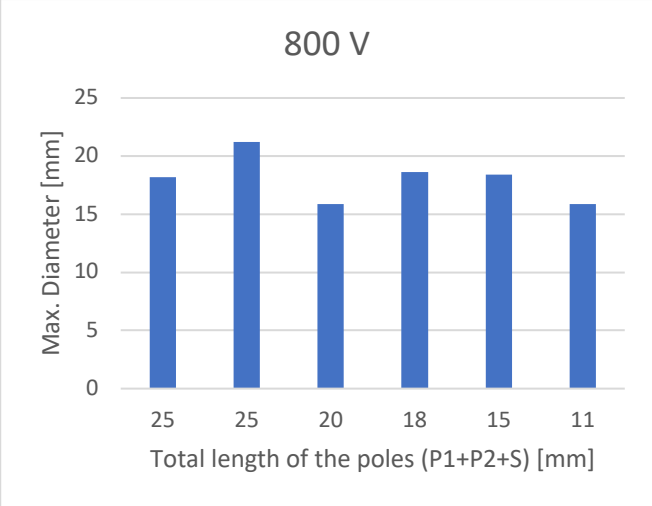

Figure 4.59 **Analysis of the vegetable model to the voltage 800 V.** Values of the maximum diameters of the electric field according to the total length of the poles.

Having carried out the tests on *Comsol Multiphysics*® and on a vegetable model it was possible to continue with a pre-clinical animal study (section 4.6).

It was possible to indicate useful electrode models for use *in vivo* on animals. These electrodes have been chosen in order to better highlight the aspects obtained in the conclusions of the study on a vegetable model, therefore voltage variation also according to the difference in the length of the poles.

4.6 Test *in vivo*

After having studied and analysed the vegetable model cases, it was concluded that pre-clinical animal studies could be done. Two animal tests were conducted during this master thesis. The device has been tested on animal in order to evaluate the usability and therefore suitability, the mechanical functionality and finally to treat the desired volume. The studies were conducted at the Istituto Nazionale Tumori – IRCCS – Fondazione G. Pascale, Napoli, Italia. The *in vivo* experiments have been conducted respecting bio-ethic principles and current Italian (art. 31 D.L. 26/2014), European regulations. The use of the animal model was authorized by the Ministry of Health (n. 15/2019-PR) within the Research Project "Expandable electrode for electroporation of tissues".

Before the device has been used, the animal (Female scrofa, 60 kg of weight) has been anaesthetized according to the following anaesthetic/analgesic protocol: zoletil anaesthesia 50/50 0.5 ml/kg i.m. + propofol 6 mg/kg i.v. + ketamine 10 mg/kg i.v + sevorane 2% by inhalation; butorphanol analgesia 0.1-0.4 mg/kg i.m. or i.v. The electrode was used in open surgery.

N. test	Electrode	P1 [mm]	S [mm]	P2 [mm]	D (P1) [mm]	D (P2) [mm]	V [V]	Pulse
1	**1**	5.00	3.00	20.00	1.80	2.00	800	80
2		5.00	3.00	20.00	1.80	2.00	1200	80
3	**2**	5.00	3.00	10.00	1.80	2.00	800	80
4		5.00	3.00	10.00	1.80	2.00	1200	80
5	**3**	10.00	3.00	5.00	1.40	0.95	500	96
6	**4**	3.00	5.00	3.00	1.40	0.95	800	96

Table 4.13 **Electrodes for test in vivo.**

Bipolar electrodes of different sizes were used in each. All tests in pre-clinical animal studies were performed with Cliniporator Vitae^{TM} (IGEA SpA, Carpi, Italy). At the end of the study the animal was sacrificed and liver specimens were removed for vital staining (Tetrazolium) and/or histology and immunohistochemistry evaluation.

The calculation of the volume of ablated areas was performed on the CT imaging data.

The electrodes used in in vivo tests are in the table 4.15.

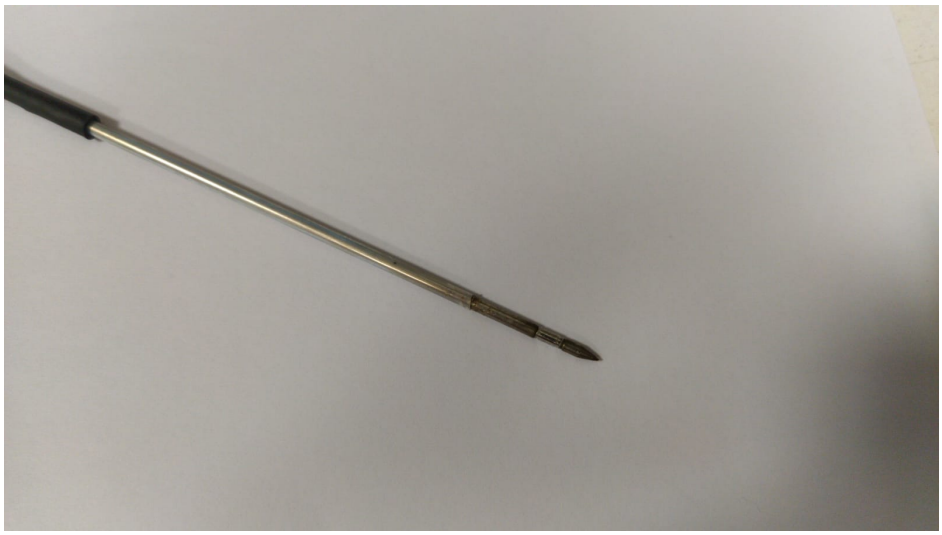

Figure 4.61 **Bipolar electrode used for first test in vivo.** P1: 5.00 mm, S: 3.00 mm, P2: 10.00 mm.

The first pre-clinical study has analysed the influence of applied tension and the difference in the total length of the electrode, in particular the influence of the length of the proximal pole (P2). Using 80 electrical pulses, the influence of the voltage of 800 V or 1200 V has been observed, and for the length of the second pole, it changes between 10 mm (figure 4.61) and 20 mm. Pulse duration was 100 μs. In this first study only two electrodes were used but 4 total tests were performed.

The second pre-clinical study was conducted with electrodes much more similar to those that will be used in clinical settings. In all the cases, the number of pulses applied was not varied and it was maintained at 96 with pulses duration of 100 μs.

The electrodes chosen in the second pre-clinical study were based on the results obtained with the vegetable model analysis. Test were conducted using:

- different voltage;
- different length of the insulating spacer and also of the conductive poles;
- the difference between a symmetrical geometry and an asymmetrical one.

Moreover, with both electrodes a rather important ablation is obtained on 1 cm of diameter of the electroporated volume.

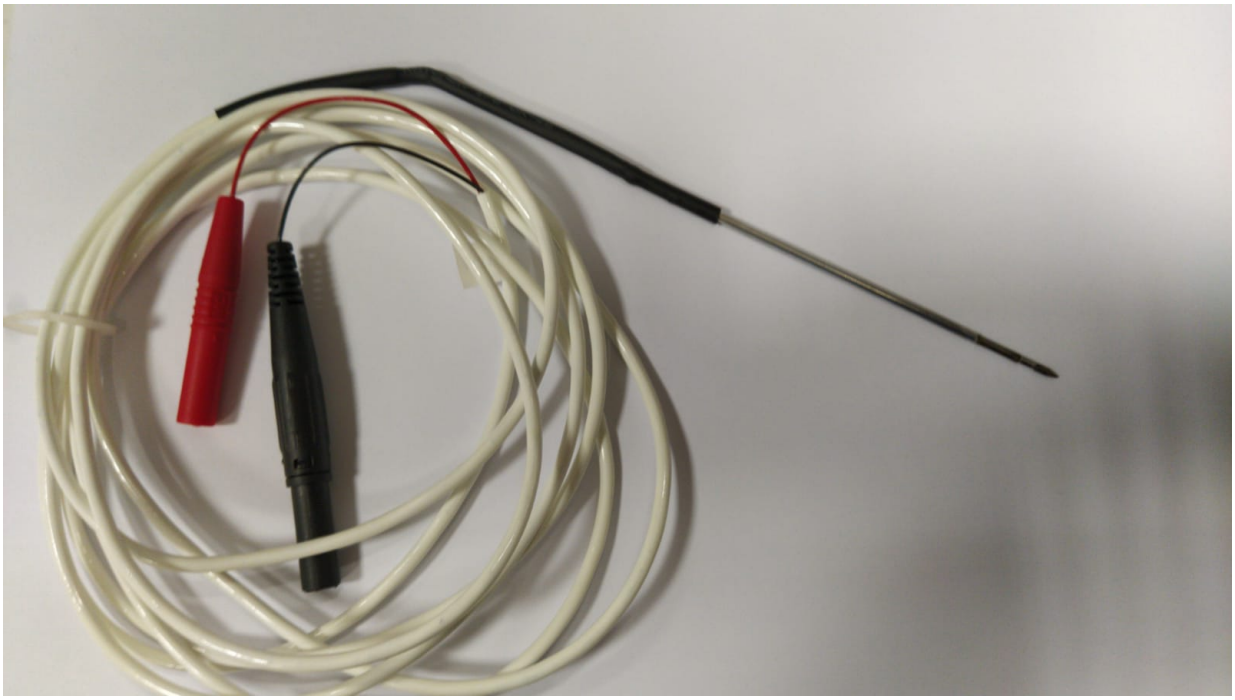

Figure 4.62 **Bipolar electrode with electrical connection.** Electrode used for the first clinical study with electrical connection for the Cliniporator™.

4.6.1 Critical analysis of the results (animal test)

Three histological results were reported for the critical analysis of animal results. In particular, the images show the cells ablated by electroporation and the shaper of the ablated area to be used to define the electroporated volume.

The first case concerns the electrode with the following characteristics:

- Distal Pole: 5.00 mm;
- Spacer: 3.00 mm;
- Proximal Pole: 20.00 mm;
- Total length of electrode: 20.00 cm;
- Pulse: 80;
- Voltage: 800 V.

The image 4.63 shows the sample taken for histology where the electrode was inserted.

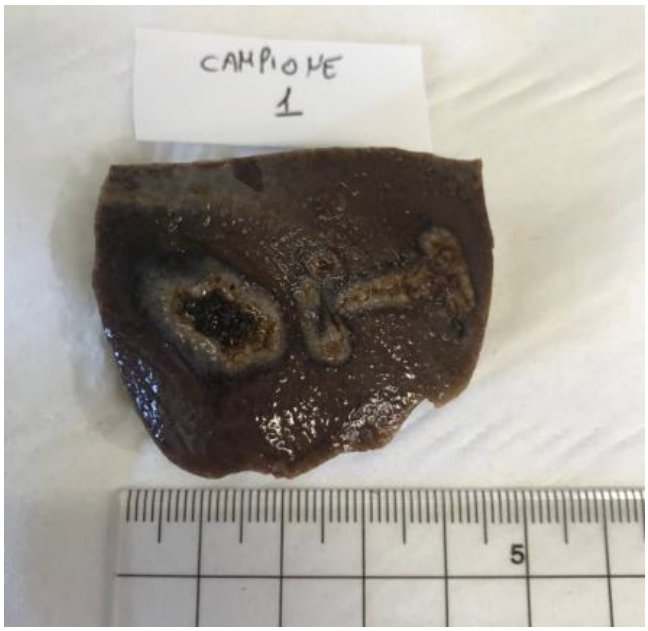

Figure 4.63 **Sample treated with bipolar electrode and taken for histology.** N. test: 1. P1 = 5.00 mm, S = 3.00 mm, P2 =20.00 mm.

The treated area is clearly visible in picture 4.64. In particular, the difference between lighter and darker staining of cells is noted, this is a sign of differentiation between dying cells and still living cells. The area treated as evidenced by the drawn circle is within the centimetre of diameter that was intended as the main purpose for this electrode. Figure 4.65 shows the magnification of the electroporated tissue and healthy tissue.

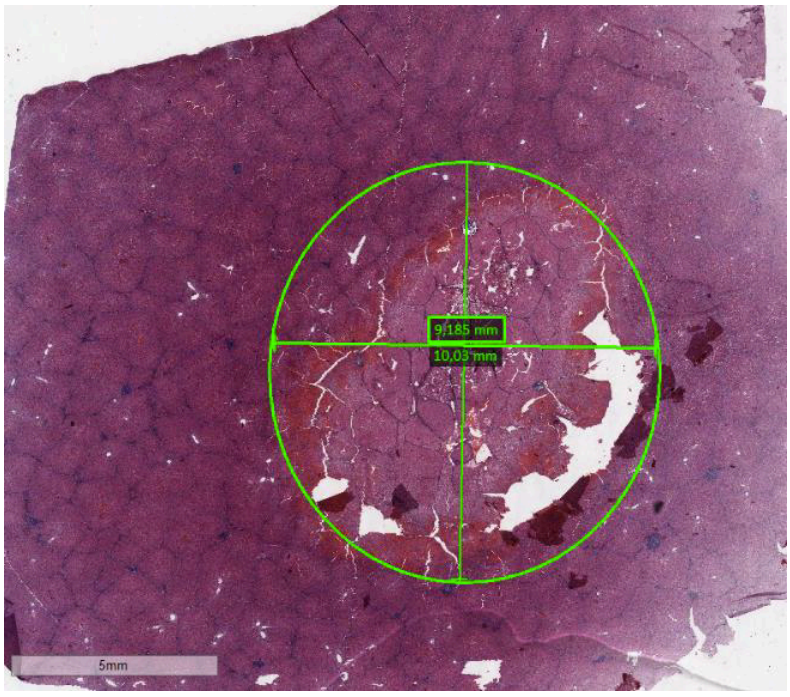

Figure 4.64 **Histology with details of the damaged parenchyma and the normal parenchyma (5 mm).** The electroporate volume about diameter of 10.00 mm.

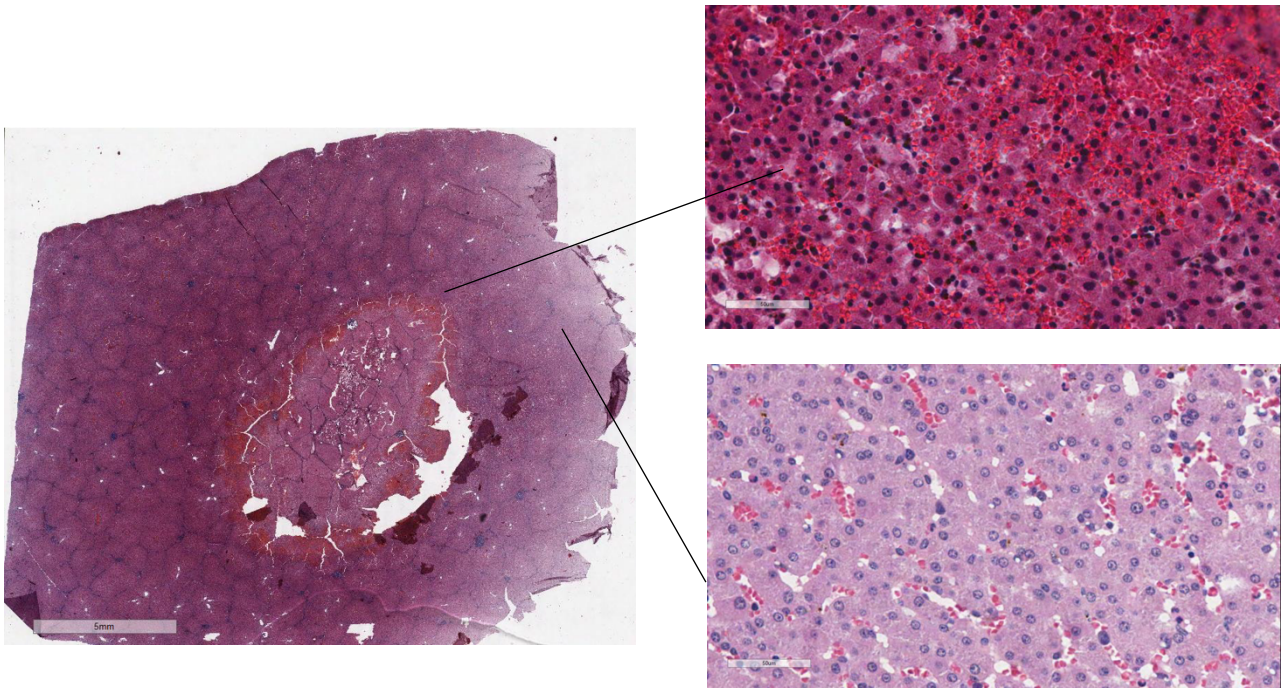

Figure 4.65 **Enlargement of the surrounding cells in the electroporate tissue and healthy tissue.** Figure top right: Electroporate tissue cells. Bottom: Healthy tissue cells.

The second sample reported in this thesis reports the results obtained with the second electrode. Two cases will be analysed. Both will have the following characteristics:

- Distal Pole: 5.00 mm;
- Spacer: 3.00 mm;
- Proximal Pole: 10.00 mm;
- Total length of electrode: 20.00 cm;
- Pulse: 80.

They will differ only for the applied voltage, which in the first case is 800 V and in the second of 1200 V.

Figure 4.66 **Sample treated with bipolar electrode and taken for histology.** N. test: 4. P1 = 5.00 mm, S = 3.00 mm, P2 =10.00 mm, Voltage = 800 V.

The electrode used in this test with respect to the previous uses the proximal pole of length half of that used with the first device. From the image 4.67 it is possible to see the diameter of the circular area ablated by electroporation, also in this case is about 1 cm. From the pictures below a clear difference between dead cells and healthy cells can be seen.

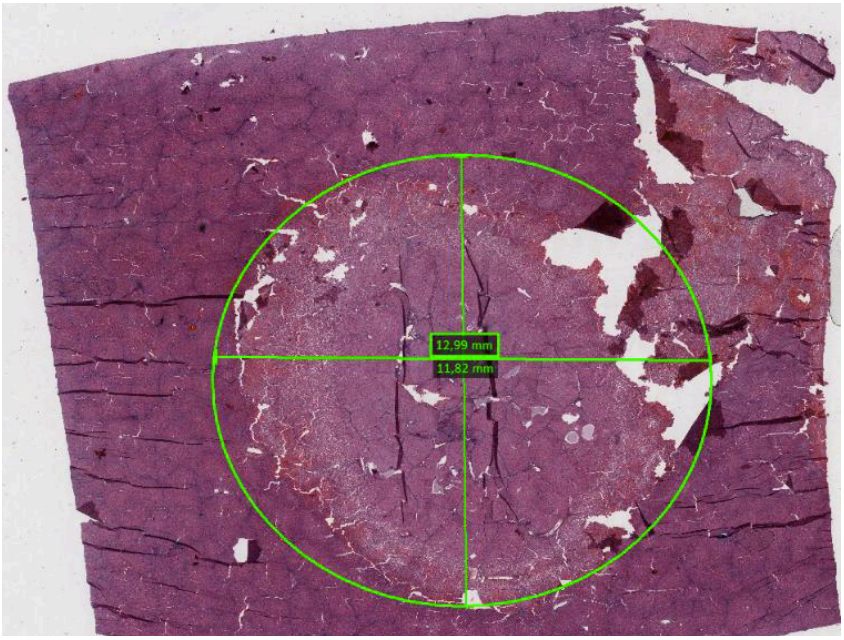

Figure 4.67 **Histology with details of the damaged parenchyma and the normal parenchyma (5 mm).** The electroporate volume about diameter of 12.00 mm.

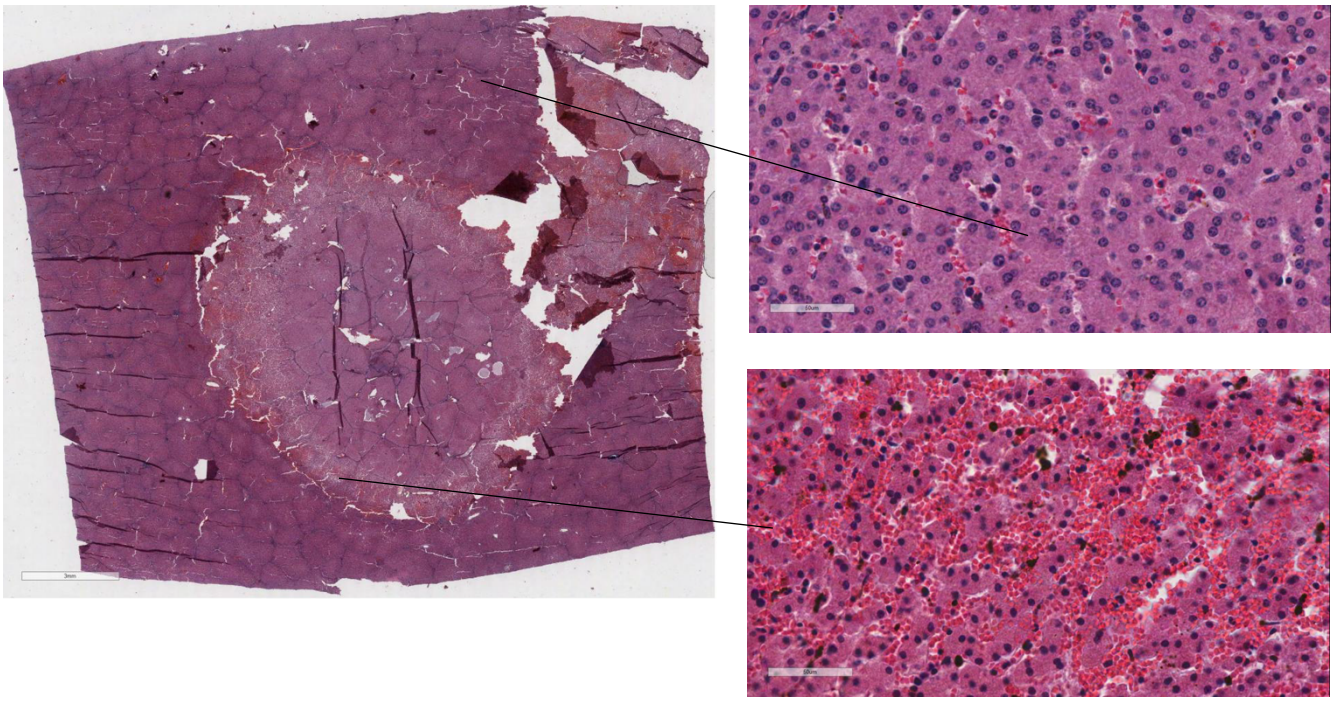

Figure 4.68 **Enlargement of the surrounding cells in the electroporate tissue and healthy tissue.** Figure top right: Healthy tissue cells. Bottom: Electroporate tissue cells.

The other test conducted with variation of the voltage alone at 1200 V is visible in the analysis of sample 5 (figure 4.69).

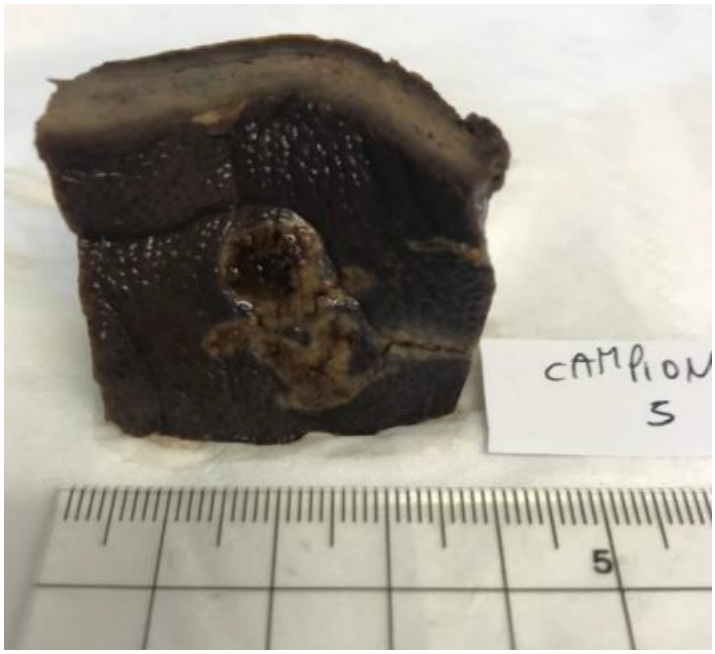

Figure 4.69 **Sample treated with bipolar electrode and taken for histology.** N. test: 5. P1 = 5.00 mm, S = 3.00 mm, P2 =10.00 mm, Voltage = 1200 V.

In this test the diameter of the electroporated zone is smaller than 1 cm although the applied voltage has increased. As in the previous tests, images of enlargement of dying tissue and tissue with cells still alive are reported.

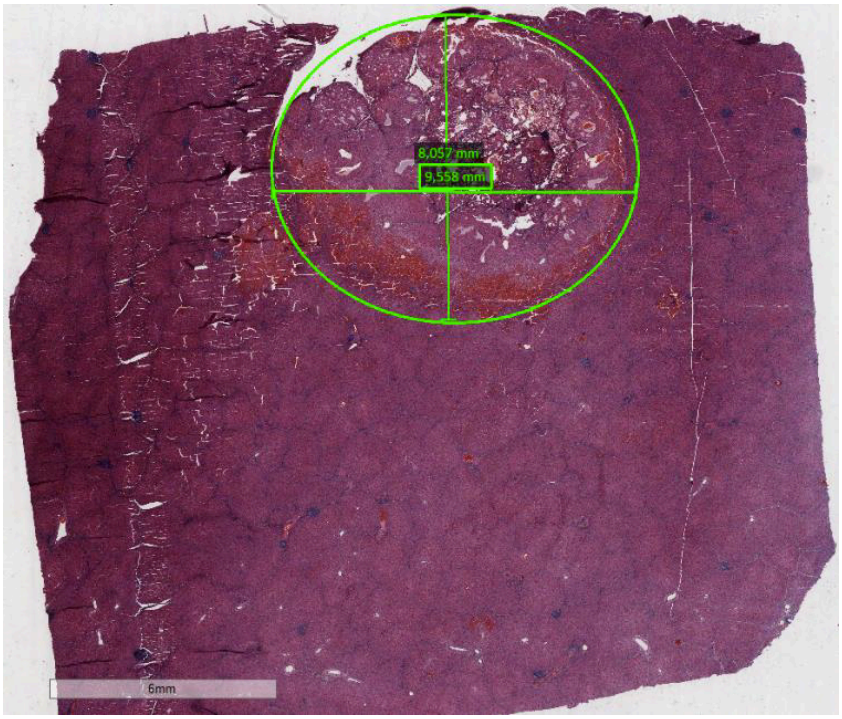

Figure 4.70 **Histology with details of the damaged parenchyma and the normal parenchyma (5 mm).** The electroporate volume about diameter of 10.00 mm.

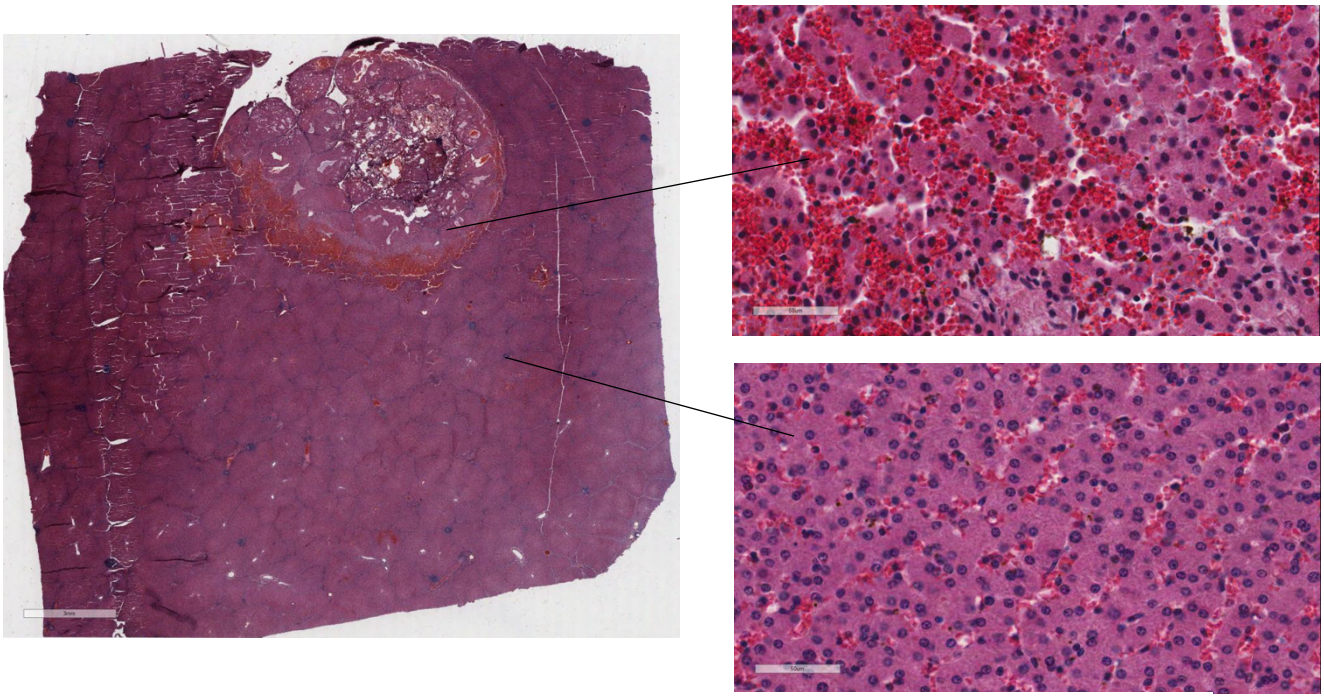

Figure 4.71 **Enlargement of the surrounding cells in the electroporate tissue and healthy tissue.** Figure top right: Electroporate tissue cells. Bottom: Healthy tissue cells Electroporate tissue cells.

In conclusion, the prototypes of bipolar electrode, tested in open surgery all result in parenchymal damage, due to irreversible electroporation, in an area always exceeding 5x6.5 mm^2. The largest damage area was obtained with 10 mm bipolar electrode and the following electrical parameters: N. 80 pulses and 800 V voltage.
Tests with the vegetable model were able to confirm the results obtained with the theoretical model of *Comsol Multiphysics* ® and finally the animal model was able to confirm the conclusions drawn from the previous studies. By analysing the variables that could most influence the electroporate volume we arrived to satisfy the aim we had initially made: reduce the invasiveness of the device and be able to cover an electroporate volume of about 1 cm in diameter. As we have seen from the histological reports above, with a diameter of about 1.80 mm it has been succeeded to satisfy these demands.

4.7 Conclusion

During this thesis work, it has been possible to prepare a prototype of electrode with the goal to develop a medical device and its certification. The initial aim, to create a device that was minimally invasive and that could cover an electroporated volume of 1 cm in diameter, has been achieved. The activity conducted begun with simulations with *Comsol Multiphysics* ® and then pre-clinical tests were completed both with potatoes and in pigs.
The prototype also met the usability and therefore suitability, the mechanical functionality analysis. The next step will be to define the characteristics of the new electrode that will be used in clinical practice.

References

[1] J. Impellizeri, L. Aurisicchio, P. Forde, and D. M. Soden, "Electroporation in veterinary oncology," *Veterinary Journal*. 2016, doi: 10.1016/j.tvjl.2016.05.015.

[2] E. W. Lee, J. Gehl, and S. T. Kee, "Introduction to Electroporation," in *Clinical Aspects of Electroporation*, 2011.

[3] R. Cadossi, M. Ronchetti, and M. Cadossi, "Locally enhanced chemotherapy by electroporation: Clinical experiences and perspective of use of electrochemotherapy," *Futur. Oncol.*, vol. 10, no. 5, pp. 877–890, 2014, doi: 10.2217/fon.13.235.

[4] A. Ongaro *et al.*, "Identification of in vitro electropermeabilization equivalent pulse protocols," *Technol. Cancer Res. Treat.*, vol. 10, no. 5, pp. 465–473, 2011, doi: 10.7785/tcrt.2012.500223.

[5] J. Kolosnjaj-Tabi, L. Gibot, I. Fourquaux, M. Golzio, and M. P. Rols, "Electric field-responsive nanoparticles and electric fields: physical, chemical, biological mechanisms and therapeutic prospects," *Adv. Drug Deliv. Rev.*, vol. 138, pp. 56–67, 2019, doi: 10.1016/j.addr.2018.10.017.

[6] N. P. Damijan Miklavcic, Selma Corovic, Gorazd Pucihar, "Importance of tumour coverage by sufficiently high local electric field for effective electrochemotherapy," *www.ejconline.com*, 2006.

[7] Y. Zhao, H. Liu, S. P. Bhonsle, Y. Wang, R. V. Davalos, and C. Yao, "Ablation outcome of irreversible electroporation on potato monitored by impedance spectrum under multi-electrode system," *Biomed. Eng. Online*, vol. 17, no. 1, pp. 1–13, 2018, doi: 10.1186/s12938-018-0562-9.

[8] L. G. Staal and R. Gilbert, "Generators and Applicators: Equipment for Electroporation," in *Clinical Aspects of Electroporation*, 2011.

[9] H. Gissel, R. C. Lee, and J. Gehl, "Electroporation and Cellular Physiology," in *Clinical Aspects of Electroporation*, 2011.

[10] "Cliniporator." [Online]. Available: https://www.igea.it/it/oncologia/area-dedicata-al-medico. [Accessed: 18-Nov-2019].

[11] J. Gehl *et al.*, "Updated standard operating procedures for electrochemotherapy of cutaneous tumours and skin metastases," *Acta Oncol. (Madr).*, vol. 57, no. 7, pp. 874–882, 2018, doi: 10.1080/0284186X.2018.1454602.

[12] G. Sersa *et al.*, "Electrochemotherapy of Small Tumors; The Experience from the ESOPE (European Standard Operating Procedures for Electrochemotherapy) Group," in *Clinical Aspects of Electroporation*, 2011.

[13] A. Silve and L. M. Mir, "Cell Electropermeabilization and Cellular Uptake of Small Molecules: The Electrochemotherapy Concept," in *Clinical Aspects of Electroporation*, 2011.

[14] "Comsol." [Online]. Available: https://en.wikipedia.org/wiki/COMSOL_Multiphysics.

[15] A. goleman, daniel; boyatzis, Richard; Mckee, "Acciai inox," *J. Chem. Inf. Model.*,

vol. 53, no. 9, pp. 1689–1699, 2019, doi: 10.1017/CBO9781107415324.004.

[16] A. Wandel *et al.*, “Optimizing Irreversible Electroporation Ablation with a Bipolar Electrode,” *J. Vasc. Interv. Radiol.*, vol. 27, no. 9, pp. 1441-1450.e2, 2016, doi: 10.1016/j.jvir.2016.06.001.